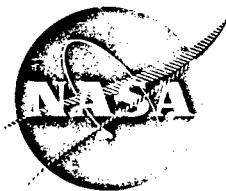


**NASA
SPACE VEHICLE
DESIGN CRITERIA
(CHEMICAL PROPULSION)**

NASA SP-8076

SOLID PROPELLANT GRAIN DESIGN AND INTERNAL BALLISTICS



MARCH 1972

NATIONAL AERONAUTICS AND SPACE ADMINISTRATION

FOREWORD

NASA experience has indicated a need for uniform criteria for the design of space vehicles. Accordingly, criteria are being developed in the following areas of technology:

Environment
Structures
Guidance and Control
Chemical Propulsion

Individual components of this work will be issued as separate monographs as soon as they are completed. This document, part of the series on Chemical Propulsion, is one such monograph. A list of all monographs issued prior to this one can be found on the final pages of this document.

These monographs are to be regarded as guides to design and not as NASA requirements, except as may be specified in formal project specifications. It is expected, however, that these documents, revised as experience may indicate to be desirable, eventually will provide uniform design practices for NASA space vehicles.

This monograph, "Solid Propellant Grain Design and Internal Ballistics", was prepared under the direction of Howard W. Douglass, Chief, Design Criteria Office, Lewis Research Center; project management was by John H. Collins, Jr. The monograph was written by W. T. Brooks of the Rocketdyne Solid Rocket Division, North American Rockwell Corporation, and was edited by Russell B. Keller, Jr. of Lewis. To assure technical accuracy of this document, scientists and engineers throughout the technical community participated in interviews, consultations, and critical review of the text. In particular, Gene O. Chan of Aerojet Solid Propulsion Company; Charles A. Chase of United Technology Center, United Aircraft Corporation; and C. A. Speak of Thiokol Chemical Corporation (Wasatch Division) individually and collectively reviewed the monograph in detail.

Comments concerning the technical content of this monograph will be welcomed by the National Aeronautics and Space Administration, Lewis Research Center (Design Criteria Office), Cleveland, Ohio 44135.

March 1972

GUIDE TO THE USE OF THIS MONOGRAPH

The purpose of this monograph is to organize and present, for effective use in design, the significant experience and knowledge accumulated in development and operational programs to date. It reviews and assesses current design practices, and from them establishes firm guidance for achieving greater consistency in design, increased reliability in the end product, and greater efficiency in the design effort. The monograph is organized into two major sections that are preceded by a brief introduction and complemented by a set of references.

The State of the Art, section 2, reviews and discusses the total design problem, and identifies which design elements are involved in successful design. It describes succinctly the current technology pertaining to these elements. When detailed information is required, the best available references are cited. This section serves as a survey of the subject that provides background material and prepares a proper technological base for the *Design Criteria* and Recommended Practices.

The *Design Criteria*, shown in italic in section 3, state clearly and briefly what rule, guide, limitation, or standard must be imposed on each essential design element to ensure successful design. The *Design Criteria* can serve effectively as a checklist of rules for the project manager to use in guiding a design or in assessing its adequacy.

The Recommended Practices, also in section 3, state how to satisfy each of the criteria. Whenever possible, the best procedure is described; when this cannot be done concisely, appropriate references are provided. The Recommended Practices, in conjunction with the *Design Criteria*, provide positive guidance to the practicing designer on how to achieve successful design.

Both sections have been organized into decimally numbered subsections so that the subjects within similarly numbered subsections correspond from section to section. The format for the Contents displays this continuity of subject in such a way that a particular aspect of design can be followed through both sections as a discrete subject.

The design criteria monograph is not intended to be a design handbook, a set of specifications, or a design manual. It is a summary and a systematic ordering of the large and loosely organized body of existing successful design techniques and practices. Its value and its merit should be judged on how effectively it makes that material available to and useful to the designer.

CONTENTS

1.	INTRODUCTION	1
2.	STATE OF THE ART	3
3.	DESIGN CRITERIA and Recommended Practices	58
	REFERENCES	81
	GLOSSARY	91
	NASA Space Vehicle Design Criteria Monographs Issued to Date	99

<u>SUBJECT</u>	<u>STATE OF THE ART</u>		<u>DESIGN CRITERIA</u>	
EVALUATION OF PARAMETERS	2.1	5	3.1	58
Independent Parameters	2.1.1	5	3.1.1	58
Ballistic Performance	2.1.1.1	6	3.1.1.1	58
Propellant Properties	2.1.1.2	7	3.1.1.2	59
Specific Impulse	2.1.1.2.1	7	3.1.1.2.1	59
Burning Rate	2.1.1.2.2	9	3.1.1.2.2	60
Density	2.1.1.2.3	13	3.1.1.2.3	61
Mission- and Vehicle-Related Constraints	2.1.1.3	13	3.1.1.3	61
Envelope	2.1.1.3.1	14	3.1.1.3.1	61
Maximum Expected Operating Pressure	2.1.1.3.2	14	3.1.1.3.2	62
Use Environment	2.1.1.3.3	14	3.1.1.3.3	62
Dependent Parameters	2.1.2	15	3.1.2	62
Average Operating Pressure	2.1.2.1	15	3.1.2.1	63
Nozzle Throat Area and Expansion Ratio	2.1.2.2	16	3.1.2.2	63
Volumetric Loading Fraction	2.1.2.3	18	3.1.2.3	64

<u>SUBJECT</u>	<u>STATE OF THE ART</u>		<u>DESIGN CRITERIA</u>	
Web Fraction	2.1.2.4	19	3.1.2.4	64
Port-to-Throat Area Ratio	2.1.2.5	19	3.1.2.5	65
Length-to-Diameter Ratio	2.1.2.6	21	3.1.2.6	66
CONFIGURATION SELECTION AND DESIGN	2.2	22	3.2	66
Principles Governing Selection	2.2.1	22	3.2.1	66
Ballistic Constraints	2.2.1.1	22	3.2.1.1	66
Processing Practicality	2.2.1.2	22	3.2.1.2	67
Structural Integrity	2.2.1.3	23	3.2.1.3	67
Geometric Definition and Analysis	2.2.2	24	3.2.2	69
Configuration Types	2.2.2.1	24	3.2.2.1	69
End Burner	2.2.2.1.1	24	—	—
Internal-External-Burning Tube	2.2.2.1.2	26	—	—
Internal-Burning Tube or Shell	2.2.2.1.3	28	—	—
Rod and Shell	2.2.2.1.4	31	—	—
Star	2.2.2.1.5	32	—	—
Wagon Wheel	2.2.2.1.6	36	—	—
Dendrite or Forked Wagon Wheel	2.2.2.1.7	37	—	—
Anchor and Dogbone	2.2.2.1.8	38	—	—
Slotted Tube	2.2.2.1.9	40	—	—
Conocyl	2.2.2.1.10	41	—	—
Finocyl	2.2.2.1.11	42	—	—
Other Configurations	2.2.2.1.12	43	—	—
Method of Selection	2.2.2.2	49	3.2.2.2	69
Geometric Analysis	2.2.2.3	50	3.2.2.3	73
Analytical Techniques	2.2.2.3.1	51	—	—
Drafting Techniques	2.2.2.3.2	52	—	—

<u>SUBJECT</u>	<u>STATE OF THE ART</u>		<u>DESIGN CRITERIA</u>	
DESIGN VERIFICATION ANALYSIS	2.3	53	3.3	75
Steady-State Mass Balance	2.3.1	53	3.3.1	75
Burning-Rate Augmentation	2.3.2	55	3.3.2	75
Performance Prediction and Iteration	2.3.3	56	3.3.3	76
MEOP	—	—	3.3.3.1	77
Average Thrust	—	—	3.3.3.2	78
Duration and Impulse	—	—	3.3.3.3	79
Design Acceptability and Optimization	2.3.4	57	3.3.4	79

LIST OF FIGURES AND TABLES

Figure	Title	Page
1	Solid propellant grain design sequence	4
2	Definition of ballistic performance parameters	6
3	Relationships among temperature-sensitivity coefficients	12
4	Nozzle divergence angles.	17
5	End-burning configuration.	25
6	Formation of equilibrium burning surface of an end-burning grain with nonuniform burning rate	26
7	Internal-external-burning tube configuration	27
8	Internal-burning tube or shell configuration	28
9	Burning characteristics, internal-burning tube	30
10	Rod-and-shell configuration	31
11	Star configuration	33
12	Wagon wheel configuration	36
13	Dendrite configuration	38
14	Anchor configuration	39
15	Dogbone configuration	39
16	Slotted-tube configuration.	40
17	Conocyl configuration	41
18	Finocyl configuration	42
19	Spherical grain configuration	44
20	Typical boost-sustain grain configurations.	45
21	Boost-sustain grain thrust schedule	46

LIST OF FIGURES AND TABLES (concluded)

Figure	Title	Page
22	Bipropellant star configuration	47
23	Typical cartridge-loaded grains	48
24	Cartridge-loaded slab	48
25	Typical multiperforated grain shapes	49
26	Burning-perimeter changes at a cusp	51
27	Simulation of grain configuration using basic figures	51
28	Typical burning perimeters from a neutral-burning star	53
29	Balance of mass flowrates	54
30	Points of discontinuity for $A_b = f(w_x)$	74
31	Dependence of thrust on pressure, nozzle throat area, and burning rate	78
Table	Title	Page
I	Suitability of Grain Configurations for Neutral-Burning Applications	71

SOLID PROPELLANT GRAIN DESIGN AND INTERNAL BALLISTICS

1. INTRODUCTION

A distinctive property of a solid propellant grain is the manner in which the burning surface changes during motor operation. The burning surface at each point recedes in the direction normal to the surface at that point, the result being a relationship between burning surface and web distance burned that depends almost entirely on the initial shape and restricted boundary. The rate of propellant consumption depends on the burning surface and other internal ballistic variables related to the dynamics of the compressible-fluid flow. Thus, the design of the grain ultimately defines the performance characteristics that can be obtained with a given propellant and nozzle.

Although grain design per se in terms of configuration is largely a geometric consideration, the particular geometry that meets specific ballistic performance requirements depends on the interrelationship of the geometric, propellant, and flow variables. Therefore, material within the scope of this monograph is organized around the logical order of the grain design sequence, including geometric definition and internal ballistic analysis, due recognition being given to processing limitations and structural requirements. The monograph is limited primarily to the ballistic aspects of grain design with the purpose of (1) outlining the ordered steps necessary to achieve a successful grain design and (2) recommending practices to accomplish each step.

The approach to grain design presented in this monograph is consistent with the practice of (1) evaluating the requirements, (2) selecting and designing the configuration, and (3) analytically verifying the design. This approach recognizes that some requirements imposed on the grain design can be treated independently whereas others must be considered as functions of the independent requirements. Failure to distinguish properly between the two kinds of requirements can result in conflicts and may compromise the design in terms of optimization, if not acceptability. Ballistic performance requirements, derived from mission analysis, are dominant in the determination of a grain design. Structural integrity requirements and processing constraints are fundamental considerations, however, and can be overriding influences in some grain design situations. Mission requirements, generally thrust and duration, usually define the independent parameters and provide the variables from which the dependent parameters can be determined. These dependent parameters include finally the web fraction, volumetric loading fraction, length-to-diameter ratio, and port-to-throat area ratio; this set of variables establishes firm criteria for configuration

selection. Quantitative evaluation of these parameters limits the number of applicable configurations, frequently to one or two. Guidelines given are to be used in selecting the configuration on the basis of the dependent parameters.

An integrated ballistic analysis is necessary as a part of the iterative grain design effort. The typical in-depth analysis treats mass addition by finite element and erosive burning at each element. Relationships of the grain design to the steady-state mass balance and erosive burning are considered. The significant influence of erosive burning on mass addition must be recognized and assessed to preclude subsequent redesign, resultant schedule delays, and unscheduled expenditures. References to appropriate internal ballistic computer programs, including a generalized three-dimensional grain design program, are cited, and recommendations are given regarding the extent and depth of analysis appropriate for a specified design.

Ballistic quality of a grain design can be evaluated by various indexes presented in the monograph, such as sliver content, volumetric loading, and configuration efficiency. These measures of merit are treated as part of design optimization for an otherwise acceptable grain design.

2. STATE OF THE ART

Much of the motor design activity depends on definition of the grain configuration (also referred to as grain perforation), and thus early completion of the grain design normally is required. Accordingly, advances in grain design technology have greatly enhanced motor design capability. Techniques have been improved to the extent that performance within the specified limits frequently is demonstrated by the first design verification firing. Performance in the first test within 10 percent of the design objective is typical, and frequently performance is better when adequate data from similar designs are available. With the benefit of one or two test firings, adjustable parameters such as burning rate can be varied to provide rated performance within 1 or 2 percent of the original design objectives, without major changes to the configuration. Improved design reliability therefore has reduced the number of development firings required for design verification, in some instances to three or four.

Computer-aided methods permitting both rigorous treatment of the gas dynamics and complete analysis of the grain geometry have contributed to the current state of the art in grain design. These analyses have been complemented by accurate methods for assessing flow and combustion inefficiencies within the motor and nozzle to permit effective and efficient grain design and analysis. In particular, the generalized three-dimensional grain-design program available in the literature (ref. 1) and the programs developed by various companies make possible the effective design and analysis of grains in envelopes with small length-to-diameter ratios where three-dimensional characteristics dominate. The complicated three-dimensional configuration no longer is avoided because of inability to compute an accurate surface area and conduct a three-dimensional grain stress analysis.

Following a logical sequence of design steps increases the chances of obtaining a grain design that is near optimum, not merely adequate. The ordered steps necessary for successful grain design are (1) evaluation of design requirements and internal ballistic parameters, (2) selection and design of grain configuration, and (3) analysis of design. The steps and their order of inclusion are identified in figure 1; normal sequence of steps is indicated by solid lines, and redirection of steps, frequently required in the iterative process, is indicated by dashed lines. The general analytical expressions presented in figure 1 attest the dependence of those parameters so designated and the necessity for treating them as dependent. Relation of configuration types to the design parameters also is depicted in figure 1.

An understanding of the evolution of the classical shapes and certain aspects of grain topology from a purely morphological standpoint enhances the ability of the grain designer. These subjects are covered in detail in references 2 through 5. It is the intent herein to give only a geometric definition for each of the classical grain configurations in terms of the necessary independent variables. No particular regard is paid to the location of a given configuration in the evolution of grain designs, but specific emphasis is placed on its area of application.

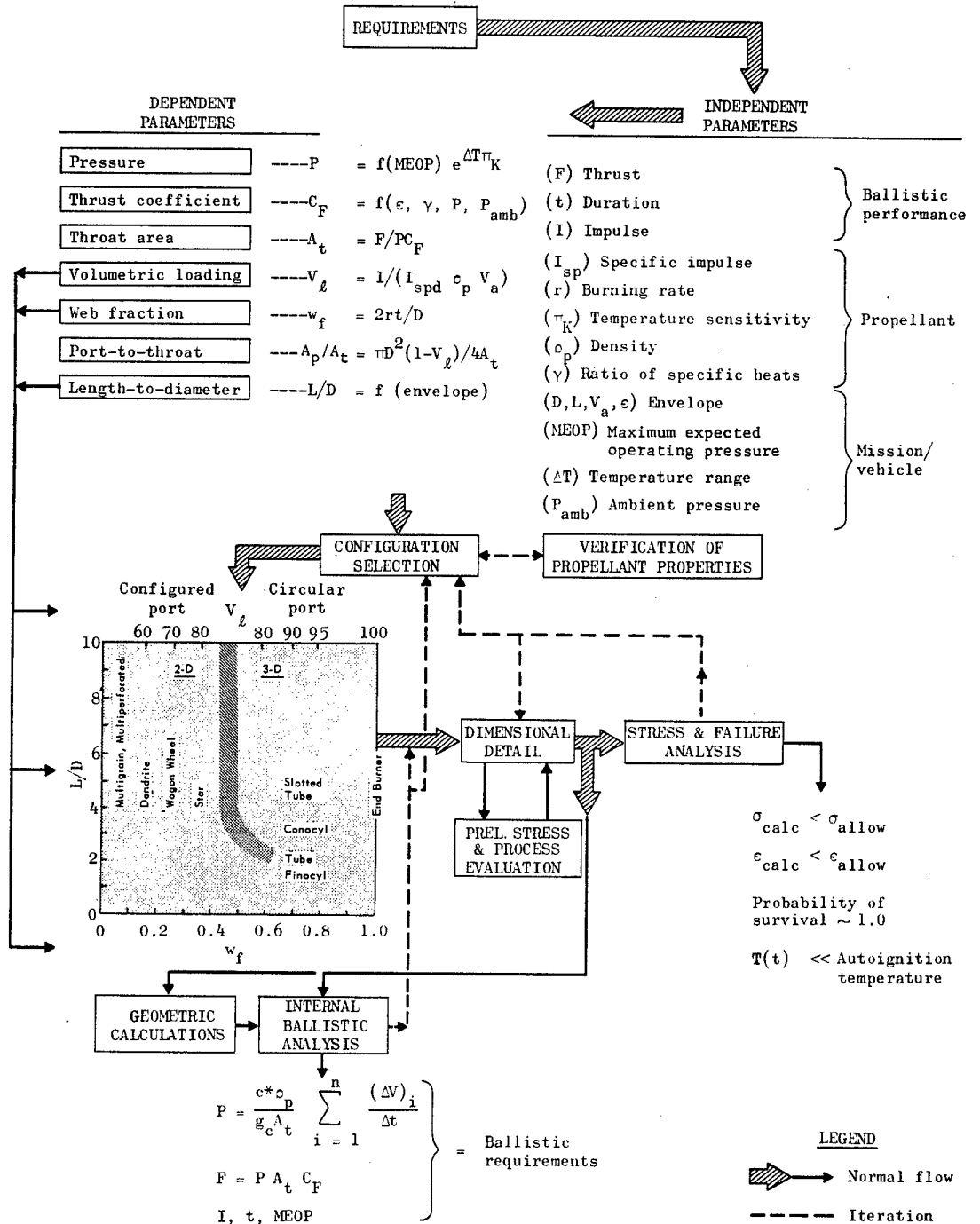


Figure 1.—Solid propellant grain design sequence.

2.1 Evaluation of Parameters

The prime objective of the solid propellant grain designer is to provide the rocket motor with a propellant grain that will evolve combustion products consistent with the thrust-time schedule required for the mission. Thus, ballistic parameters deduced from thrust-time performance stipulated for the rocket motor are the primary requirements imposed on the grain design. These requirements provide the basis for establishing quantities applicable to the grain design parameters.

The parameters fall into two categories: (1) independent parameters and (2) dependent parameters. Recognition of this distinction prevents conflicting requirements and provides the grain designer with the maximum degree of freedom permitted by the design problem. For example, average pressure, a dependent parameter, cannot be established without regard for the maximum expected operating pressure and propellant temperature sensitivity, both of which are independent (fig. 1).

Grain design is not accomplished independently of system analysis and inert components design. There is a necessary interaction between the grain design and other design areas with which the grain interfaces. For example, burnout velocity may be a stipulated requirement in lieu of total impulse. In this case, total impulse would be an implicit requirement necessitating feedback to system analysis and further design iteration. Nevertheless, grain design is a loop within the total motor design procedure, although the loop may not always be continuous as presented herein.

Compatibility of the igniter and grain is a requirement commonly imposed on the igniter design rather than on the grain design (ref. 6). Although the igniter normally can be accommodated in the internal free volume of the propellant grain without significant alteration of the adjacent grain perforation, there are instances in which the total motor design benefits from early consideration of igniter requirements in the grain design.

2.1.1 Independent Parameters

Requirements and constraints that are specified to the grain designer without regard to the grain configuration are defined herein as independent parameters. These parameters include ballistic performance characteristics, propellant properties, and mission- and vehicle-related requirements. Within the boundaries of the grain design process as charted in figure 1, they are independent parameters, for they define the values that constitute the basis for selection of the grain geometry. Typically, they originate from the specification for motor performance and optimization studies performed before the grain design process begins.

2.1.1.1 Ballistic Performance

Performance requirements that satisfy the mission objectives are given in terms of impulse and time or thrust level, frequently with a limiting value of instantaneous thrust, acceleration, or maximum dynamic pressure. When considering these requirements, one must recognize that impulse, time, and thrust level cannot all be specified independently. Therefore, typical specifications will include impulse and one of the three parameters: average thrust, burning duration, or impulse-time limit.

Definitions of ballistic performance parameters are related to the thrust- and pressure-time curves for the motor (fig. 2). Averages are defined in terms of time intervals on either the thrust- or pressure-time curve. The two common intervals are burning time t_b and action time t_a .¹ Burning time is well established as the interval from 10-percent maximum thrust (or pressure) to web burnout, usually taken as the aft tangent-bisector point (fig. 2). Action time typically is the time interval from initial to final 10-percent maximum thrust (or pressure). However, action time may be defined as the interval between specific pressure or thrust values or in terms based on other references. Definitions customarily specified and used in the industry are given in reference 7.

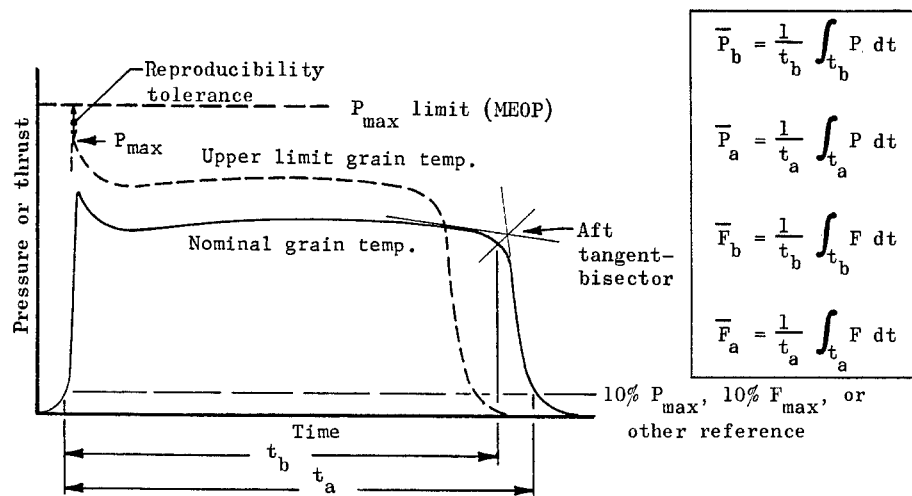


Figure 2.—Definition of ballistic performance parameters.

Burning time is always less than action time. The two may differ by only 2 percent or less for a sliverless design with insignificant erosive burning. The same sliverless design, however, with significant erosive burning likely will have an action time significantly greater (5 percent or more) than burning time. Sliver tends to increase the difference even more, the amount depending on the sliver content.

¹Symbols and terms are defined in the Glossary.

Frequently, a requirement limiting the maximum thrust of the motor is imposed; this limitation may be given in terms of an absolute maximum force permitted by the structure or it may be specified as maximum acceleration or maximum dynamic pressure. A shape of the thrust-time curve may be implied, and a non-neutral, regressive trace that limits terminal acceleration is not uncommon.

2.1.1.2 Propellant Properties

The specification of burning rate, specific impulse, and density, with due regard for the required propellant mechanical properties, often dictates the applicable propellant formulations. Although ballistic properties of the propellant usually are dominant in propellant selection, the processibility of the propellant and properties required for structural integrity of the grain also influence the choice of propellant formulation. Exhaust products may be of concern and hence may influence propellant selection if flame impingement, exhaust plume, or microwave attenuation is a predominant consideration.

This monograph considers that propellant properties are specified and therefore included in the category of independent requirements. In practice propellant selection commonly is accomplished in conjunction with configuration selection and grain design. (Details of propellant selection are provided in reference 8). Web fraction, for example, frequently is taken as an independent variable, and the required burning rate is determined therefrom. Furthermore, burning rate has been shown to have a slight dependence on the given thrust and duration in terms of the ratio F/t^2 without regard to motor size or other considerations (ref. 9). However, it will be assumed that propellant properties, including a burning rate range that encompasses a value suitable for an acceptable web fraction, are specified.

2.1.1.2.1 Specific Impulse

Specific impulse I_{sp} is a measure of the impulse or momentum change that can be produced per unit mass of propellant consumed. In terms of grain design, I_{sp} is the ratio of motor thrust to mass flowrate, and hence its value is most significant in the determination of propellant weight necessary to meet the ballistic requirements. Specific impulse frequently is defined in general terms¹ as

$$\begin{aligned} I_{sp} &= \frac{c^* C_F}{g_c} \\ &= \frac{C_F}{C_D} \end{aligned} \quad (1)$$

¹Alternate forms of an equation here and elsewhere in the monograph give the expression for a parameter in the form appropriate to the unit system involved, i.e. customary engineering units or SI units, as shown.

where

I_{sp} = propellant specific impulse, lbf-sec/lbm or N-sec/kg

c^* = characteristic exhaust velocity, ft/sec

C_F = nozzle thrust coefficient, dimensionless

g_c = gravitational conversion constant, 32.17 lbf-ft/lbf-sec²

C_D = discharge coefficient, kg/(N-sec)

The characteristic exhaust velocity is a function of the propellant combustion process; c^* is proportional to $\sqrt{T_c/\bar{M}}$, where T_c is the propellant flame temperature and \bar{M} is the average molecular weight of the gas, and therefore has a slight dependence on chamber pressure. Actual c^* and I_{sp} delivered in the motor are less than theoretical values by a significant amount. The reductions in values are the result of (1) fluid flow losses including two-phase flow in which particles fail to achieve kinetic and thermal equilibrium, (2) heat losses to motor hardware, and (3) combustion inefficiency. Those losses occurring upstream of the nozzle throat plane are inherent in the delivered c^* , and the total value of these losses is indicated in a factor η_θ defined as the c^* efficiency factor. Performance losses in the nozzle are expressed by λ (correction factor for nozzle divergence loss calculated as shown in sec. 2.1.2.2) and η_F (nozzle efficiency factor experimentally determined and usually in the range 0.96 to 0.99).

An accurate estimate of delivered specific impulse in the motor is obtained from the expression

$$I_{spd} = \eta_\mu I_{spd}^o \quad (2)$$

where

I_{spd} = measured (delivered) propellant specific impulse, lbf-sec/lbm (N-sec/kg)

η_μ = deliverable motor efficiency ($\approx \eta_\theta \eta_F$)

I_{spd}^o = theoretical delivered propellant specific impulse, lbf-sec/lbm (N-sec/kg)

This estimate requires calculation of theoretical I_{sp} at motor operating conditions. Frequently the I_{spd} is a value corrected from the standard deliverable specific

impulse I_{sp_s} , a value of I_{sp} delivered at 1000 psia (6.895 MN/m²) at sea level with an optimum nozzle having no divergence loss ($\alpha = 0$). The I_{sp_s} is related to the standard theoretical specific impulse $I_{sp_s}^o$, the value of theoretical I_{sp} at the same conditions given for I_{sp_s} , by an expression equivalent to equation (2). The correction of I_{sp_s} to I_{sp_d} is based on equation (1) and requires values of C_F and c^* at standard conditions of I_{sp_s} and motor conditions of I_{sp_d} .

For metallized propellants, the magnitude of η_μ varies directly with motor size and with mass flowrate (ref. 10). Further, metal oxides tend to decrease I_{sp} efficiency, and the variation of η_μ with aluminum content is less in large motors than in small ones. In general, the optimum I_{sp_s} occurs at an aluminum content of 10 to 16 percent for small motors (less than 20 in. [50.8 cm] in diameter) and at an aluminum content of 20 to 21 percent for much larger motors. The value of η_μ varies from 0.93 or less in small motors to approximately 0.96 in large motors.

In some designs, a short residence time of metal particles and gases within the combustion chamber results in significant losses in I_{sp_d} . Residence time varies with the characteristic length L^* (ratio of the instantaneous free volume of the combustion chamber to the nozzle throat area V_c/A_t), and this relation provides a geometric measure of the I_{sp_d} losses. Specific impulse efficiency decreases as residence time decreases; for typical propellants η_μ commences to drop sharply at a residence time of approximately 10 msec (ref. 8) or L^* of 160 in. (4.06 m) (ref. 10). During the early phases of burning, when L^* is below this value, I_{sp_d} may vary by 5 percent or more because of the less efficient combustion.

2.1.1.2.2 Burning Rate

The rate at which a propellant burns usually is described by a reference value at a specific pressure (usually 1000 psia [6.895 MN/m²]). With appropriate constants, the burning rate can be represented by an analytical expression that defines burning rate as a function of pressure at a given grain conditioned temperature. Additional constants termed "temperature-sensitivity coefficients" are required to define burning-rate values at other grain temperatures. Values for these coefficients are derived from the results of tests of 2- to 6-in. (5.08- to 15.24-cm) diameter subscale motors.

Actual burning rate in the motor is subject to the effects of erosive burning (sec. 2.3.2); consequently, burning rate is one of the most difficult internal ballistic variables to evaluate. Knowing exactly the burning rate at each station along the grain length, one could predict precisely (within a percent or so) the pressure and thrust as a function of time. Frequently the difference between estimated and actual performance can be attributed largely to the difference between estimated and actual burning rate.

2.1.1.2.2.1 Pressure Sensitivity

The rate of heat transfer from flame to propellant usually responds to the magnitude of local static pressure. Burning rate responds to this change in heat-transfer rate, thereby providing the basis for equating burning rate to a function of pressure. Over specific intervals of pressure, when pressure is the only significant variable, a log/log plot of burning rate versus pressure at a given temperature frequently approximates a straight line, particularly for composite propellants. In this case the analytical expression most frequently used in the industry to describe burning rate (ref. 11) and the one preferred by most propellant investigators (ref. 12, p. 92) is de Saint Robert's burning-rate law

$$r = aP_c^n \quad (3)$$

where

r = propellant burning rate, in./sec (m/sec)

a = coefficient of pressure

P_c = chamber pressure, lbf/in.² (N/m²)

n = pressure exponent

This empirical expression defines the burning rate of the propellant; values for a and n usually are derived from data obtained with subscale burning-rate motors 2 to 6 inches (5.08 to 15.24 cm) in diameter.

Other notable expressions for burning rate include

$$\frac{1}{r} = \frac{a}{P_c} + \frac{b}{(P_c)^{1/3}} \quad (\text{ref. 13}) \quad (4)$$

and

$$r = a + bP_c \quad (\text{ref. 14}) \quad (5)$$

where a and b are constants as applicable. Some propellants have burning-rate characteristics that require more than one straight line segment; these propellants are called plateau- and mesa-burning propellants (ref. 15).

The grain designer must know the burning-rate properties and permissible range for burning-rate adjustment appropriate for the selected propellant. Further, burning rate typically scales upward in the full-scale motor, from 1 to 5 percent (refs. 16 and 17).

Occasionally, however, there is a one-to-one correspondence between subscale and reference (non-erosive) full-scale burning rates. Scale factors usually are applied to burning rates obtained from a subscale motor. Burning rates of uncured propellant strands generally are used only for process control. However, a substantial method for correlating strand burning rates with motor burning rates is shown in reference 18; variables correlated are ratios of pressure to burning rate for the uncured propellant strand and for the motor.

2.1.1.2.2.2 Temperature Sensitivity

Motor burning rate and operating pressure are dependent on the conditioned temperature of the propellant grain T_i . The sensitivity of motor ballistics to grain temperature is characterized by various propellant temperature-sensitivity coefficients. Each coefficient is defined in terms of a proportionality constant in a specific partial differential equation. The coefficients customarily used in ballistic analysis are (refs. 7 and 15)

$$\begin{array}{l} \text{Temperature sensitivity of} \\ \text{pressure at a particular} \\ \text{value of } K_n, \%/\text{°F } (\%/K) \end{array} \quad \pi_K = \left[\frac{\partial \ln P}{\partial T_i} \right]_{K_n} \quad (6)$$

$$\begin{array}{l} \text{Temperature sensitivity of} \\ \text{burning rate at a partic-} \\ \text{ular value of } P, \%/\text{°F } (\%/K) \end{array} \quad \sigma_P = \left[\frac{\partial \ln r}{\partial T_i} \right]_P \quad (7)$$

$$\begin{array}{l} \text{Temperature sensitivity of} \\ \text{burning rate at a partic-} \\ \text{ular value of } K_n, \%/\text{°F } (\%/K) \end{array} \quad \sigma_K = \left[\frac{\partial \ln r}{\partial T_i} \right]_{K_n} \quad (8)$$

$$\begin{array}{l} \text{Temperature sensitivity of} \\ \text{pressure at a particular} \\ \text{value of } P/r, \%/\text{°F } (\%/K) \end{array} \quad \pi_{P/r} = \left[\frac{\partial \ln P}{\partial T_i} \right]_{P/r} \quad (9)$$

where

K_n = burning surface-to-throat area ratio, A_b/A_t

T_i = grain conditioned temperature, °F (K)

A_b = area of propellant burning surface, in.² (m²)

A_t = flow area at nozzle throat, in.² (m²)

Subscripts to the bracketed terms indicate the constant conditions shown in figure 3 with specific variables applicable to each of the coefficients.

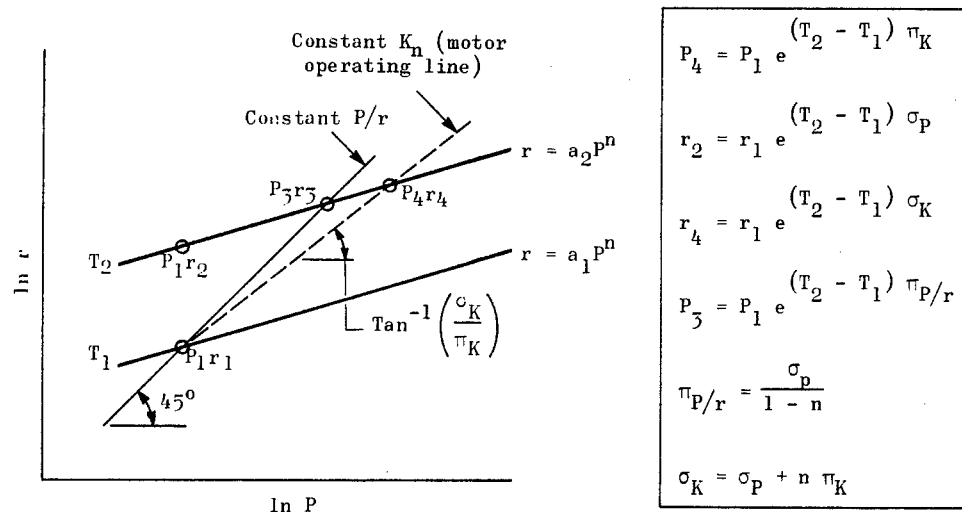


Figure 3.—Relationships among temperature-sensitivity coefficients.

Constants σ_P and $\pi_{P/r}$ are properties of the propellant independent of motor design. They are related by the pressure exponent n as indicated in figure 3. Constants π_K and σ_K reflect not only the sensitivity of burning rate to T_i , but also the variation of c^* with T_i , primarily, and with other variables related to the motor design. Hence, π_K and σ_K characterize the temperature sensitivity of the overall motor, whereas σ_P and $\pi_{P/r}$ characterize the temperature sensitivity of the propellant only.

The values of σ_K , σ_P , and $\pi_{P/r}$ derived from motor test data depend on assumed variability of web with grain temperature. In practice, K_n usually is considered constant, and burning rate at each temperature T_i is calculated on the basis of a constant web. Under these conditions, when P/r is constant as T_i varies, the pressure-time integral likewise is constant. Pressure and rate variations with temperature are then determined with $\pi_{P/r}$, and the motor operating line when plotted on logarithmic coordinates will have a constant slope of 1.0. If the motor operates at a higher grain temperature ($T_i = T_2$) with the same reference burning rate but with variables such as c^* inducing a higher pressure, the pressure-time integral and P/r are greater. Percentage increase in pressure will be greater than the percentage increase in burning rate, and π_K will be greater than σ_K . The motor operating line on logarithmic coordinates again is a straight line, but with a slope of σ_K/π_K .

When the constant conditions noted in figure 3 are not restricted to a specific value of pressure P_1 at T_1 or to a reference pressure at T_2 , definitions of the four temperature-sensitivity coefficients (eqs. (6) through (9)) assume that the pressure exponent

n does not vary with temperature and pressure. Frequently, however, n may vary slightly with temperature and pressure; many propellants in fact do not have the constant-slope property depicted in figure 3 (refs. 11, 19, and 20). When n at T_2 is significantly different from n at T_1 , values for all the coefficients depend on the reference pressure. If the slope of the burning-rate/pressure curve at a given temperature changes in the range of operating pressure (i.e., within the range P_1 to P_4 in fig. 3), the relationships among n and the temperature-sensitivity coefficients given in figure 3 may not be valid.

2.1.1.2.3 Density

When propellant weight is not limited in a volume-limited system, the product of propellant density and specific impulse becomes the important factor in determining volumetric loading fraction. Propellant density is calculated from the density of the ingredients, due account being given to chemical reactions during mixing and residual material from volatile solvents. These factors usually do not affect the calculations significantly. Calculated density is one of the most dependable of the propellant parameters and essentially coincides with measured values. In composite propellants, variations greater than 1 percent may indicate problems such as voids and fissures.

Application of density to determination of propellant weight requirements and subsequent ballistic analysis is straightforward. It is important, however, to associate a given density with a specific grain temperature. Volumetric change in the propellant grain from the uncured high temperature state to cured ambient conditions (normally 77°F [298K]) usually produces a density increase of 1.0 to 1.5 percent, depending on thermal expansion properties of the specific grain configuration. Neglect of this increase in dimensioning the casting mandrel can result in a deficiency in propellant weight of the same magnitude. Furthermore, the decrease in port-to-throat area ratio at the upper temperature limit may have a significant effect on erosive burning and initial chamber pressure.

2.1.1.3 Mission- and Vehicle-Related Constraints

Certain requirements imposed on the grain design depend directly on related vehicle and motor dimensions. The overall envelope allotted the grain and the constraints on nozzle length and exit diameter usually are specified independently of ballistic performance and propellant requirements (within the context of grain design); in some cases, however, the results from grain design may feed back into mission analysis, where the envelope and nozzle dimensions are reevaluated. Maximum expected operating pressure MEOP is the basis for motor operating pressure; MEOP usually is derived from preliminary systems analysis, where it is optimized with respect to ideal velocity increment, motor weight, total impulse, or some other figure of merit. Further, the mission of the vehicle often produces environmental requirements that may influence the grain design.

2.1.1.3.1 Envelope

The allowable envelope defining the physical boundaries for the grain is a fundamental constraint on the grain geometry. Total volume available and its shape in terms of length-to-diameter ratio provide a basis for selecting the configuration type and also define the limit on maximum grain weight achievable.

Required dimensions for the envelope are total length, inside diameter of the insulated case, and definition of volume in the end closures available for propellant. In practice, a trade-off frequently exists between configuration types and required amount of liner, where the regressive elements of the configuration expose the chamber wall to gas flow. In such cases the grain outer diameter might depend on configuration characteristics and would not be a fixed independent dimension.

The vehicle envelope may further impose a limit on the nozzle exit diameter. This constraint prevents the nozzle expansion ratio from being selected independently. In this event, the expansion ratio is implicit in determination of nozzle throat area.

2.1.1.3.2 Maximum Expected Operating Pressure

In most grain design efforts, a limit on maximum pressure (MEOP) has been established at the time grain design activity commences. Concurrent with grain design, the motor case and other components are being designed and analyzed for conformance with the MEOP. Therefore, the grain designer must respect MEOP as an independent requirement and perform whatever design iterations are necessary to provide predicted performance within the limitations of the MEOP. Costly delays may result when the operating pressure is established without due consideration of the expected pressure-time neutrality and resultant MEOP.

2.1.1.3.3 Use Environment

Many environmental conditions may be imposed on the rocket motor, and often the motor cannot be protected from environmental extremes without resorting to complicated and costly measures. Some of the environmental conditions have a significant effect on the ballistic and structural performance of the propellant grain and must be considered carefully in all phases of the grain design analysis.

Operating temperature range, altitude, vibration, temperature cycling, rough handling, aerodynamic heating, and spin are typical environments that must be given special consideration. If a motor will be subject to severe vibration, applicable grain configurations are limited; those with relatively large portions of unsupported mass (e.g., the wagon wheel) may be excluded. Requirements for temperature cycling frequently result in grain dimensions that reflect a compromise between ballistic and structural interests.

Aerodynamic heating and acceleration, principally spin, likewise may influence the burning rate and therefore have significant effect on motor performance. These influences on burning rate are particularly significant in the evaluation of maximum pressure, burning duration, and thrust level.

Environments such as rain, dust, salt spray, etc. have little if any influence on the grain design. Motors subject to exposure to these environments usually are fitted with environmental seals to preclude problems.

2.1.2 Dependent Parameters

The grain design parameters herein termed "dependent parameters" include those grain design attributes that are dependent on the parameters given in section 2.1.1 and that must be evaluated before grain configuration or analysis is considered. The dependent parameters are average operating pressure, nozzle throat area and thrust coefficient, volumetric loading fraction, web fraction, port-to-throat area ratio, and length-to-diameter ratio. Quantitative independent consideration of these variables can result in conflicting requirements and may weaken the analytical base for the grain design.

2.1.2.1 Average Operating Pressure

Typical preliminary optimization studies consider average operating pressure on a preliminary basis in establishing an MEOP for the motor. Also, preliminary consideration is given to expected pressure-time neutrality to relate MEOP and average pressure. When the grain design is to be considered in detail, however, the MEOP customarily is specified; and average pressure is estimated therefrom. An estimate of the pressure is made for the primary purpose of determining a nozzle throat area, propellant weight for initial grain dimensions, and burning rate for web fraction.

Quantities considered for nozzle throat area, specific impulse, and web fraction depend on average pressure over particular intervals of time. The value applicable to specific impulse determination usually is the average over the action-time interval. Average pressure applicable to the throat area (sec. 2.1.2.2) applies to the same interval as that for average thrust, which may not be over action time. Web fraction is based on the burning rate corresponding to the burning-time interval.

Relationships between MEOP and average pressure values are illustrated in figure 2. Equations in figure 3 define the variation of corresponding average pressure with respect to temperature. Relating MEOP, average pressure over burning time \bar{P}_b , and average pressure over action time \bar{P}_a at a given temperature prior to analysis of the grain design, however, requires an estimate with little analytical basis. Until the performance of a particular grain design is predicted, the pressure neutrality and initial pressure overshoot (frequently

maximum pressure) can only be estimated, either by comparison with similar motors or by intuitive judgement.

2.1.2.2 Nozzle Throat Area and Expansion Ratio

The flow area at the nozzle throat A_t is the predominant nozzle parameter. It is evaluated in conjunction with the variables associated with thrust coefficient: expansion ratio, exit diameter, ambient pressure, chamber pressure, and nozzle inefficiencies. Proper treatment of these variables is necessary for accurate grain design.

The ideal thrust coefficient C_F° is defined (ref. 21, p. 54; ref. 22, p. 101) by

$$C_F^\circ = \sqrt{\frac{2\gamma^2}{\gamma-1} \left(\frac{2}{\gamma+1}\right)^{\frac{\gamma+1}{\gamma-1}} \left[1 - \left(\frac{P_e}{P_c}\right)^{\frac{\gamma-1}{\gamma}}\right]} + \left(\frac{P_e - P_{amb}}{P_c}\right) \epsilon \quad (10)$$

where

C_F° = ideal thrust coefficient

$\gamma = \frac{\text{specific heat at constant pressure}}{\text{specific heat at constant volume}}$

P_e = exit plane pressure, lbf/in.² (N/m²)

P_{amb} = ambient barometric pressure, lbf/in.² (N/m²)

ϵ = nozzle area expansion ratio, A_e/A_t

A_e = flow area at nozzle exit plane, in.² (m²)

The ideal thrust coefficient in a vacuum $C_{F,vac}^\circ$ ($P_{amb} = 0$) is a function only of ϵ and γ , and it is convenient to consider the actual thrust coefficient $C_{F,act}$ in terms of $C_{F,vac}^\circ$. The factors λ and η_F are applied to the momentum term in the expression for ideal thrust coefficient (ref. 23, p. 88) to obtain the actual thrust coefficient $C_{F,act}$ by

$$C_{F,act} = \lambda \eta_F \left(C_{F,vac}^\circ - \frac{P_e}{P_c} \epsilon \right) + \left(\frac{P_e - P_{amb}}{P_c} \right) \epsilon \quad (11)$$

where

$C_{F,act}$ = actual thrust coefficient reflecting all nozzle losses

$C_{F,vac}^o$ = ideal thrust coefficient in vacuum

λ = nozzle divergence correction factor

$\eta_F = C_F$ efficiency factor

For a conical nozzle, λ is defined by

$$\lambda = \frac{1}{2}(1 + \cos a) \quad (12)$$

where

a = nozzle divergence half angle, deg

Frequently the nozzle exit cone is contoured to reduce divergence losses for expansion of gases within the same length of nozzle. Both the contour configuration and λ usually are based on a method-of-characteristics flow analysis. For a contoured nozzle, an approximate value of λ is (ref. 10)

$$\lambda = \frac{1}{2} \left[1 + \cos \left(\frac{a + \theta_{ex}}{2} \right) \right] \quad (13)$$

where a and θ_{ex} are defined as shown in figure 4.

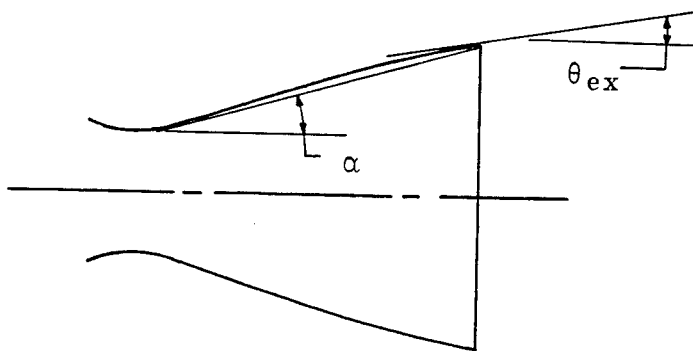


Figure 4.—Nozzle divergence angles.

A widely used equation for thrust (ref. 24) contains the expression for $C_{F,act}$ in equation (11). Applying also the nozzle efficiency factor, thrust typically is defined by

$$\begin{aligned} F &= \lambda \eta_F (P_c A_t C_{F,vac}^\circ - P_e A_e) + (P_e - P_{amb}) A_e \\ &= P_c A_t C_{F,act} \end{aligned} \quad (14)$$

where

$$F = \text{thrust, lbf (N)}$$

When A_e is stipulated as a constant or is limited to a maximum value by the envelope constraints, A_t is the only unknown. The equation must be solved by iteration, however, as ϵ and therefore $C_{F,vac}^\circ$ depend on A_t . When A_e is not limited, ϵ may be chosen independently and equation (14) can be solved explicitly for A_t . The expansion ratio ϵ usually is chosen to provide maximum performance to the system. Although the maximum C_F for non-vacuum conditions occurs when $P_e = P_{amb}$ (ref. 21, pp. 57 to 59), the optimum value for ϵ frequently depends on the effect of ϵ on motor size and weight. The optimum ϵ for a motor having a submerged nozzle depends on a tradeoff among available propellant volume, degree of submergence, nozzle weight, and related flow losses.

It has been shown that the exit pressure and velocity under assumption of point-source flow should correspond to expansion of gas to the spherical area, which is somewhat larger than the area at the nozzle exit plane on which ϵ is based (ref. 25). Failure to account for this difference results in a small error, acknowledged to be negligible in the range of expansion ratios usually of interest. Additional comments on minor inaccuracies due to throat-area assumption are given in reference 24.

2.1.2.3 Volumetric Loading Fraction

In grain design, volumetric loading fraction V_ℓ is defined as the fraction of available chamber volume required for propellant. The available chamber volume is defined to be the volume within the boundaries of the insulated case, including the heads. Although V_ℓ is usually evaluated in terms of the two-dimensional cross-sectional loading fraction, it may be expressed equally well in terms of performance and propellant requirements; thus

$$V_\ell = \frac{V_p}{V_a} = \frac{I_{tot}}{I_{sp} \rho_p V_a} \quad (15)$$

where

$$V_\ell = \text{volumetric loading fraction}$$

V_p = propellant volume (W_p/ρ_p), in.³ (m³)

V_a = chamber volume available for propellant, in.³ (m³)

I_{tot} = total impulse ($W_p \cdot I_{sp}d$), lbf-sec (N-sec)

W_p = propellant weight, lbm (kg)

ρ_p = propellant mass density, lbm/in.³ (kg/m³)

Burning neutrality limits the application of each grain configuration to a specific range of values for V_ℓ , as is illustrated in figure 1. Required V_ℓ therefore will have a significant bearing on selection of a suitable grain configuration.

2.1.2.4 Web Fraction

Web fraction w_f (the ratio of web to grain outer radius) is one of the most significant parameters influencing the selection of configuration type. The range of applicable web fractions depends on the range of available propellant burning rates. Burning rate and duration define the required w_f for internal-burning grains from the equation

$$w_f = \frac{2rt_b}{D} \quad (16)$$

where

w_f = web fraction (ratio of web to grain outer radius, frequently written $(D-d)/D$ after d has been determined)

t_b = burning time, sec

D = outside diameter of grain, in. (m)

d = inside diameter of grain, in. (m)

2.1.2.5 Port-to-Throat Area Ratio

Average initial cross-sectional area of the flow channel (port area A_p) is dependent on volumetric loading requirements and envelope constraints as shown in the expression

$$A_p = \frac{\pi}{4} D^2 (1 - V_\ell) \quad (17a)$$

For strictly two-dimensional grain configurations in which end configurations are insignificant, port-to-throat area ratio A_p/A_t is approximated by

$$\frac{A_p}{A_t} = \frac{\pi D^2 (1 - V_\ell)}{4A_t} \quad (17b)$$

where

$$\frac{A_p}{A_t} = \text{port-to-throat area ratio (the symbol } 1/J \text{ is also used)}$$

$$A_p = \text{flow area at grain port, in.}^2 \text{ (m}^2\text{)}$$

Gas velocity along the flow channel is influenced significantly by the magnitude of A_p/A_t . The limit of A_p/A_t at the aft end for choked flow at the nozzle is 1.0 when the port area equals the throat area. The practical limit generally is greater than 1.0, although the ratio less than 1.0 could be considered, depending on other variables discussed in section 2.3. Frequently the port area in the forward portion of the grain is equal to or less than the nozzle throat area. This relationship is typical of (1) the slotted tube in which slots are aft, (2) ports that have been tapered to minimize erosive burning, and (3) boost-sustain configurations. A typical configuration with $A_p/A_t < 1$ is an internal-burning tube having a small diameter and a large length-to-diameter ratio (ref. 26, units 370 and 371). Motors with high thrust levels and short durations frequently have a throat area that is a sizable fraction of the chamber cross-sectional area. Requirements for such motors may result in port-to-throat area ratios that approach 1.0 at some point in the flow channel.

The criticality of the port-to-throat area ratio at a particular station in the grain depends on the mass flowrate at that station. Thus, the port can be tapered to maximize volumetric loading fraction. Tapering or coning (ref. 27) of the flow channel at the aft end is a method whereby designs already committed to tooling can be modified to increase the effective port-to-throat area ratio.

The port-to-throat area ratio provides an index from which both pressure drop and erosive burning tendencies can be established, thus generally dictating the lower practical limit for a ported grain as well as indicating the depth of analysis advisable before release of design to manufacturing. Very low values for A_p/A_t , including $A_p/A_t \leq 1.0$, can be accommodated by proper provision in the design (e.g., a relatively small initial burning surface or a structure adequate for a significantly large initial pressure peak). However, when

reasonably neutral-burning grains are considered for neutral pressure-time performance, the port-to-throat area ratio becomes a significant limitation. The allowable ratio depends on the configuration complexity, reference value of burning rate, and operating pressure. When the burning rate is relatively high ($r > 0.5$ in./sec [12.7 mm/sec]) and the port is circular, $A_p/A_t < 2.0$ usually can be accommodated. Erosive burning and hence initial pressure peaks for a given port-to-throat area ratio become more severe when the complexity of the configuration increases and burning rate decreases. Thus, port-to-throat area ratios greater than 2.0 and even up to 3.0 or more may be a limitation for highly configured grains with low burning rates ($r < 0.30$ in./sec [7.62 mm/sec]). A measure of configuration complexity is (ref. 28)

$$X = \frac{Q^2}{4\pi A_p} \quad (18)$$

where

X = configuration factor

Q = burning perimeter of grain, in. (m)

The value of X is 1.0 for a circular port and greater than 1.0 for a non-circular port.

In certain grain designs, gas dynamic effects cause the effective port-to-throat area ratio to be less than the geometric value. In grain designs having circumferential slots in the vicinity of the aft end, mass flow from the burning surface within the slots is added to the primary flow at right angles. An aerodynamic restriction occurs in the flow channel at the location of the slot, and its effect may be sufficiently large to create a substantial static pressure drop across the slot. The resultant forces acting on the grain tend to induce an inward deflection of the propellant downstream of the slot. This coupling between the aerodynamically induced pressure drop across the slot and the propellant deformation subjects the motor to a failure mode (ref. 29).

2.1.2.6 Length-to-Diameter Ratio

The ratio of grain length to diameter L/D is derived from the envelope dimensions stipulated in the independent requirements. This parameter is significant in three important aspects of grain design and analysis:

- (1) The significance of end effects in burning geometry increases as L/D decreases. Thus L/D is a significant parameter in selection of a grain configuration for neutral-burning requirements. The dependence of grain configuration on L/D is evident in the region of three-dimensional configurations in the graph in figure 1.

- (2) Erosive burning, sensitive also to other factors, tends to be greater in motors with large L/D.
- (3) High L/D values may increase the tendency for combustion instability to occur.

2.2 Configuration Selection and Design

A reasonably methodic procedure usually is followed in selecting and designing the specific grain geometry. Limitations imposed by processing capability and cost constraints restrict the characteristic shape of a solid propellant grain to specific configuration types having exact geometric definition. Propellant burning rate jointly with motor performance requirements further reduces the number of configuration types relevant to a particular application. Thus, there have evolved certain principles that govern the selection of a suitable configuration type. Grain design encompasses configuration selection based on these principles and subsequent analysis that provides dimensional detail to the satisfaction of all requirements.

2.2.1 Principles Governing Selection

2.2.1.1 Ballistic Constraints

The dependent parameters (sec. 2.1.2) characterize the significant ballistic constraints on grain design. Specific values for these variables, particularly w_f , V_f , and L/D, indicate directly the applicable configuration types (fig. 1). The most significant variable is web fraction, which depends directly on the given propellant burning rate, duration requirement, and envelope. Volumetric loading fraction generally is limited by the web fraction. An iteration in propellant selection may be necessary to provide a propellant with burning rate high enough to accommodate a larger web fraction and loading fraction. The influence of length-to-diameter ratio on the gas dynamics, in particular erosive burning, may be a constraint limiting the geometric complexity of the grain cross section.

2.2.1.2 Processing Practicality

Flexibility in grain design is limited by processing techniques and rheological properties of the propellant. Without consideration of the state of technology related to manufacturing of solid motors, more elaborate grain designs would prevail. However, neglect of the processing requirements leaves the grain design subject to failure on the basis that (1) it simply cannot be fabricated with existing technology or (2) the cost of sophisticated tooling is prohibitive.

Perhaps the two most important areas that the grain designer must consider are mandrel removal techniques and provision for unrestricted end areas. Through advances in propellant

casting technology that have introduced collapsible and consumable mandrels, the finocyl and conocyl configurations have become commonplace in operational motors. Without these improved techniques, consideration of designs that required forward slots would be futile.

Further information on processing factors related to motor design can be found in reference 30.

2.2.1.3 Structural Integrity

Throughout the grain design, the grain designer must continually consider the structural integrity of the grain from fabrication through performance of the motor's mission. Structural failures can occur in any of four modes—cracking, debonding, excessive deformation, and autoignition. Cracking and debonding are the more prevalent types of structural failures leading to (1) abnormal burning geometry and potential malfunction from over pressurization, or (2) case structural failure from premature exposure of the case to excessive heat. Cracking can be caused by loadings from ignition pressurization, temperature changes, and acceleration (including vibrational). Geometric design considerations can minimize the tendency of the grain to crack by decreasing the regions of high stress concentration, by adding reinforcements or stress reducers where the high stresses cannot otherwise be avoided, and by giving proper attention to chemical and processing details that may degrade the structural properties. Excessive deformations may come from long-term creep or from the large body forces generated by high accelerations. The deformations may reduce port area or alter burning surface and significantly affect motor ballistics. Grain deformation under pressure may alter the geometric surface area, particularly in large motors with fiberglass cases, and thus become important to a precise ballistic calculation. Autoignition is likely to occur during vibration when the viscous nature of the propellant causes a temperature buildup due to internal heat generation.

Adequacy of the grain design is predicated on acceptable results from the stress analysis. The structural integrity of the grain is verified first on a preliminary basis when the configuration type has been selected (fig. 1). Predominant ballistic variables assessed at this point are web fraction and length-to-diameter ratio. Large values for either variable may require the use of circumferential slots, specific configuration of slot termination, or other stress-relief mechanisms in the grain design. Burning geometry usually is altered by these features, and provision must be made in the overall grain design to accommodate these effects. Subsequent dimensioning of the grain is accomplished in view of grain stress as well as ballistic performance requirements. Finally, acceptability of the complete grain design is dependent on final evaluation of structural integrity. Guidelines to the complete treatment of structural integrity are given in reference 31.

2.2.2 Geometric Definition and Analysis

2.2.2.1 Configuration Types

Thrust was defined in equation (14) as a function of pressure and nozzle variables. It may be expressed also by

$$F = \dot{m} I_{sp} d = A_b \rho_p r I_{sp} d \quad (19)$$

where

\dot{m} = propellant mass flowrate, lbm/sec (kg/sec)

The tradeoff between burning rate and propellant burning surface in grain design is evident in equation (19). This relation was the motivation for development of the current variety of grain configurations that makes available to the grain designer configuration types adaptable to a variety of burning rate—thrust combinations. For example, the requirement for high thrust-to-weight ratio that preceded the general availability of high burning rates (greater than 0.3 in./sec [7.62 mm/sec]) necessitated configurations with large burning surface, e.g., the dendrite and wagon wheel.

With respect to configuration selection, grain configurations are best classified according to their web-fraction capability. They are ordered in this section, however, to retain a continuity in geometric definition. Certain features of the star, for example, are contained in the wagon wheel, and elements of both the star and wagon wheel comprise the dendrite. Further, they are grouped according to the primary orientation of burning in the order of (1) the end burner, with burning only in the longitudinal direction, (2) radial-burning grains, frequently identified as two-dimensional grains, and (3) grains that burn both radially and longitudinally, frequently identified as three-dimensional grains.

With few exceptions, each grain configuration reported in the compilation of motor designs of reference 26 may be defined in terms of the variables of one of the configurations of this section. Some may appear to be still another unique configuration type. For example, the rayside of a star configuration (sec. 2.2.2.1.5) does not exist when $r_2 = Y^*$, and the grain may no longer have the appearance of a star configuration. It is still defined geometrically by the seven independent variables, however, and is by definition and function a star.

2.2.2.1.1 End Burner

The end-burning grain (fig. 5) is distinguished from all other configurations by the orientation of burning, which is totally in the longitudinal direction. Its burning surface is defined by the end area, with all other surfaces restricted. In its simplest form the end-burning grain is defined by two variables, length L and diameter D .

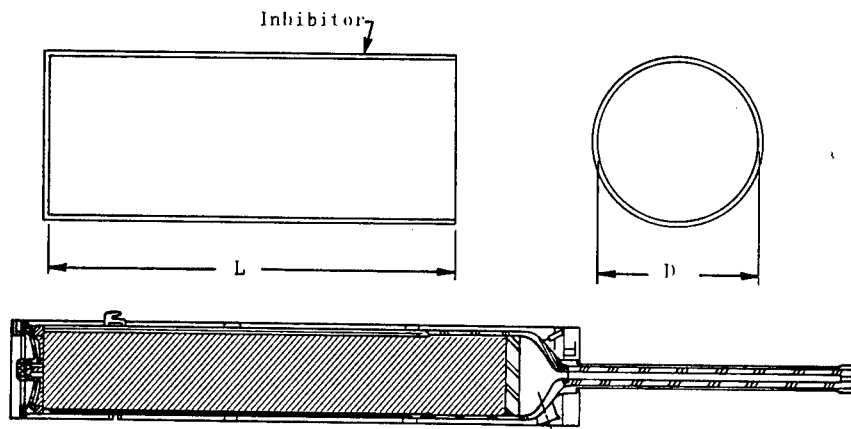


Figure 5.—End-burning configuration (ref. 26, unit 402).

The end-burning grain continuously exposes the chamber wall to hot gases; therefore, the motor case requires significantly more insulation than that required for internal-burning grains. This imposes an additional weight penalty on the motor from added insulation as well as a sacrifice in chamber volume available for propellant. Depending on motor diameter and firing duration, the case liner may displace 5 to 10 percent of the volume inside the case wall, the range indicating the penalty of reduced volume available for propellant that must be charged against the end burner. Even so, other configurations usually cannot compete with the end burner on the basis of total propellant volume achievable.

End burners typically are applicable to missions requiring relatively long durations and low thrust levels. Recent advancements in technology related to stress-relieving grain support and retention systems (ref. 32) have made the end-burning grains suitable for large-diameter motors. Upper limit on propellant burning rate, however, usually prohibits the use of end-burning grains for many applications, simply because the burning surface is not sufficient to provide the required mass flowrate (eq. (19)).

Ideally, burning surface of an end-burning grain is independent of web burned and is defined simply by the cross-sectional area of the grain. Factors that promote non-parallel regression of burning surfaces frequently become significant, however, and result in non-neutral pressure-time traces from an end-burning grain. Typical of these factors is a nonuniform burning rate at the propellant/liner interface that causes the surface to develop into a cone shape during operation (fig. 6). This coning results from heat transfer along the liner to propellant ahead of the flame front (backside heating [ref. 33]), from chemical migration between propellant and liner, or from concentration of fine particles at the interface. Propellant characteristics at the liner/propellant interface are known to be influenced by liner primer, proximity of insulating materials, and processing techniques (ref. 34).

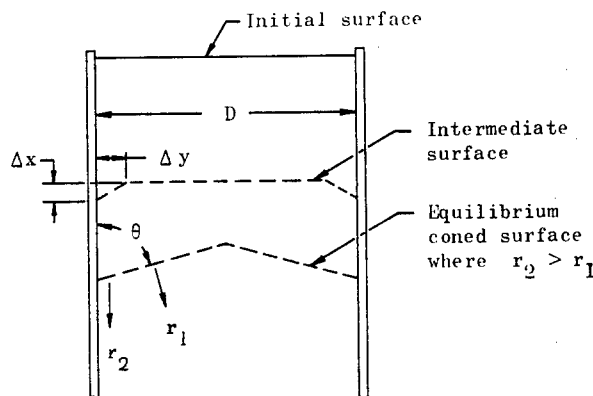


Figure 6.—Formation of equilibrium burning surface of an end-burning grain with nonuniform burning rate.

The burning rate r_1 (fig. 6) is the reference burning rate of the grain. Rate r_2 is the rate at the propellant/liner interface. Angle θ and thus burning surface are defined by the relative values of r_1 and r_2 . Intermediate surfaces depend on time and are based on the frustum of a cone defined by the values of Δx and Δy .

Several methods for achieving greater mass flowrates from end-burning grains have been proposed: (1) a higher-burning-rate strand coincident with the grain's longitudinal axis to promote a coned surface (ref. 35), (2) techniques described in reference 36, and (3) wires imbedded in the grain to induce an increase in burning rate by enhancing heat transfer. Practicality of these methods is limited by manufacturing complexity, dependence on relative burning-rate values, and uncertain reproducibility in providing the greater mass flowrate.

2.2.2.1.2 Internal-External-Burning Tube

The internal-external-burning tube (fig. 7, ref. 37) is a grain that burns radially both inward and outward. Neglecting end effects and structural facets for a tube with a relatively large L/D , the grain is neutral burning. It is defined simply by two diameters, D and d , and a length L , with the web w equal to half the grain thickness.

Cross-sectional volumetric loading fraction of the configuration in terms of web fraction is

$$V_l = w_f (1 - w_f) \frac{\pi D^2 L}{V_a} \quad (20)$$

where

L = grain length, in. (m)

Volumetric loading fraction depends on the web fraction and therefore cannot be considered independently of web requirement.

Chief ballistic advantages of the internal-external-burning tube are its neutral-burning characteristics and lack of sliver. In lieu of case bond, a support system is required to retain the grain within the chamber. The chamber wall is exposed continuously to combustion gases and thus requires additional liner. Typical support methods include retainer pads bonded to grain and case liner (ref. 38). Bonded interface of grain and retainer pad is restricted from burning and provides a progressive burning element to offset the regressive end element, thereby neutralizing burning when ends are unrestricted. This is a practical support method for propellants with low flame temperature.

A more elaborate support design is depicted in figure 7. The propellant is cast into a mold-and-mandrel assembly containing the grain support tube/molded cap/forward head assembly. The grain assembly is loaded into the motor case, where it is supported at the forward end and positioned by small support structures extending from the support tube through the propellant to the chamber wall. Predominant requirements influencing selection of the configuration in this application were aerodynamic heating and upper limit on thrust (ref. 37). The air gap between the grain and case insulation provided sufficient protection to the grain from aerodynamic heating and its effect on burning rate and maximum thrust.

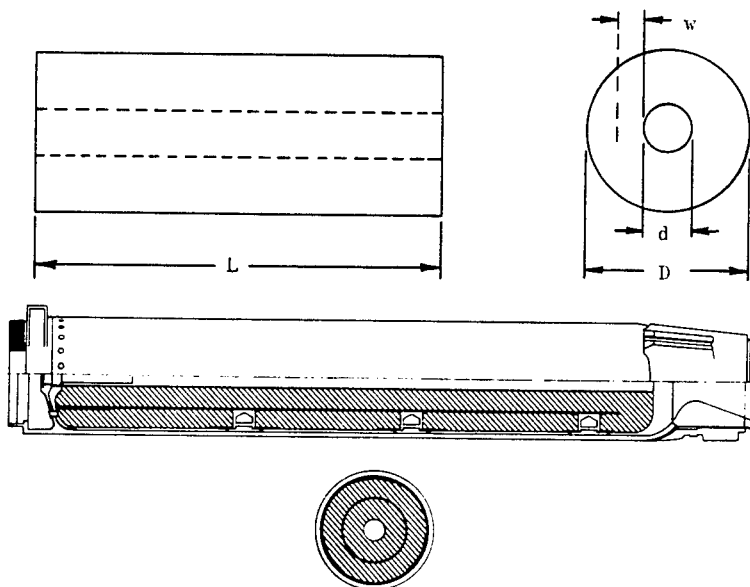


Figure 7.—Internal-external-burning tube configuration (ref. 37).

2.2.2.1.3 Internal-Burning Tube or Shell

The internal-burning tube (fig. 8) is one of the most practical and preferred configurations when web fraction and length-to-diameter ratio will permit its use. It is a radially burning grain with ends usually unrestricted to function as a burning-surface control; otherwise, it burns progressively. It is typically case bonded, which inhibits the outer surface. The internal-burning tube is defined by a length L and two diameters D and d .

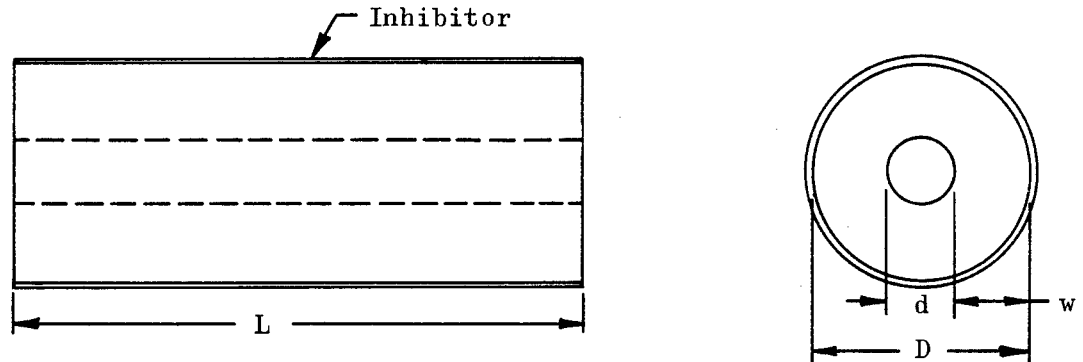


Figure 8.—Internal-burning tube or shell configuration.

Volumetric loading fraction is a function of the web fraction, i.e.,

$$V_L = w_f (2 - w_f) \quad (21)$$

Thus web fraction and loading fraction cannot be considered independently.

If required web fraction satisfies the loading fraction requirement and if length-to-diameter ratio is such that the required degree of neutrality is obtained, the tube with its inherent simplicity, case-bonded feature, and lack of sliver is an excellent candidate design. It is the least susceptible of all configurations to the erosive burning that results from configuration complexity (eq. (18)). In the range of L/D in which the configuration typically is applicable from a ballistic standpoint ($L/D < 2$), stress relief provided by end effects permits a much larger web fraction. For a case-bonded tube with $w_f = 0.8$, inner bore strain when $L/D = 2$ is approximately half the value when $L/D \geq 6$.

For many applications, however, the L/D requirement frequently dictates a tube that burns too progressively. There are two exceptions for which an $L/D > 2$ is practical:

- (1) Prevailing erosive burning will interact with the progressively burning surface sufficiently to neutralize the pressure-time delivery.

- (2) The grain can be segmented, thus adding two regressively burning ends for each segment and in effect reducing the L/D to a point that will yield a sufficiently neutral pressure-time delivery. Cartridge-loaded, internal-burning tubes provide flexibility in the use of the tube in that sufficient neutrality can be achieved by utilizing the proper number of segments.

Burning surface for the internal-burning tube with both ends unrestricted is given by

$$A_b = \pi (d + 2w_x) (L - 2w_x) + \frac{\pi}{2} [D^2 - (d + 2w_x)^2] \quad (22)$$

where

$$w_x = \text{variable web burned, in. (m)}$$

Equation (22) provides the basis for graphical presentation of geometric parameters in normalized units (refs. 39 and 40). One such graph is shown in figure 9 (ref. 40).

Equation (22) also provides a model for generalized analysis of the internal-burning tube. The first derivative of A_b with respect to w_x equated to zero yields

$$w_x = \frac{L - 2d}{6} \quad (23)$$

This is the value of w_x when maximum A_b is attained. The second derivative

$$\frac{d^2 A_b}{dw_x^2} = -12\pi \quad (24)$$

is negative, indicating that the burning surface curve is always concave downward or rainbow shaped. The negative second derivative has been given as a goal of grain design for applications when a requirement for pressure neutrality is inferred (ref. 4). The relatively low initial surface is desirable in view of initial erosive burning, and the relatively low final surface minimizes terminal acceleration.

To obtain equal initial and final burning surfaces, L/D must be satisfied by

$$\frac{L}{D} = \frac{4 - w_f}{2} \quad (25)$$

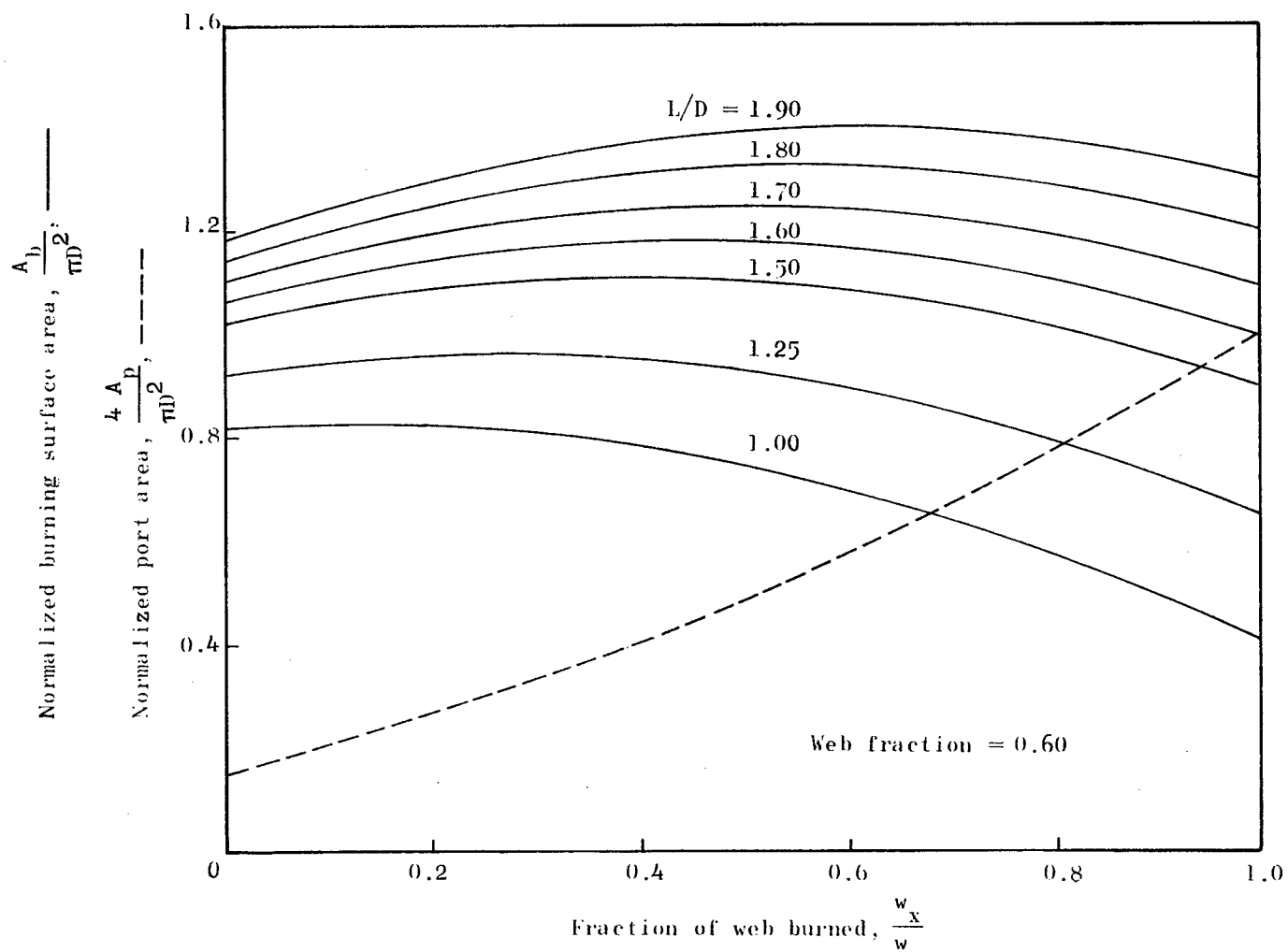


Figure 9.—Burning characteristics, internal-burning tube (ref. 40).

Thus, it is evident that the internal-burning tube becomes significantly progressive for $L/D > 2$.

2.2.2.1.4 Rod and Shell

The rod-and-shell configuration consists of a regressively burning rod with a shell configuration (fig. 10). It is a neutral-burning, sliverless configuration from which a reasonable volumetric loading fraction combined with moderate web fractions can be obtained.

The shell is restricted on the outer surface and may be case bonded. This feature protects the case wall from high combustion temperatures. Neutral burning surface is maintained by opposing functions of the two elements. When ends of the grains are restricted from burning, the burning surface is constant and independent of web burned.

Volumetric loading fraction, neglecting volume displaced by support elements, is a function of web fraction, being simply

$$V_l = 2 w_f \quad (26)$$

Hence, the rod-and-shell configuration is a candidate only when the required web fraction is sufficient to provide the required loading fraction. The predominant disadvantage is the requirement for support of the rod. For a given support system, the structural

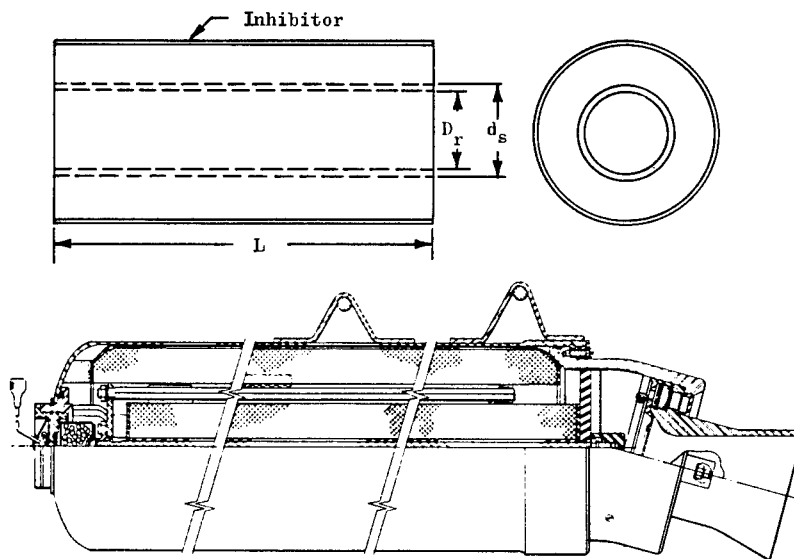


Figure 10.—Rod-and-shell configuration (ref. 26, unit 211).

requirements further imposed by temperature cycling and other environmental stipulations might prove to be too severe for acceptability, particularly in view of the relatively high flame temperatures of current propellants.

2.2.2.1.5 Star

The star is a radially burning cylindrical grain with distinctive geometric properties (fig. 11). Neutrality is provided in two dimensions by the interaction of the regressive-burning star wedges and the progressive-burning tube. Seven independent geometric variables defined in figure 11 characterize the star. Only one of the two angles η and α is necessary for definition; angle η is more commonly used. Angle α , however, is a measure common to the star, wagon wheel, and dendrite, so both α and η are shown. Descriptive terms given in figure 11 have been affixed to the functional parts of the star (ref. 2). These terms are pertinent to an understanding of the quantitative evaluation of the variables.

In a tabulation of grain designs used in 129 operational motors, presented in reference 9, it was noted that the star configuration is utilized in about 40 percent of the motors. A 3-point star configuration was the grain of the largest (260-in. [6.6 m] diam.) solid propellant motor ever developed and tested (refs. 41 and 26, unit 472). Design flexibility of the star configuration accounts for its wide application. It is a case-bonded configuration that protects the chamber wall from consequences of gas temperature and erosion, thereby eliminating the need for wholesale case insulation. With seven variables available, it is easy to achieve desirable volumetric loading fraction and relatively neutral burning with stars having web fractions of 0.3 to 0.4. Sliver, however, is an inherent characteristic of the star, the amount depending on the specific design.

The star configuration appears to have originated in England as early as 1935 (ref. 42, ch. 16, p. 8). Internal-burning configurations of this type were used in experiments at the Jet Propulsion Laboratory, California Institute of Technology, in 1947 (ref. 43). About this time, the case-bonded star configuration evolved. The early literature (ref. 44) contained geometric equations for the star geometry and dimensionless expressions for parameters such as sliver content and progressivity ratio. Parametric presentations were devised for convenient analysis of the geometric variables (ref. 43). Various graphical presentations based on this analysis have been presented (refs. 45 and 46, p. 609).

In zone 1 (fig. 11) the predominant variable is the radius r_2 , which limits the duration of burning in this zone. When $w_x < r_2$, the perimeter-web function $S = f(w_x)$ is progressive.

The progressivity in zone 2 can be determined analytically by evaluating the derivative of the function S . The perimeter (taking $r_2 = 0$) in zone 2 at the distance burned w_x is

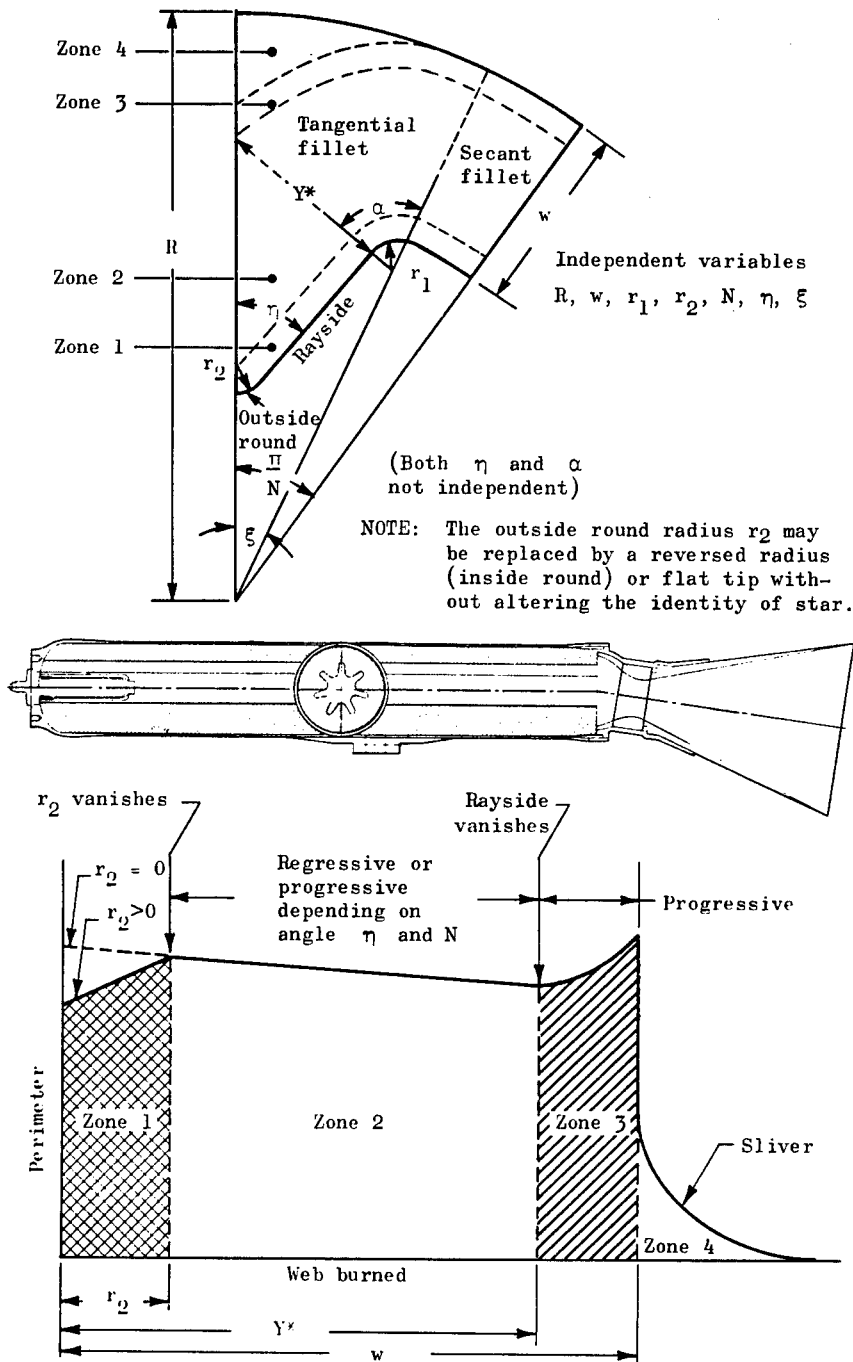


Figure 11.—Star configuration (ref. 26, unit 479).

the sum of the arc $(R - w + w_x) (\pi/N - \xi)$, the arc $(r_1 + w_x) \alpha$, and the rayside of the star $(R - w - r_1) (\sin \xi / \sin \eta) - (r_1 + w_x) \tan (\pi/2 - \eta)$.

$$\frac{dS}{dw_x} = 2N \left[\frac{\pi}{2} - \eta + \frac{\pi}{N} - \tan \left(\frac{\pi}{2} - \eta \right) \right] \quad (27)$$

where

S = burning perimeter varying with w_x , in. (m)

η = angle (fig. 11), deg

N = number of star points (symmetry number)

The value of dS/dw_x obtained from equation (27) for a given symmetry number N is determined by η independently of ξ and establishes the progressivity in zone 2.

In zone 3 the surface-web trace basically tends to be progressive, being composed of arcs defined by continuously increasing radii. The sliver, zone 4, is regressive, since the arcs involved are continuously decreasing in length.

Inert slivers may be used to displace the propellant in zone 4 when a sharp tailoff with the star is a requirement. This is not a frequent practice, however, because of the added processing complexity and cost.

Equation (27) indicated conditions for burning neutrality in the star. When $dS/dw_x = 0$, η is defined implicitly as a function of N , the expression being

$$\eta = \frac{\pi}{N} - \tan \left(\frac{\pi}{2} - \eta \right) + \frac{\pi}{2} \quad (28)$$

Thus, for a given number of star points N , a unique value of η is defined for neutrality in zone 2, independent of the value of ξ . Values for N and η satisfying equation (28) are

<u>N</u>	<u>η, deg</u>	<u>π/N, deg</u>	
3	24.55	60.00	} $\xi < \pi/N$
4	28.22	45.00	
5	31.13	36.00	

<u>N</u>	<u>η, deg</u>	<u>π/N, deg</u>	
6	33.53	30.00	} $\xi \leq \pi/N$
7	35.56	25.71	
8	37.31	22.50	
9	38.84	20.00	
10	40.20	18.00	

When $\eta < \pi/N$, a secant fillet $\xi < \pi/N$ may be necessary, depending on values of r_1 and r_2 , to prevent the raysides from overlapping (fig. 11). Considering N as a symmetry number rather than an integral number of star points, the minimum value of N permitting $\xi = \pi/N$ for which neutral burning is achieved is $N = 5.54$. This would represent a neutral star configuration with a symmetry N of 5.54, $\eta = \pi/N = \xi = 32.48$ deg, and volumetric loading fraction of 1.0. The value of N is integral, however; and for $N = 6$, for example, $\eta = 33.53$ deg and $\xi \leq \pi/6$.

Neutrality is maintained only in zone 2. Hence, for total neutrality, the condition $Y^* = \text{web}$, which eliminates burning in zone 3, must be imposed (ref. 2). When $r_1 = r_2 = 0$, this condition restricts the value of ξ to

$$\xi = \sin^{-1} \left[\frac{w_f}{1 - w_f} \cos \eta \right] \quad (29)$$

where

$$\xi = \text{angle (fig. 11), deg}$$

When the secant fillet is nonexistent ($\xi = \pi/N$ in eq. [29]), the value of N for a neutral star with $r_1 = r_2 = 0$ determines both η and w_f .

References 44 through 47 employ a common set of four independent variables instead of the seven variables normally used in defining a particular star geometry. Treating the configuration in dimensionless form reduces the number to six, and letting $r_1 = r_2 = 0$ reduces the variables to w_f , N , ξ , and η . The ballistic parameters port-area fraction, sliver fraction, initial perimeter-to-charge-circumference ratio, and minimum-to-initial-perimeter ratio are defined in terms of these variables. Equations and graphical presentations are given in reference 45. Additional star configuration analyses are presented in references 48 through 55.

2.2.2.1.6 Wagon Wheel

The wagon wheel (fig. 12), originally called the H-R design (ref. 56), is an internal-burning cylindrical configuration. It is an extension of the star configuration, having the seven independent variables of the star (fig. 11) and three additional variables (β , L_a , and r_3) for defining the break in the rayside that distinguishes it from the star.

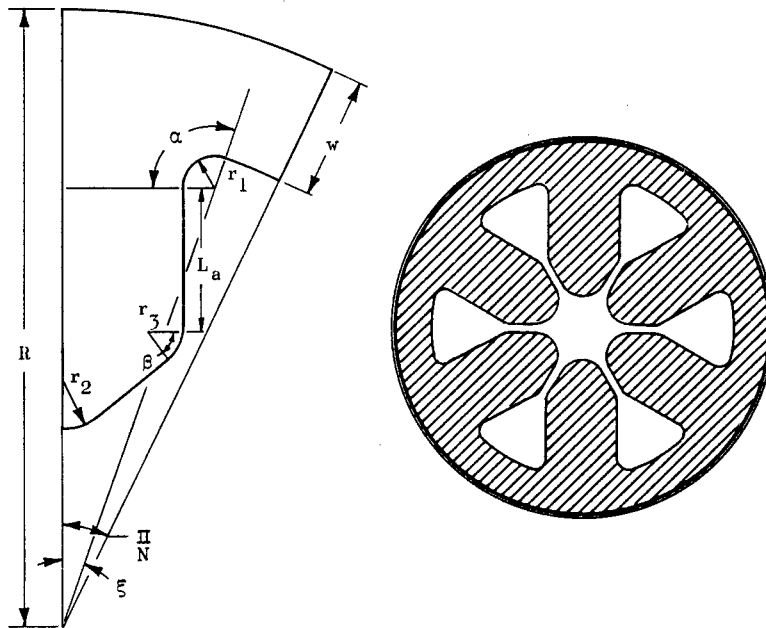


Figure 12.—Wagon wheel configuration.

The wagon wheel is used when web fractions of approximately 0.15 to 0.25 are required. Typical volumetric loading fraction is 0.70, the actual value depending primarily on specific values for web fraction and number of spokes. However, vibration and shock considerations are significant in the wagon wheel because of the thin-web, cantilevered spoke.

The conventional wagon wheel usually has parallel raysides, with angle α defined by

$$\alpha = \frac{\pi}{2} + \xi \quad (30)$$

where

α = angle (fig. 12), deg

ξ = angle (fig. 12), deg

For the condition of parallel raysides, α becomes dependent, the number of independent variables is reduced to nine, and, more importantly, the web in the spoke is constant. If this web is equal to the major web, the most common condition, the angle ξ also becomes dependent in the equation

$$\xi = \sin^{-1} \left(\frac{w + r_1}{R - w - r_1} \right) \quad (31)$$

where

w = web thickness of propellant, in. (m)

r_1 = outside round radius (fig. 12), in. (m)

R = outer radius of grain, in. (m)

This reduces the number of variables to eight. Furthermore, volumetric loading fraction is enhanced when $\beta = \pi/N$. Thus, a typical, workable wagon wheel can be defined with seven independent variables.

Reference 57 uses 13 independent variables to define the configuration. The additional variables provide a third flat side to the spoke compared with two for the standard wagon wheel. Other analyses for the wagon wheel are given in references 48 and 49 and in the references cited in section 2.2.2.1.7.

2.2.2.1.7 Dendrite or Forked Wagon Wheel

The dendrite configuration (fig. 13), or forked wagon wheel (ref. 57), is composed of combinations of elements from the wagon wheel and star configuration. Typically the dendrite contains alternate long and short wagon-wheel spokes. The computer program discussed in reference 57 provides an additional break in the rayside of the long spoke, which adds a radius, an angle, and a length for a total of 20 independent variables. Degrees of freedom on the dendrite permitted in two computer programs (refs. 57 and 58) are compared in reference 3.

Application of the dendrite is similar to that of the wagon wheel except for the range of web fraction, which is approximately 0.10 to 0.15. Volumetric loading fraction is 0.60 to 0.65 in this range.

References 59 through 61 contain comprehensive tabulations of geometric detail for the dendrite. A graphic presentation of grain design characteristics for the dendrite is presented in reference 62.

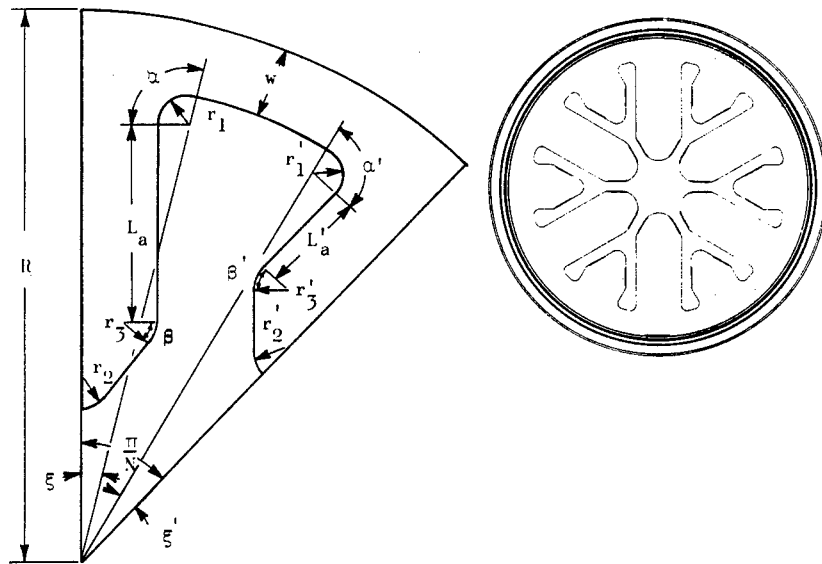


Figure 13.—Dendrite configuration (ref. 26, unit 330).

2.2.2.1.8 Anchor and Dogbone

The anchor configuration (fig. 14), defined with seven independent variables (ref. 63), is more noteworthy for its position as a morphological reference than for its actual use in motors (ref. 3). The anchor has elements that function as the shell, rod, star, and wagon wheel. Sliver is a characteristic feature of this design, and improper dimensioning of the grain can result in unsupported or detached sliver. Because of the large mass of unsupported propellant, the configuration is subject to shear failure. Although the anchor has little general application, its use in specialized application may be practical, e.g., extension of the transverse slot and termination of the radial slots at a transition point within the grain to provide a dual thrust level.

A configuration (fig. 15) recently developed for its superior structural qualities is the dogbone (ref. 19). It is classed with the anchor, since its morphological characteristics suggest that it may have been derived in part from the anchor, particularly in view of the possibility of detached sliver (ref. 3). Ideally the tips of the slot form a true ellipse for the best structural characteristics. In practice, however, an elliptical shape is only approximated, and frequently the configuration can be described by the variables that define the wagon wheel. Dogbone tips to a slot are more often the result of a structural rather than a ballistic requirement.

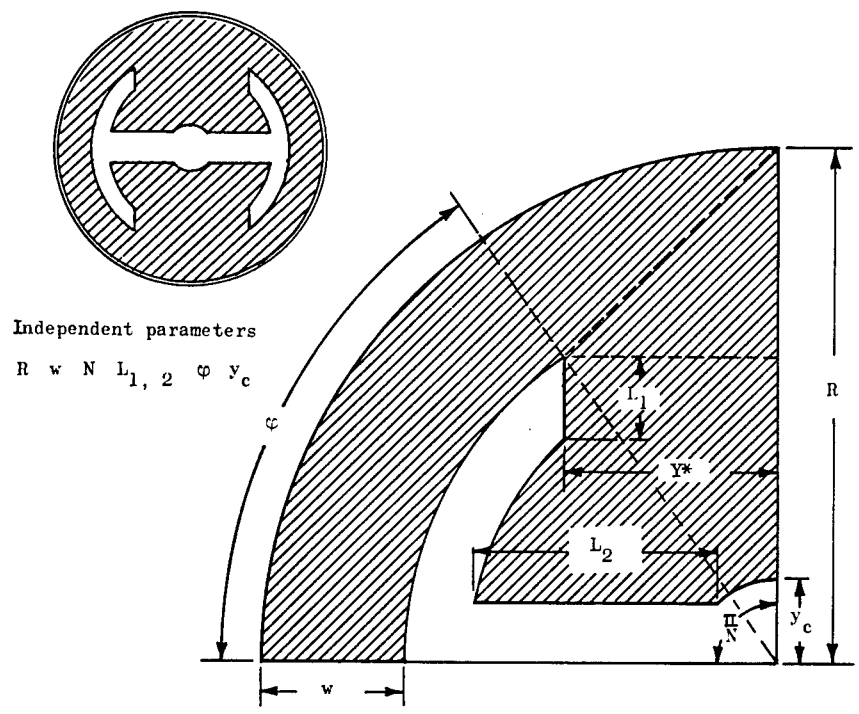


Figure 14.—Anchor configuration (ref. 63).

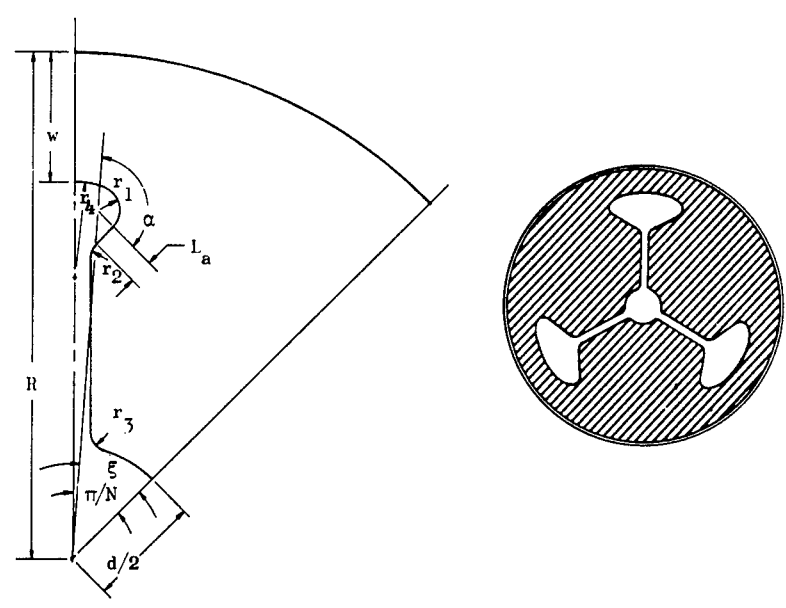


Figure 15.—Dogbone configuration.

2.2.2.1.9 Slotted Tube

The slotted tube (fig. 16) is a conventional internal-burning tube that has been slotted with one or more longitudinal slots that connect the flow channel with the insulated case wall. The slotted portion provides a regressive element to offset the progressivity of the internal-burning tube. In terms of a grain design principle, this feature is described as control of burning surface by exposure of the chamber wall (ref. 3). Burning front progresses in both the radial and longitudinal directions.

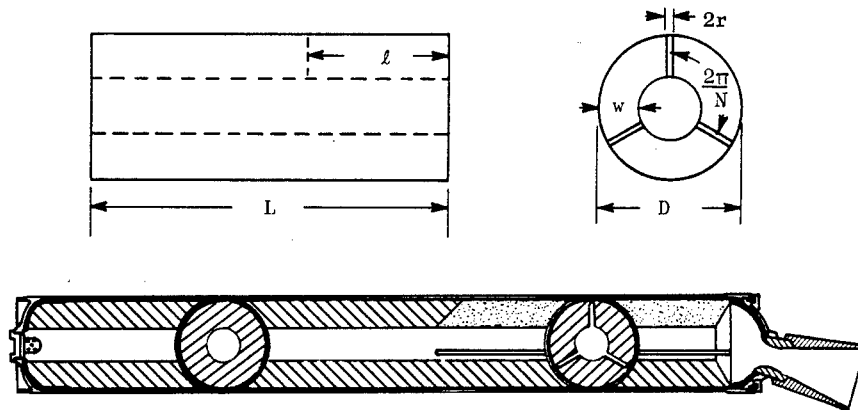


Figure 16.—Slotted-tube configuration (ref. 26, unit 442).

Geometric analysis of the slotted tube has been developed in detail (refs. 64 and 65). Equations derived were programmed for computer calculation, and data were generated for graphical presentation. An excellent set of usable curves is contained in reference 64. The graphs display initial surface, progressivity ratio, and volumetric loading fraction in terms of combinations of web fraction, slot length, grain length, and number of slots.

Advantages of the slotted tube cited in reference 64 are

- Inherent lack of sliver
- Relative freedom from regions of stress concentration (excepting the region at the slot end and the thick web)
- Design simplicity in mandrel fabrication
- Slots on the aft end can provide reasonable port-to-throat area ratios with very high loading fraction

Volumetric loading fraction of the slotted tube, as with the other tubular configurations, is basically a function of the web fraction. Therefore, the slotted tube would be applicable

only when the required web fraction satisfies the loading fraction requirement. Perhaps the most notable disadvantage of the slotted tube is the exposure of the case insulation to the high-velocity hot gases. Liner erosion is severe during the first portion of motor operation, and provision for added liner at the base of the slots usually is necessary (ref. 66). Initial exposure of the case liner to the gas flow can be delayed by a modification of the slotted tube that reduces the slot dimension corresponding to w (fig. 16) to a value less than the web. This modification, however, alters the normal burning characteristics of the slotted tube, the extent depending on the reduction in slot depth. The relationships among number of slots, slot length, and case liner requirements at the slotted section may provide tradeoff variables in determining the number of slots to use in a specific application of the slotted tube. The slot length, being an independent variable, can be used to advantage in partial compensation for erosive burning (ref. 67).

2.2.2.1.10 Conocyl

The conocyl (acronym for "cone in cylinder") is a three-dimensional grain configuration (fig. 17) utilizing the two-dimensional progressive characteristic of an internal-burning circular cylinder and the regressive feature of an external-burning cone formed in the forward end (ref. 68). Interaction of the two elements provides a ballistically acceptable grain configuration in terms of burning neutrality for a range of values for L/D with an upper limit of approximately 4.

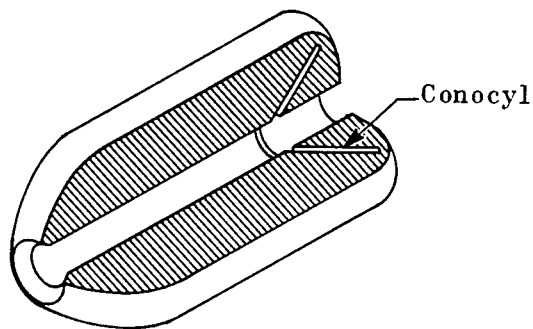


Figure 17.—Conocyl configuration.

The designer has at his disposal the cone angle, web fraction, and cavity dimensions between the cone and cylinder for optimization. Beyond that, the fixed chamber envelope, particularly the shape of the forward closure, dictates the burning characteristics. Disadvantages of the conocyl configuration include processing difficulties, high-stress region at the cone tip, and slow-ignition characteristics.

Geometric analysis of the conocyl has not been generalized, perhaps because of its dependence on the shape of the forward closure. The conocyl is symmetrical with respect to

the longitudinal axis and therefore is readily adaptable to drafting techniques for analysis; computer programs include a number of proprietary programs written specifically for the conocyl and the three-dimensional grain design program of reference 1.

2.2.2.1.11 Finocyl

The finocyl (acronym for "fin in cylinder") is a three-dimensional grain configuration (fig. 18) specifically applicable to long-duration motors with relatively low L/D values requiring internal-burning grains (ref. 69). Also called "winged slot" and "star-in-a-pocket," the finocyl is distinguished from the conocyl primarily in that axial rather than radial slots are used, and the surface control may or may not be accomplished by exposure of case wall. No generalized analysis providing definition in terms of a fixed number of variables for the finocyl grain has been proposed (ref. 3). Like the conocyl, the chamber shape and degree of nozzle submergence in addition to the number and geometry of slots are significant variables in determining the characteristics of burning.

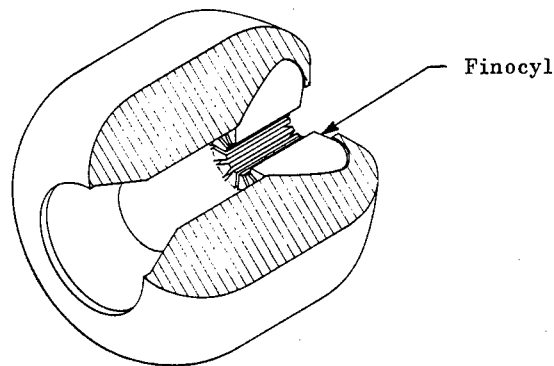


Figure 18.—Finocyl configuration.

Experience has shown that a finocyl with a web fraction of 0.8 will have approximately the same strain capability as a star with a web fraction of 0.6 (ref. 70), both providing approximately the same volumetric loading fraction. The finocyl provides approximately the same ballistics as the conocyl, and some manufacturers find the finocyl easier to fabricate. Frequently, however, other system requirements such as thrust reversal ports that require added flow channel volume in the forward end prevail over purely ballistic considerations. A submerged nozzle may require forward slots to obtain required burning geometries. In either design situation, the finocyl may be the only applicable configuration.

The grain geometry typically is analyzed by generalized three-dimensional programs such as that in reference 1 or similar proprietary programs including those prepared specifically for the finocyl configuration. A desired surface-versus-web performance may be established and dimensions of the functional elements of the finocyl varied until the desired geometry is

obtained. This practice is common when graphics display equipment, in conjunction with computer facilities, is available. Graphics programs have the facility for simultaneously displaying a previously determined and a calculated surface-web curve. The desired curve satisfies the grain design parameters known at this stage of the design phase and is tempered with a knowledge of what can reasonably be expected from the configuration. Preliminary dimensioning of the configuration, then, will consider a reasonable match of a calculated curve with the reference curve. With the display equipment, repeated runs are made, with a brief analysis between each run.

2.2.2.1.12 Other Configurations

Grain geometries are not necessarily limited to the exact geometric shapes described in the previous sections. Combinations of shapes frequently satisfy certain requirements, in particular dual thrust levels. Depending on the boundaries, slot geometries may be varied to give desired results; this technique is used in the finocyl configuration. When surfaces may be freely inhibited, the flexibility of a surface-web program for a given web fraction essentially is limited only by the practicality of and process requirements for installing the inhibitor pattern. However, inhibited surfaces other than the bonded interface between propellant and case wall generally are not preferred, because they are less reliable and are relatively expensive.

Very short duration motors ($t_b \ll 0.5$ sec) with very small webs ($w_f \ll 0.10$) requiring support are reported in references 71 and 72. Reference 73 gives an example of the use of inhibitor in the bore of an internal-burning grain to provide an effective web greater than the radius. The flexibility inherent in solid propellant grain design has resulted in numerous other configurations, including thin-web grains (used in early motors and in special application) and dual-propellant configurations.

2.2.2.1.12.1 Spherical Grain

In outer space, where aerodynamic drag is not a significant factor and the shape of the performance curve has less influence on optimum performance, the spherical motor may be the optimum motor design. Occasionally in other applications, the envelope for the rocket motor may be utilized more efficiently by a spherically shaped motor, or the spherical geometry may be more adaptable to other system requirements (e.g., limits on moment of inertia and weight). The sphere provides benefits of minimum case wall stress and minimum surface area for a given volume, and hence the spherical motor has the potential of having a relatively high mass fraction.

The first major development of the spherical motor was conducted by the National Advisory Committee for Aeronautics (ref. 74). This effort produced a spherical grain configuration called "melon slice" (fig. 19), which has become a typical grain design for the spherical envelope (ref. 75). It is an internal-burning star configuration with a constant web

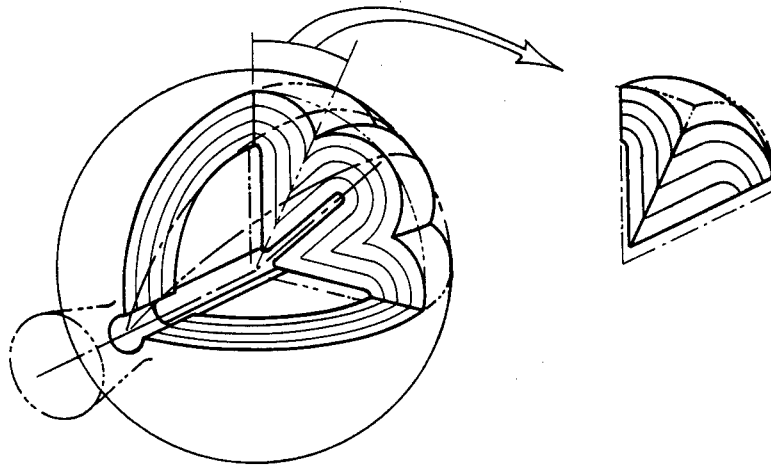


Figure 19.—Spherical grain configuration (ref. 77).

throughout. Grains of seven and eight star points typically are used. Volumetric loadings of 95 percent with sliver of approximately 5 percent and burning-surface area variation less than 6 percent are easily attained (ref. 76).

Analytical methods for geometric analysis of this configuration include those discussed in references 74 and 77 through 80 as well as the generalized three-dimensional analysis presented in reference 1. Reference 75 reviews development of the spherical motor as a propulsion system for space and upper-stage application and presents a performance table of recently developed spherical motors.

2.2.2.1.12.2 Dual Thrust Grain

Dual-thrust-level (boost-sustain) motors frequently provide a more effective delivery of impulse than those with an all-boost schedule and are, therefore, specified for some applications (refs. 81 through 83). Required delivery of mass flowrate versus time to provide the boost-sustain thrust schedule is obtained by grain design involving the same principles applicable to all-boost, neutral-burning grains. Typical boost-sustain motors (fig. 20) contain grain designs of two basic configurations composed of one or two propellants, depending on achievable web fractions, burning-rate characteristics, and relative values of thrust and duration (fig. 21).

Dual-thrust configurations generally are combinations of those discussed in previous sections. The geometric transition from boost to sustain is used to advantage in tailoring the burning geometry. The general relation of web fraction to burning-rate availability influences the selection of the configuration and establishes either a dual- or single-propellant system. For a single-propellant system, the limit on sustain web fraction

Single Propellant Systems	
	<p>Boost: radial burning Sustain: end burning</p>
	<p>Boost: radial burning Sustain: radial burning</p>
Dual Propellant Systems	
	<p>Boost: radial burning Sustain: radial burning Concentric full length</p>
	<p>Boost: radial burning Sustain: radial burning Concentric in aft end</p>
	<p>Boost: radial burning Sustain: radial burning Tandem with boost aft</p>
	<p>Boost: radial burning Sustain: radial burning Tandem with boost forward</p>
	<p>Boost: end burning Sustain: end burning Tandem with boost aft</p>

Figure 20.—Typical boost-sustain grain configurations.

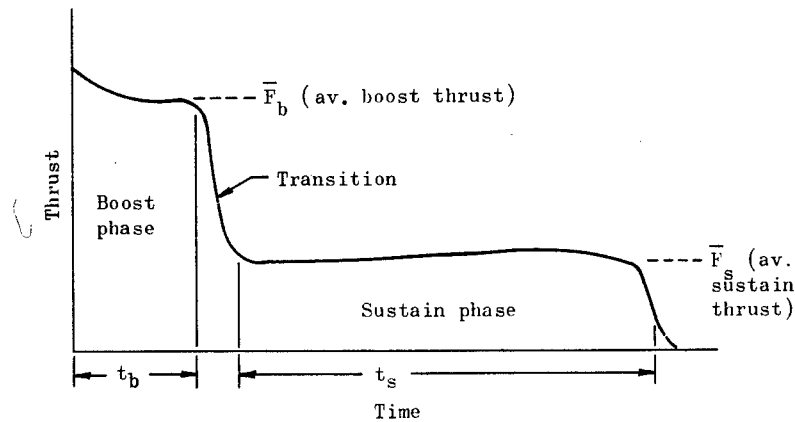


Figure 21.—Boost-sustain grain thrust schedule.

and the propellant burning rate selected for sustain define the boost burning rate at boost pressure, and the required web fraction and complexity of the boost grain are thus established. For a dual-propellant system, however, the sustain-propellant properties can be treated independently of boost-propellant properties. This feature permits independent treatment of the boost-phase web fraction and more flexibility in the design.

Current dual-thrust motors satisfy requirements for a wide range of boost-to-sustain thrust ratio and of distribution of impulse. Both requirements as well as web fraction significantly affect selection of the grain configuration. Concentric configurations are applicable when the boost impulse requirement can be satisfied by an inner grain that allows sufficient web in the outer grain for sustain duration. Frequently a single-propellant, tandem grain design with a low-web-fraction boost grain and a high-web-fraction sustain grain satisfies typical requirements. Sliver characteristic of low-web-fraction boost configurations, however, increases the transition time. An upper limit on this parameter is not uncommon. A dual-propellant application may be necessary when required sustain duration exceeds the burning-rate capability of the boost propellant at the lower sustain operating pressure.

Additional flexibility in boost-sustain design can be provided by a dual-area nozzle (ref. 84), which permits the motor to operate at a high pressure during the sustain phase as well as during the boost phase. Although not presently operational, this nozzle concept has performed as expected in engineering development programs. Notable advantages of the dual-area nozzle in addition to flexibility in thrust-time scheduling are (1) increased total impulse at the higher sustain pressure (data cited in ref. 84) and (2) burning-rate enhancement for end-burning sustain grains. Disadvantages compared with a conventional nozzle include higher cost and relative mechanical complexity.

2.2.2.1.12.3 Bipropellant Star

An internal-burning grain composed of two cylinders of distinct propellants can provide a sliverless design with high volumetric loading fraction. Such a configuration is the bipropellant star (fig. 22). The configuration is applicable to motors with web fractions of approximately 0.6 requiring a high loading fraction and neutral-burning features that do not produce sliver. The control of mass flowrate depends on the differential in burning rates and the evolution of burning surface from the interaction at the line of propellant interface.

Geometric equations providing a detailed method of analysis for the bipropellant star are reported in reference 85. The equations describe the surface areas as a function of the distance burned into the propellant. The distance burned in turn is a function of burning rate and time. The initial star perforation is a standard star except for the omission of the secant fillet angle (i.e., $\pi/N = \xi$) and the outside round radius r_2 (fig. 11). Graphical methods for analysis are given in references 86 and 87.

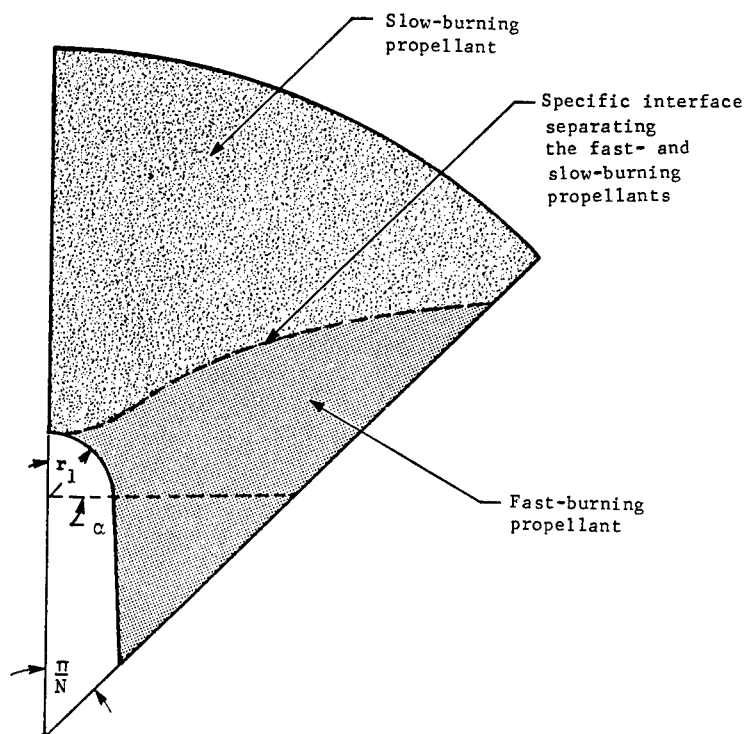


Figure 22.—Bipropellant star configuration (ref. 85).

2.2.2.1.12.4 Modular and Cartridge-Loaded Grain

Cartridge-loaded grains (fig. 23) were used extensively in earlier rockets, particularly artillery rockets and JATO's (ref. 88). Castable propellants, advanced technology, and much higher burning-rate ranges have brought about the case-bonded grains, which are generally favored over cartridge-loaded grains. In certain recent applications, however, modular grains of ammonium nitrate propellant have been used. A notable application is one that satisfies the requirement for a very-low-web-fraction, short-duration, relatively-high-thrust booster for launching jet aircraft from a platform. Such systems using restricted triform and slab grains (fig. 24) have been developed and qualified (refs. 89 through 91).

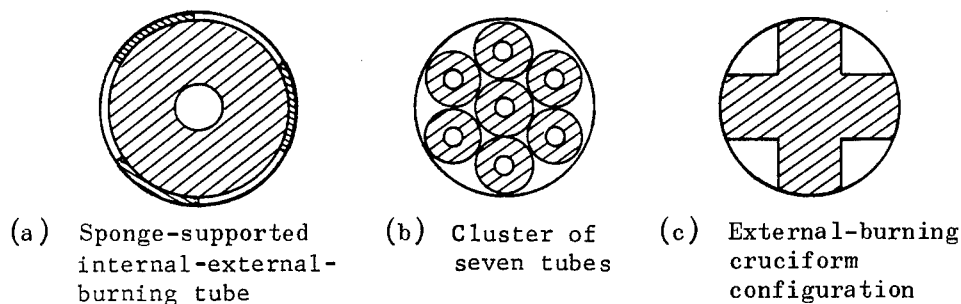


Figure 23.—Typical cartridge-loaded grains.

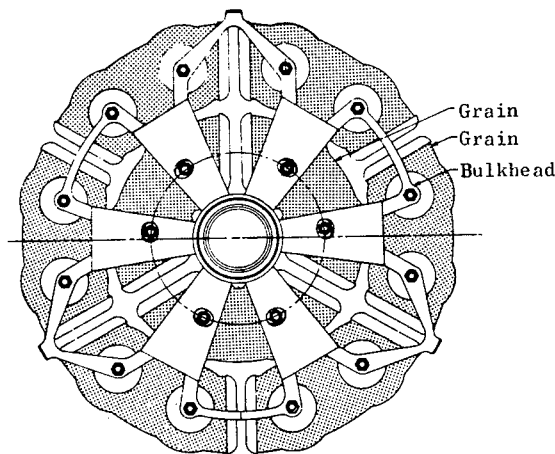


Figure 24.—Cartridge-loaded slab (ref. 89).

2.2.2.1.12.5 Multiperforated Grain

Multiperforated configurations, which permit a much thinner web than does the case-bonded dendrite, were used in early motors when burning-rate limits were lower. Illustrations of typical multiperforated grain shapes are shown in figure 25.



Figure 25.—Typical multiperforated grain shapes.

The seven-perforate design (Rodman design) is internal-external burning, slightly progressive, and has detached sliver (ref. 4). A similar design, with seven individual grains with circular ports, but internal burning, was used in a gas generator design requiring extreme progressivity (ref. 92).

2.2.2.2 Method of Selection

Application of the grain configuration types is considered in terms of the limits on web fraction and volumetric loading fraction within which neutral burning is achieved. Neutral pressure-time performance may be stipulated as an explicit requirement. Regardless of specific requirements, however, a neutral-burning configuration is desirable in many applications because of the increased efficiency in delivery of total impulse associated with neutral-burning conditions (ref. 93).

In applications requiring nonneutral thrust-time performance, the limits on web fraction and loading fraction may not apply. System requirements may dictate regressive thrust-time characteristics for conformance to acceleration constraints. In some applications (e.g., an apogee motor using an eroding nozzle and a progressive burning surface), a motor can deliver more total impulse for a given MEOP and propellant with a progressively burning grain because of the greater expansion ratio permitted by the smaller initial burning surface and nozzle throat diameter.

The three dependent parameters—web fraction, volumetric loading fraction, and length-to-diameter ratio—underlie the method of selecting a general type of grain configuration. Each configuration (sec. 2.2.2.1) applies to a range of web fraction and length-to-diameter ratio. The volumetric-loading capability can be varied over a limited range with a fixed web fraction on those configurations having non-circular cross sections. Volumetric loading fraction for circular-ported grains, however, depends directly on the web fraction. Hence, these grains can be assessed quickly for applicability.

A preliminary evaluation of maximum pressure is made during the configuration selection phase. The configuration not only must be capable of meeting the propellant weight and web-fraction requirements but also must show promise of providing estimated performance in the final analysis under the influence of erosive burning (sec. 2.3.2). A typical deleterious

effect is an initial pressure and hence MEOP greater than anticipated. In general, propellants with low burning rate ($r < 0.3$ in./sec [7.62 mm/sec]) or grains with complex cross sections are more susceptible to erosive burning. However, motors operating at low pressures (< 500 psia [3.45 MN/m²]) have relatively high erosive-burning threshold velocities that tend to lessen the erosive effect when $r < 0.3$ in./sec (7.62 mm/sec) (sec. 2.3.2).

The selected configuration usually is based on preliminary analysis of the dependent parameters. Further preliminary calculations are sufficient to dimension the grain for detailed ballistic analysis and performance prediction. Subsequent iterations typically are necessary for adjusting dimensions to provide predicted performance within the prescribed limits. The basic configuration type, however, ordinarily survives the ballistic analysis.

2.2.2.3 Geometric Analysis

When the type of configuration has been selected, initial grain dimensions are determined and intermediate burning surfaces or perimeters and areas are calculated. Initial dimensions may be calculated by formula, preliminary computer run, or comparison with similar design; determined by drafting techniques; or obtained from graphs or tables. Intermediate surfaces are then determined by (1) computer programs that consider the geometry in conjunction with or separate from internal ballistic calculations, (2) analytical geometry, or (3) drafting techniques.

The manner in which a cylindrical propellant grain burns (ref. 94) is fundamental to the analysis. The term "cylindrical configuration" is taken in the mathematical sense to mean essentially any two-dimensional grain configuration, not necessarily a right circular cylinder. Thus, only the perimeter defined by the directrix of the cylinder need be considered (ref. 94). During propellant combustion, the burning perimeter at each point recedes in the direction normal to the surface at that point; this generalization is identified as Piobert's Law (ref. 95, p. 516). In general the burning surface conforms to Piobert's Law when (1) erosive burning or pressure drop along the grain length is insignificant and (2) grain temperature is uniform. As an example of the effect of this law on the burning characteristics of a grain, it has been noted (ref. 94) that a cusp convex toward the gas phase remains a cusp and that a cusp initially concave toward the gas phase becomes an arc of a circle with its center at the original cusp (fig. 26).

In motors where erosive burning and pressure drop are predominant variables, however, only perimeters at specific stations along the grain length function as depicted in figure 26. In still other configurations such as the wagon wheel and dendrite, two-dimensional flow effects may cause perimeter regression to be nonparallel even at one station.

Intersection of burning surfaces during propellant combustion may cause portions of the grain to become unsupported. These unsupported or detached slivers induce anomalous

performance when ejected. The anchor, dogbone, and wagon wheel are configurations that may produce this condition when dimensioned improperly.

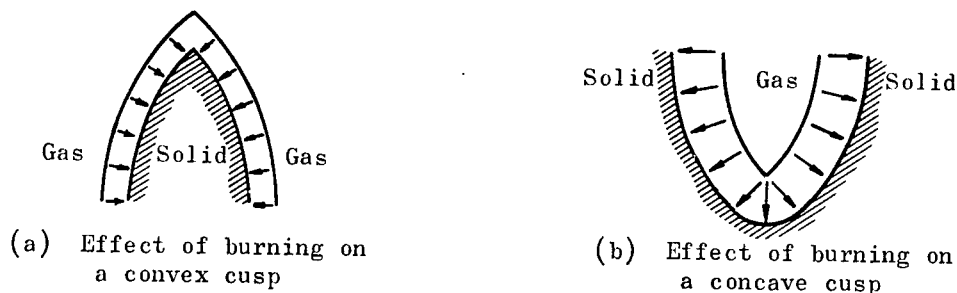


Figure 26.—Burning-perimeter changes at a cusp (ref. 94).

2.2.2.3.1 Analytical Techniques

Several analytical capabilities with computer programs have been reported (refs. 1, 57, and 58). The generalized three-dimensional grain design program in reference 1 is capable of calculating burning surfaces and other geometry for virtually any grain design. The geometry is generalized to the extent that the shape can be described by a combination of intersections of cones, spheres, cylinders, and right triangular prisms (fig. 27). This is sufficient for analytical definition of essentially any practical configuration.

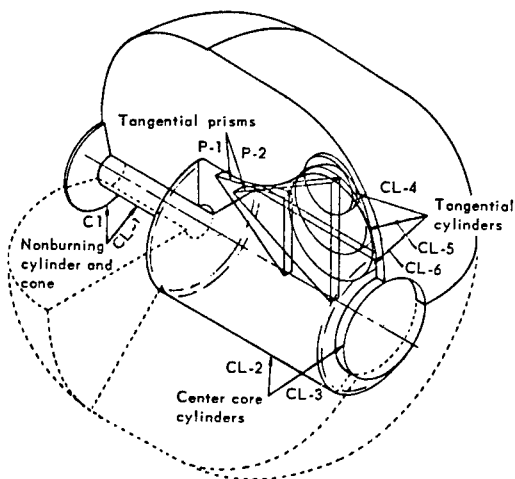


Figure 27.—Simulation of grain configuration using basic figures (ref. 96).

Surfaces are not calculated explicitly, but are derived numerically from the fact that surface at a given value of web distance is the rate of change of volume with respect to web:

$$A_b = \frac{dV_p}{dw_x} \cong \frac{\Delta V_p}{\Delta w_x} \quad (32)$$

In the finite-element form, the derivative is treated as $\Delta V_p / \Delta w_x$. The mean-value theorem states that A_b corresponds to a point somewhere in the open interval $(w_x, w_x + \Delta w_x)$. The midpoint was arbitrarily chosen as the value of w_x corresponding to A_b .

The program uses the geometric data computed at each increment to generate the internal ballistics data for the motor. A one-dimensional steady-state model of the internal gas flow is used. Burn rates are computed at discrete positions along the motor length as functions of pressure and gas velocity at those locations.

References 57 and 58 contain detailed descriptions of programs capable of calculating grain geometry variables as well as other ballistic parameters. The program in reference 58 will either accept tabulated input for geometric variables or will calculate the necessary perimeters and areas from any one of five standard configurations—star, wagon wheel, dendrite, shell, or slotted tube. The program also can select the best configuration and detail its dimensions. The selection is limited, however, to a star, wagon-wheel, or slotted-tube configuration. The program in reference 57 is similar, but it cannot select a configuration. Grain design options are similar except that the latter program includes the general forked wagon wheel (sec. 2.2.2.1.7).

Generalized two-dimensional analyses frequently are used by companies that have developed their own computer programs. These analyses usually are proprietary and unpublished. A generalized two-dimensional method is described in references 97 and 98, however, and is applicable to any two-dimensional cross section of an internal-burning, case-bonded, monopropellant grain for which the initial configuration can be described mathematically by equations of intersecting straight lines and arcs of circles.

2.2.2.3.2 Drafting Techniques

Although computer methods have almost replaced drafting techniques, a detailed scale drawing of the configuration with its intermediate surfaces scaled on the drawing still is considered an accurate method of analysis. In a typical design analysis, some part of the final grain design usually requires scaling. This requirement results from indentations and other minor alterations made on the grain by features of the final hardware design. Perimeters and port areas are measured or calculated from a sketch depicting the intermediate burning surfaces (fig. 28); simple devices such as scales, map measures, and planimeters are used.

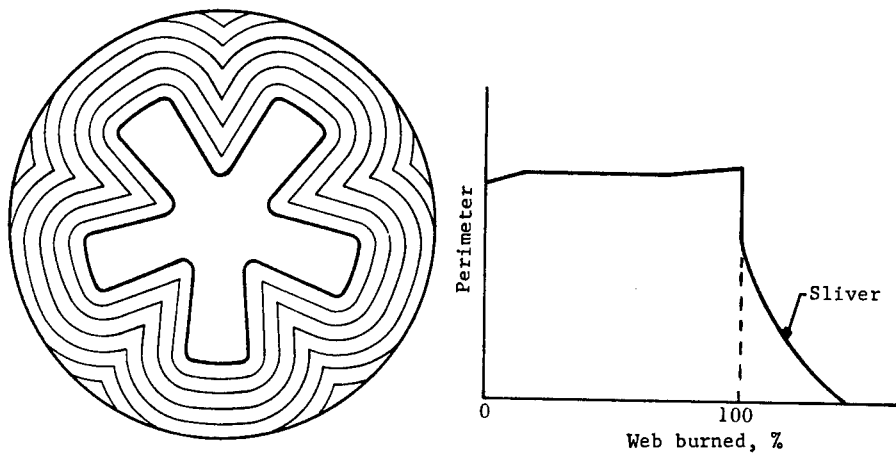


Figure 28.—Typical burning perimeters from a neutral-burning star.

2.3 Design Verification Analysis

Initial dimensioning of the grain configuration to define a specific grain design usually is accomplished independently of detailed gas dynamic calculations, with dimensions being subject to subsequent refinement. Although there are integrated techniques for complete design of a grain including automated configuration selection and performance prediction (ref. 58), treatment of grain geometry independent of performance prediction is more common. Thus, the analysis phase of grain design normally is comprised of performance prediction for a specific grain design and subsequent iteration of the grain design variables to satisfy requirements.

Rocket motor performance (sec. 2.3.3) is predicted by well-established techniques (refs. 99 and 100). Areas within the framework of performance prediction that are related directly to grain design include mass balance (sec. 2.3.1) and burning-rate augmentation (sec. 2.3.2).

2.3.1 Steady-State Mass Balance

The primary function of the propellant grain is to produce combustion products at a prescribed mass flowrate defined by

$$\dot{m}_g = A_b \rho_p r \quad (33)$$

where

\dot{m}_g = propellant mass flowrate generated in the chamber, lbm/sec (kg/sec)

The rate of gas products discharged through the nozzle is expressed as

$$\begin{aligned}\dot{m}_e &= \frac{g_c}{c^*} P_c A_t \\ &= C_D P_c A_t\end{aligned}\quad (34)$$

where

\dot{m}_e = propellant mass flowrate consistent with nozzle discharge capability,
lbm/sec or kg/sec

The condition for equilibrium operation is the mass balance $\dot{m}_g = \dot{m}_e$ (neglecting mass stored in the chamber). On the basis of this condition, a combination of equations (3), (33), and (34) leads to the following equation relating motor performance to the propellant burning surface:

$$\begin{aligned}P_c &= \left(\frac{A_b \rho_p c^* a}{g_c A_t} \right)^{\frac{1}{1-n}} \\ &= \left(\frac{A_b \rho_p a}{C_D A_t} \right)^{\frac{1}{1-n}}\end{aligned}\quad (35)$$

Equilibrium flow exists at some pressure for $n \neq 1$ ($\dot{m}_g = \dot{m}_e$, fig. 29).

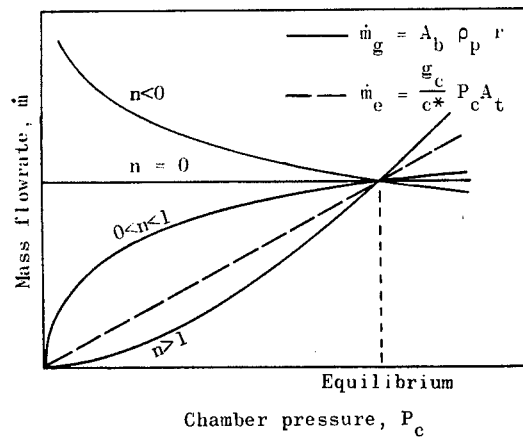


Figure 29.—Balance of mass flowrates.

When $n < 1$, $\dot{m}_g > \dot{m}_e$ at pressures below equilibrium and $\dot{m}_g < \dot{m}_e$ at pressures above equilibrium. Therefore, the motor operates stably at the equilibrium pressure when $n < 1$, a condition that encompasses the range $0 < n < 1$ of typical propellants. When $n > 1$, the mass flow process is not stable at the equilibrium pressure. Disturbances below this value will cause pressure to decrease to zero, and disturbances above it will increase the pressure to values beyond the structural capability of the case. Reference 101 noted that a stable point exists for $n > 1$ when change in volume accessible to \dot{m}_g is considered. The pressure value is exorbitant, however, far beyond the usual range of pressure for solid propellant motors.

2.3.2 Burning-Rate Augmentation

Motor burning rate frequently is greater than that indicated by expressions that are only pressure and temperature dependent (eqs. (3) through (5)). The most common augmentation is induced by the hot gas flow in the flow channel and customarily is called "erosive burning." The degree to which burning rate is augmented depends on other design characteristics such as mass flux (refs. 102 and 103), port-to-throat area ratio, reference burning rate (refs. 102 and 104), and complexity of the grain geometry (ref. 28). The erosive-burning sensitivity of propellant is influenced strongly by the binder system used in the propellant formulation (ref. 105). Many analytical expressions for erosive burning have been reported (refs. 28, 102 through 104, 106, and 107), as well as results of evaluations (refs. 105, 108, and 109) and methods of measurement (refs. 110 through 112). Some of the most successful prediction methods include a measure of all of the above-mentioned influences.

Erosive burning is a common occurrence in high-thrust, short-duration rocket motors. For these applications, total-impulse requirements demand a grain with substantial volumetric loading fraction. The commensurate requirement for a large nozzle throat area typically results in a relatively low port-to-throat area ratio. The resulting gas velocity will tend to increase the burning rate in the aft portion of the flow channel at ignition, the magnitude depending on the propellant characteristics and grain geometry. The influence on initial chamber pressure can be substantial. Even in motors with port-to-throat area ratios of 4 to 6, pressure overshoots of 100 percent have been observed in many instances (ref. 105).

Impact on motor design is readily apparent. Even discounting catastrophic failure from excessive chamber pressure, underestimated erosive burning can necessitate a decrease in motor operating pressure during development testing so that pressure can be maintained within the MEOP limits of the motor case. This decrease can be accomplished independently of the grain configuration by increasing the nozzle throat area and propellant burning rate to deliver the same thrust at lower pressure. Delivery of the stipulated total impulse, however, was predicated on operating at the original pressure level. The motor, then, probably would be deficient in required propellant, and reliability in terms of mission

capability might be compromised at the lower total impulse level. Thus, an analysis that will accurately predict erosive burning is fundamental to successful design analysis.

A design feature that has been used successfully to offset initially high erosive-burning rates without significantly affecting subsequent burning geometry is initial surface restriction with narrow strips (ref. 113). The method may rely on timely ablation of the restrictor strips when applied to a high-velocity region. Otherwise, the burning surface will be progressive as cusps form under the strips, forming a relative maximum point at a web equal to half the strip width. This feature generally is applied as a last resort when initial mass flowrate and pressure cannot be contained within limits by other methods.

Another factor that may influence burning rate is acceleration, such as that from spinning a rocket motor to provide dynamic stability. Effects from this environment may induce burning-rate augmentation and thus increase propellant mass flowrate and chamber pressure to undesirable levels. Propellant surfaces subjected to the greatest change in burning rate are those normal to the acceleration vector (ref. 114). Metallized propellants are significantly more sensitive to spin than are nonmetallized propellants because of the increased rate of heat transfer from the molten metal particles retained at the propellant surface by the acceleration forces (refs. 115 through 118). Data in the cited references indicate burning-rate augmentation of 20 to 30 percent or more. Although quantitative assessment of the effects of acceleration on potential ballistic aberration is not yet a state-of-the-art technique, the grain designer must be mindful of the potential effect of this environment on the performance of the grain design (ref. 99).

Other mechanisms that influence burning rate have been identified and studied. Burning rate at the propellant/liner interface may be augmented by variables other than pressure and temperature (sec. 2.2.2.1.1). Typical effects from this type of burning-rate augmentation are nonneutral end-burning grains and burnout pressure of internal-burning grains greater than that indicated by the final burning surface and reference burning rate. Propellant strain has shown a tendency to increase burning rate in certain types of propellant (refs. 119 and 120) because of the compressibility of the propellant; however, an opposite effect also has been reported (ref. 121).

2.3.3 Performance Prediction and Iteration

The mass-balance relationship implied in equation (35) is fundamental to prediction of ballistic performance. Most prediction methods, regardless of their sophistication, treat mass discharged in the simple terms of equation (34) (refs. 1, 57, 58, and 122). Furthermore, a treatment by equation (33) of mass generated in the chamber may be sufficient for motors having end-burning grains or internal-burning configurations with large port-to-throat area ratios. In such cases, equation (35) is sufficient for calculation of chamber pressure.

In many cases, however, mass is being added to a relatively high-velocity flow stream. Gas density, pressure, velocity, temperature, and flow area are changing continuously with respect to time and position along the motor axis (ref. 123, p. 48). Complexity of the resulting gas dynamic problem is such that computer methods must be used to determine the total mass flowrate and aft-end stagnation pressure versus time. This complexity prevents exact determination of burning rate, in particular, and of detailed dimensions for the grain that will yield the desired predicted performance the first time. Therefore, input values to the initial performance calculation frequently are only estimates, and the analytical phase of grain design entails evaluation and adjustment of the appropriate design variables for subsequent performance prediction.

Grain dimensions are the more reliable inputs inasmuch as the initially determined propellant weight requirement is relatively accurate. Erosive burning, on the other hand, can only be estimated prior to the first performance calculation, and the extent of erosive burning will directly influence the initial burning-rate input. An inaccurate assessment of burning rate typically will result in a predicted MEOP different from the initial MEOP estimate. This inaccuracy usually is reconciled after the first performance prediction by changing the motor operating pressure, the change being effected by altering both propellant burning rate and nozzle throat diameter. Depending on the extent of pressure change necessary, the grain dimensions may require revision.

2.3.4 Design Acceptability and Optimization

The basis for design acceptability is a satisfactory correspondence between predicted performance and stipulated requirements, including ballistic, structural integrity, and processing. The depth of analysis undertaken and the degree of tolerance permitted in the design nominal values dictate the degree of correlation necessary for acceptability. Depending on the particular design problem, if subsequent changes in nozzle throat diameter and burning rate are not permitted because of schedule or other factors, extreme care must be taken to ensure that the analysis is accurate and completely reliable.

Measures of design optimization depend on the particular requirements of the motor; and the degree to which a grain design can be optimized usually is restricted by schedule, economy, and practicality. Within the constraints of structural integrity and manufacturing capability, parameters such as volumetric loading fraction, sliver content, neutrality of thrust-time, and configuration efficiency (ref. 93) are common measures of design merit. However, regressive thrust-time performance may be required when terminal acceleration is limited. Sliver likewise may be a desirable or necessary feature if a requirement for gradual thrust decay is stipulated. Ballistic optimization may be extremely limited, if not prohibited, if structural, system, or process requirements dominate in the grain design process. Generally, however, the optimum design from a ballistic standpoint is the one that delivers the maximum impulse within the pressure capabilities of the case or the stipulated impulse with minimum propellant weight, consistent with other ballistic requirements.

3. DESIGN CRITERIA and Recommended Practices

3.1 Evaluation of Parameters

3.1.1 Independent Parameters

The grain design shall be based on explicit ballistic performance parameters and related motor attributes derived from mission requirements, stated propellant properties, and stipulated envelope and environmental constraints.

It is recommended that specific motor parameters having influence on the grain design be established as set forth in section 3.1.1.1 if they are not otherwise stated explicitly. These parameters should be used together with propellant ballistic properties (sec. 3.1.1.2) and mission- and vehicle-related constraints (sec. 3.1.1.3) as the basis for determining the dependent grain design parameters of section 3.1.2. It is important to consider the parameters that are specified independently before considering any of the parameters of section 3.1.2 so that imposition of conflicting requirements on the grain design is precluded.

3.1.1.1 Ballistic Performance

Specified ballistic performance requirements shall be evaluated in terms suitable for identifying applicable grain configurations.

Ballistic performance requirements imposed on the grain design must ultimately correspond (within limits) to the predicted performance of the motor. Initially, however, thrust and duration must be considered in evaluating the parameters that form the basis for configuration selection. If average thrust, duration, and total impulse are not stated explicitly, it is recommended that these values be derived from the performance requirements given and then applied to the determination of the dependent variables of section 3.1.2.

Values of average thrust and pressure are necessary in the initial estimate of nozzle throat area. These averages may be treated as the average over burning time or action time; therefore, the values stipulated or derived are sufficient. With respect to grain configuration and propellant burning rate, however, the time necessary to burn the propellant web is of principal concern. Hence, burning time normally is used in these instances. Therefore, if the specified or derived duration corresponds to another time interval, the burning time should be estimated. Initial estimates provide the first assumption of burning-rate or web

requirement in the iterative grain design problem; hence, their accuracy is important in consideration of the number of iterations and therefore design time required. Estimates preferably should be based on data from similar motors.

When a limit on maximum thrust is imposed, an estimated reproducibility of thrust-time performance must be established, preferably based on related experience. The estimated maximum thrust then must be within the limits stipulated when the tolerance is applied to the estimated value. The designer should consider that typical reproducibility in average thrust at a given temperature is ± 7 percent (3σ) if no special provision for manufacturing control above the ordinary is made (ref. 124). Point values are not so reproducible, however, ranging typically to ± 10 percent. Additional allowance should be made for maximum thrust at ignition, which generally will not be as reproducible as the maximum value during the latter part of the firing, because of the influence at ignition of additional variables such as port-to-throat area ratio, configuration effects, igniter mass, and propellant flame spread characteristics.

The impulse requirement may be given in terms of action-time or burning-time impulse instead of total impulse, the latter implying the total integral under the thrust-time curve. In the calculation of propellant weight, impulse should be treated as recommended in section 3.1.2.3.

3.1.1.2 Propellant Properties

The candidate propellants shall have ballistic properties that are well characterized over the ranges of pressure, temperature, and environment stipulated in the grain design requirements.

Although propellant selection is beyond the scope of this monograph, applicable propellants depend on the ballistic performance requirements as well as requirements for structural capability and other considerations. Tradeoff studies and considerations substantiating selection should be accomplished in accordance with the guides presented in reference 8 and with the practices presented in sections 3.1.1.2.1 through 3.1.1.2.3.

3.1.1.2.1 Specific Impulse

The design value of propellant specific impulse delivered by the motor shall reflect all losses related to the particular motor design.

It is recommended that the design value for specific impulse be based on the theoretical value at motor conditions in accordance with equation (2). This practice is preferred when it is practical to perform the required theoretical calculations (refs. 10 and 125). The value of η_{μ} should reflect in particular the motor size or mass flowrate, the aluminum content of

the propellant, and residence time. Reference 99 outlines subscale testing methods for substantiating I_{sp} and identifies other design characteristics that influence η_μ . Other applicable information on scaling can be found in references 126 and 127.

When I_{spd} is estimated from the standard value I_{spS} , one should recognize that I_{spS} , although given at standard conditions, still reflects certain inefficiencies attributable to the motor from which the data were obtained. These inefficiencies may or may not be applicable to the design under consideration. Further, c^* has a slight dependence on chamber pressure that should be considered when basing I_{spd} on I_{spS} .

3.1.1.2.2 Burning Rate

3.1.1.2.2.1 Pressure Sensitivity

Propellant burning rate shall be defined as a function of pressure.

It is recommended that variation of propellant burning rate with pressure be defined in terms of de Saint Robert's burning-rate law (eq. (3)). The constants a and n should be established by subscale test methods cited in reference 99. When the values a and n are constant only over limited pressure ranges, these ranges should be known. Scaleup for use in large motor analysis should be based on data from similar motors. When no basis for scaleup is available, it is recommended that the value of burning rate from the subscale motor be applied as the nonerosive burning rate in the grain design.

3.1.1.2.2.2 Temperature Sensitivity

3.1.1.2.2.2.1 Variation of Chamber Pressure with Temperature

Preliminary estimate of chamber pressure variation with temperature shall reflect a dependence on overall motor and grain design.

It is recommended that a value for π_K be established on a preliminary basis and used in determination of pressure variation with temperature for purposes of establishing average pressure. The value for π_K should either be based on data from motors with similar propellant formulation and design or be estimated from the burning-rate sensitivity σ_P and pressure exponent n . The constant $\pi_{P/T}$ is directly a function of n and σ_P , and the difference in $\pi_{P/T}$ and π_K reflects primarily the increase in c^* resulting from the higher sensible heat of the propellant at higher temperature T_2 (fig. 3). The c^* usually will vary 0.5 to 0.75 percent for each 100-degree variation in propellant conditioned temperature. Therefore, an approximation of π_K can be calculated from the equation

$$\pi_K \cong \frac{1}{1-n} \left[\sigma_P + \frac{1}{T_2 - T_1} \ln \left(\frac{c^*_2}{c^*_1} \right) \right] \quad (36)$$

where the subscripts 1 and 2 correspond to temperature conditions.

3.1.1.2.2.2 Variation of Burning Rate with Temperature

Variation of the design value of nonerosive burning rate with temperature shall be independent of configuration features.

It is recommended that the propellant nonerosive burning rate at temperature extremes be based on the coefficient σ_P (fig. 3). This constant is independent of c^* , whereas π_K reflects c^* variation with temperature (eq. (36)). Burning rate for analysis at temperature T_2 should be determined as indicated in figure 3.

When the pressure exponent n does not vary with temperature, the temperature sensitivity coefficients will have constant values regardless of reference pressure P_1 (fig. 3). When n varies with temperature, values for all of the coefficients depend on the value for P_1 . Therefore, when n varies with temperature, it is recommended that the analysis include burning-rate variation with temperature based on (1) a value for σ_P established at a particular value of pressure such as 1000 psia (6.895 MN/m²), or (2) the value of $r = f(P)$ determined at each temperature.

3.1.1.2.3 Density

The value for propellant density used in grain design shall reflect the variation of density with temperature.

It is recommended that applicable coefficients of thermal expansion be applied to the grain design to account for density variation with temperature. Density variation should be accounted for with particular care when one is dimensioning the ballistic mandrel to ensure the required propellant weight, and also when one is attempting to assess port-to-throat conditions accurately at the upper temperature limit.

3.1.1.3 Mission- and Vehicle-Related Constraints

3.1.1.3.1 Envelope

Dimensions of the grain design shall conform to the limits imposed by the envelope.

The envelope dimensions in terms of length, diameter, and end configuration should be established and treated as independent variables throughout the grain design process.

3.1.1.3.2 Maximum Expected Operating Pressure

The design limit on MEOP shall not exceed the MEOP on which hardware design is based.

The initial estimate of average operating pressure should be based on the MEOP at the upper temperature limit as outlined in section 3.1.2.1 and adjusted in the design iteration as outlined in section 3.3.3 to ensure that the MEOP requirement is satisfied.

3.1.1.3.3 Use Environment

Effects on internal ballistics induced by exposure of the motor to stipulated extreme environments shall not cause motor performance to vary beyond acceptable limits.

It is necessary to evaluate all environmental influences on the grain design per se in terms of structural adequacy and on burning rate in particular in terms of the resulting effect on chamber pressure. Applicable configurations for motors that are subject to vibration, temperature cycling, and acceleration should depend on results from appropriate structural and dynamic analyses as well as on the ballistic requirements. It is recommended that these analyses be accomplished in accordance with guidelines presented in reference 31. Burning-rate variation induced by temperature variation resulting from aerodynamic heating should be based on temperature gradient from thermal analysis and applied to the internal ballistic analysis. Guidelines for evaluating the augmentation of burning rate induced by acceleration are given in reference 99. Temperature limits must be applied to evaluation of performance extremes.

3.1.2 Dependent Parameters

Values assigned to the dependent ballistic variables shall be consistent with the given (independent) parameters.

It is recommended that (1) average operating pressure, nozzle parameters, volumetric loading fraction, web fraction, port-to-throat area ratio, and length-to-diameter ratio be treated as dependent on the given requirements of section 2.1.1, (2) values for the dependent parameters be calculated on a preliminary basis for configuration selection as outlined in section 2.1.2, and (3) operating pressure and nozzle parameters be adjusted in the detailed analysis phase as appropriate, any adjustment being consistent with other variables. If any of the parameters of this section are considered independently, care should be taken to preclude the development of conflicting requirements.

3.1.2.1 Average Operating Pressure

The average operating pressure used for determining pressure-dependent parameters shall be consistent with the MEOP and anticipated pressure neutrality.

Prior to actual calculation of chamber pressure in the design analysis, preliminary values of average pressure should be established for use in determining the pressure-dependent parameters. Variation of \bar{P}_b and \bar{P}_a with temperature should be based on equations in figure 3. Pressure ratios relating MEOP, \bar{P}_b and \bar{P}_a (fig. 2) at the upper temperature limit should be estimated as a basis for estimating average pressure. The relationships may be based on one or a combination of the following:

- (1) Performance characteristics of similar motors
- (2) An estimate of initial pressure overshoot based on anticipated erosive-burning tendencies
- (3) Preliminary computer calculations simulating probable motor characteristics of port-to-throat area ratio, configuration, burning rate, and nozzle erosion rate

Success of the first performance prediction (sec. 3.3.3) depends on the accuracy of initial estimates. From the first results, however, nozzle dimensions, burning rate, nozzle erosion rate, or grain dimensions can be adjusted with accuracy for subsequent iterations.

3.1.2.2 Nozzle Throat Area and Expansion Ratio

The nozzle geometry and dimensions shall provide the required thrust and system performance within the constraints specified.

It is recommended that the design value of nozzle throat area be based on the given thrust and nozzle parameters and derived pressure (eq. (14)). This throat area is the approximate average during motor operation. Initial throat diameter therefore should be a smaller value, less than the average by approximately half the total throat erosion. Assessment of nozzle throat erosion rate usually is based on empirical data related to pressure, duration, mass flowrate, and nozzle material, and is backed by analysis if warranted.

When the optimized expansion ratio ϵ is not provided from systems optimization studies, ϵ should be chosen to provide optimum performance for the chamber operating pressure and the ambient pressure at operating altitude. In general, the optimum ϵ should be slightly less than that corresponding to the maximum thrust coefficient, because the lower thrust coefficient for ϵ near optimum is offset by a lighter weight nozzle. When the

optimum ϵ is to be determined for a length-limited system with a submerged nozzle, the effect of ϵ on propellant weight should be taken into account.

For conical nozzles, the divergence correction factor λ should be obtained from equation (12). Minor corrections that may be made to this expression are given in reference 99. Values for λ for contoured nozzles usually are available from the design analysis substantiating the contour. When this analysis is not available, the recommended practice of reference 99 should be followed in determining both λ and η_F .

3.1.2.3 Volumetric Loading Fraction

The volumetric loading fraction shall satisfy the propellant weight requirement and shall indicate applicable configuration types.

Volumetric loading requirements should be based on equation (15). Generally the value of impulse should be the total deliverable, in which case it corresponds to the total weight of propellant. However, when action-time impulse is the stipulated requirement and the configuration will have sliver, it may be more convenient to consider the action-time impulse in equation (15) and apply this to the propellant weight in the effective grain cross section (total weight minus sliver weight).

When significant liner or other inert material will be consumed and thus provide a propulsive contribution during motor operation, the consumed inerts should be accounted for in the calculation of propellant weight; analytical techniques are given in reference 128. A simplified treatment based on experience assigns to the expended inerts a specific impulse value equivalent to one-half that of the propellant.

It is recommended that the volumetric loading fraction be considered jointly with web fraction (sec. 3.1.2.4) and length-to-diameter ratio (sec. 3.1.2.6) in selecting the applicable grain configuration as outlined in section 3.2.2.

3.1.2.4 Web Fraction

The web fraction shall satisfy the burning duration requirement, consistent with the range of available burning rates, and shall indicate applicable configuration types.

The web fraction should be calculated from equation (16) with the variables defined as follows:

- (1) Duration t should be the burning time (t_b , fig. 2) corresponding to web burnout.

- (2) Burning rate r should be the value of burning rate expected in the motor at average burning-time pressure and motor reference temperature, with allowance where applicable for erosive burning. In assessing the given propellant burning rate from subscale test data, one should consider requirements for scaling. Ratios of full-scale to subscale motor rates typically vary from 1.01 to 1.05 (ref. 16). When no verified method for scaling is available, the burning rate in equation (16) should be based on factors established from demonstrated correlations for similar operational ranges, motor sizes, and propellant formulation.

Advantage should be taken of available burning rates to provide a web fraction well-suited to a particular configuration.

3.1.2.5 Port-to-Throat Area Ratio

The port-to-throat area ratio shall not be less than the minimum value permitted by the ballistic performance requirements, grain geometry, and propellant properties.

The port-to-throat area ratio should be based on the initial values of port area and nozzle throat area. It is recommended that low values for A_p/A_t be accepted on the basis of an in-depth performance prediction and analysis (refs. 99 and 100), including erosive burning evaluation for MEOP verification, when $A_p/A_t < 2.0$ or when $r < 0.3$ in./sec (7.62 mm/sec) and $A_p/A_t < 4.0$. For complex grain configurations such as the dendrite, effects of gas velocities on motor ballistics should be evaluated in detail regardless of the values of A_p/A_t and r . A configuration factor (eq. (18) and ref. 28) substantially greater than 1 (in general greater than 6 to 8) identifies a complex grain.

Particular attention should be given to grain cross-sectional changes induced by thermal expansion and shrinkage for grains with marginal port-to-throat area ratios. The grain cross section can increase in area by 1 percent or more from room temperature to the upper temperature limit, depending on the configuration, thermal properties, and temperature range. This change could be an order of magnitude greater in terms of port area reduction. Calculation of grain dimensional changes with temperature should be based on the coefficient of thermal expansion. Applicable data usually are available from the grain stress analysis.

Acceptability of port-to-throat area ratio at a station upstream of the aft end of the grain should be based on computed mass flowrate at the station. A simplified expression suitable for preliminary assessment of the adequacy of the local port-to-throat area ratio is

$$A_p/A_t = \left(\frac{\sum_i A_{b,i}}{A_t} \right) \left(\frac{A_p}{A_b} \right) \quad (37)$$

where A_p is the port area at the station, A_b is the total burning surface, and $A_{b,i}$ is a burning surface upstream of the i^{th} station. If the value of A_p/A_t at the aft end does not exceed the value calculated from equation (37), velocity distribution along the grain usually will be acceptable.

The effective port-to-throat area ratio should be evaluated in terms of aerodynamic restrictions as well as geometric port area. It is recommended that reference 29 or an equivalent work be consulted when the grain design includes circumferential slots located near the aft end of the grain.

3.1.2.6 Length-to-Diameter Ratio

The grain configuration shall make maximum use of the degree of freedom permitted by the length-to-diameter ratio.

Contribution of end effects in burning geometry should be evaluated (in particular when $L/D < 4$) in the process of identifying applicable grain configurations by L/D as illustrated in figure 1. Specific recommended practices for using L/D jointly with web fraction and volumetric loading fraction in selecting the appropriate configuration are given in section 3.2.2.

3.2 Configuration Selection and Design

3.2.1 Principles Governing Selection

3.2.1.1 Ballistic Constraints

All grain configurations identified as applicable by the ballistic constraints shall be evaluated.

Dependent parameters (sec. 2.1.2) should be applied to the analysis leading to a configuration type as outlined in section 3.2.2.2. These parameters usually will indicate some configurations that may be discarded later because of processing influences (sec. 3.2.1.2) or structural integrity considerations (sec. 3.2.1.3). All configurations with some promise of meeting ballistic requirements, however, should be identified. They should be evaluated first on the basis of ballistic merits and subsequently screened as other constraints are applied. For example, the web fraction may be on the lower end of the range applicable to a star and on the upper end applicable to a wagon wheel, with both having adequate volumetric loading capability. Both should be identified as grain design candidates and their processing and structural integrity merits then assessed.

3.2.1.2 Processing Practicality

The grain configuration shall be suitable for fabrication within cost and schedule requirements, and the fabrication method shall not compromise ballistic features of the grain geometry.

Applicable configuration types within the ballistic constraints should be screened for manufacturing complexity. The required casting and core technology necessary for fabrication of the grain is of primary concern to the designer. The grain designer should work closely with responsible manufacturing engineers, tool designers, and propellant processing engineers to ensure the successful design of a processible grain within the limits of allowable cost and required reliability. Usually the manufacturing aspects of grain design can be assessed during the evaluation for a suitable configuration type, and subsequent design detail can be performed independently of further consideration for process complexity. It is recommended that adherence to the criteria of this monograph be consistent with the practices recommended in reference 30.

3.2.1.3 Structural Integrity

The grain geometry shall not violate the requirements for structural integrity.

To minimize the chance for grain failure, ballistic and stress analyses should be coordinated from the time specific configurations are considered to the end of the grain design process. After the applicable configurations have been screened in the process evaluation, each configuration should be assessed from a structural standpoint to identify the most favorable candidates. Preliminary acceptability of a configuration should be established at the point indicated in figure 1. This may be predicated on the addition of slots or other stress-relieving features to the basic grain configuration.

Evaluation on which final acceptance for structural integrity will be based should be performed simultaneously with detailed ballistic analysis and performance prediction. Results from the final stress analysis may require the grain to have additional stress relief features, larger fillet radii, smaller web fraction, etc. Specific modifications required are peculiar to the particular design problem. Recommended practices in any significant detail therefore are prohibited by the number of possibilities. In general, however, a grain design deemed unacceptable on the basis of a final stress analysis usually can be modified to satisfy the structural analysis within the limits of the ballistic constraints without changing the basic configuration type.

Typical modifications that may be employed as a result of stress analysis are the following:

Decrease the web fraction.—Normally the burning-rate flexibility of a given propellant will permit a degree of reduction to the web fraction. This reduction generally

decreases the volumetric loading, and the grain designer must utilize the degree of freedom permitted by the remaining geometric variables to maintain the required volumetric loading fraction. This tradeoff of web fraction and geometric variables is usually possible in all grain designs except those with circular cross sections.

Add stress-relief features.—Normally, the requirements for stress relief are defined at the time the configuration is first selected. If, however, additional stress relief is required, necessary modifications usually can be accommodated. Incorporation of end-release mechanisms tends to reduce the propellant weight and to complicate the processing methods. However, necessity for circumferential slots in motors with large L/D and transition areas of boost-sustain grains usually will require modification to the grain cross section to accommodate the altered burning pattern. On the other hand, stress-relieving slots may be used to advantage in the ballistic design.

Increase the fillet radii.—Detailed stress analysis may indicate a requirement for a larger fillet radius such as that in the star configuration valleys (r_1 in fig. 11). This is an area where optimum ballistic design (small radius) for minimum sliver with a fixed star-point configuration opposes optimum structural design (large radius for stress relief). Again, depending on specific performance requirements, grain dimensions frequently can be altered to accommodate a larger fillet radius.

Change the propellant or the configuration.—When all alternatives for grain dimensional changes still violate either the ballistic or structural requirements, the only solution may be to change the propellant or the configuration or both. For example, circular-port configurations with thick webs ($w_f > 0.6$) may exceed the structural capability, thereby necessitating a reduction in web fraction. Volumetric loading capability in circular-port configurations depends on the web fraction; therefore, propellant weight will become deficient. It is then necessary to either change to a propellant with increased strain capability or change to a configuration having the same volumetric loading fraction with a lower web fraction (e.g., the star).

Establish limits on grain deformation.—If the stress analysis reveals that grain deformations from environmental factors or from chamber pressure will occur, it is recommended that the ballistic performance for extreme grain shapes be estimated so that limits on deformation may be established. Particular regard should be given to possible decreases in grain port area when grain-deforming conditions exist.

It is recommended that adherence to the criteria of this monograph be consistent with the practices recommended in reference 31.

3.2.2 Geometric Definition and Analysis

3.2.2.1 Configuration Types

Grain configurations shall be identified in terms of accepted nomenclature or variations thereto.

It is of more than academic importance to identify a specific grain configuration properly, when possible, in terms of the nomenclature defined in section 2.2.2.1. The configuration name implies certain significant aspects of the grain that are important to the various disciplines involved in rocket motor design. For example, the identification "slotted tube" conveys to the stress analyst a potential structural problem in the slot termination, whereas a star (which could be erroneously identified as a slotted tube when $\eta = \pi/N$ [fig. 11]) poses no such problem. For another example, the name "wagon wheel" implies to the process engineer and tool designer, a complex configuration; to the stress analyst, a configuration that may be subject to structural failure when subjected to large acceleration forces; and to the grain designer, a low-web-fraction grain with limited volumetric loading and significant sliver. The grain configurations given in the Rocket Motor Manual (ref. 26) can easily be identified as specific types conforming to the section 2.2.2.1 definitions. Those excluded are either unique dual-propellant grains or variations to the standard slotted tube; they are easily identified by similar descriptions.

3.2.2.2 Method of Selection

The method of selection shall produce the least complex grain design that (1) will evolve combustion products consistent with the stipulated ballistic requirements and (2) will withstand the specified environmental extremes without structural or ballistic degradation below allowable limits.

The following steps are recommended for identifying the applicable grain configuration: (1) evaluate the independent requirements, (2) calculate the dependent requirements, and (3) select the configuration applicable to w_f , V_l , and L/D .

Evaluation of the independent requirements.—The independent requirements (sec. 2.1.1) should be established from the mission requirements and the given propellant properties. Performance requirements usually are given in the motor specification, and propellant properties are selected from an applicable available formulation. These properties should be treated as independent variables in the relationship to the dependent grain design parameters. Generally each of the variables can be considered independently, with the exception of a slight dependence of thrust and duration on other ballistic variables (ref. 9).

Calculation of the dependent parameters.—With the given requirements established as recommended in section 3.1.1, parameters of section 2.1.2 can be calculated. Some of these

are preliminary in the sense that the final analysis probably will result in refinements to the values. Average pressure, for example, is necessary for determination of web fraction and propellant weight. It is based on anticipated pressure neutrality that may prove in the final analysis to be different from that estimated. Particular attention should be given to the calculation of web fraction and volumetric loading fraction. Full advantage should be taken of the available burning rate range in determining the corresponding web fraction range. Web fraction should be varied to the extent permitted by the burning rate range to permit flexibility in detailing the configuration.

Selection of configuration.—Table I summarizes the application of grain configurations with respect to web fraction and length-to-diameter ratio. In retaining the neutral-burning characteristic, each configuration is limited in its volumetric loading capability. In general, the dependent requirements (w_f , L/D , and V_ℓ) should identify one or more applicable configurations.

The recommended procedure for selecting the configuration is outlined below. The sequence follows the flow diagram shown in figure 1.

Web fraction less than 0.3.—Below a web fraction of 0.1, volumetric loading of case-bonded grains may not be sufficient to meet the propellant weight requirement; multiperforated grains and multigrain assemblies, however, are applicable. Variations of these configurations that have been used in the industry are illustrated in reference 26. Extremely small web fractions ($w_f \ll 0.1$) can be achieved by special provision for support of the thin layer of propellant (refs. 71 and 72). When the design calls for a very low web fraction, the burning-rate capability of the selected propellant and other applicable propellants with high burning rates should be thoroughly considered to make sure that a low web fraction is really necessary.

The dendrite and wagon wheel have the lowest web-fraction capability of the case-bonded grains having a single perforation. When $w_f = 0.1$ to 0.15, the dendrite is recommended; it will provide loading fraction of approximately 0.60 to 0.65. For $w_f = 0.15$ to 0.25, the wagon wheel is the recommended configuration; it will satisfy loading fraction requirements of approximately 0.7. For web fractions near 0.3, both a wagon wheel and a star may apply; selection should be based on tradeoffs among the ballistic parameters and structural and process considerations. For $w_f < 0.3$, the anchor also applies; however, the anchor has structural and ballistic disadvantages (sec. 2.2.2.1.8), and generally is not a preferred configuration.

The choice of a low-web-fraction configuration may depend on considerations other than strictly ballistic requirements (e.g., the structural requirement to withstand the large forces resulting from high acceleration levels). Length-to-diameter ratio usually is not a factor in initial configuration selection when $w_f < 0.3$.

Web fraction from 0.3 to 0.6.—When $w_f = 0.3$ to 0.5, the star satisfies typical requirements. The star can be configured to provide both acceptable burning

Table I.—Suitability of Grain Configurations for Neutral-Burning Applications

Configuration	Length-to-diameter ratio	Web fraction in typical applications						
		<0.1	0.1-0.2	0.2-0.3	0.3-0.5	0.5-0.6	0.6-0.9	>1.0
End burner	NA ¹							X
Internal-external-burning tube	NA				X			
Internal-burning tube	<2					X	X	
Segmented tube	>2					X	X	
Rod and shell	NA				X			
Star	NA				X	X		
Wagon wheel	NA		X	X				
Dendrite	NA		X					
Anchor	NA			X				
Slotted tube	>3					X	X	
Conocyl	2 to 4					X	X	
Finocyl	1 to 2						X	
Multigrain, multiperforated	NA	X						

¹not applicable

characteristics and reasonably high volumetric loading fraction. A star is ideally suited for $w_f = 0.3$ to 0.4 ; the progressivity of a star tends to increase with web fraction, however, when $w_f > 0.4$. The internal-external-burning tube and the rod and shell provide neutral-burning characteristics and also are applicable when $w_f < 0.5$; these tubular configurations are not preferred, however, because of problems related to grain support.

Requirements for both high volumetric-loading fraction and neutral burning frequently are more difficult to satisfy when $w_f = 0.5$ to 0.6 . If loading fraction can be satisfied by circular ported grains ($V_\ell = 0.75$ when $w_f = 0.5$, and $V_\ell = 0.84$ when $w_f = 0.6$),

an internal-burning tube (for $L/D < 2$), a conocyl (for $L/D = 2$ to 4), or a slotted tube (for $L/D > 3$) is applicable. Segmented tubes may also apply when $L/D > 2$. Frequently, however, required V_0 is greater than 0.85, and the additional propellant that can be provided by star points is required. If the progressivity of a high-web-fraction star cannot be tolerated, end effects from end burning may be sufficient to neutralize burning for $L/D < 4$. For larger L/D , a high-web-fraction star can be slotted (as in a slotted tube) to achieve a greater degree of neutrality.

Web fraction greater than 0.6.—Grain configurations that satisfy requirements for large web fractions generally are three dimensional; hence, length-to-diameter ratio is a significant variable in achieving burning neutrality. High-web-fraction configurations generally have circular ports, and control of burning surface is provided by unrestricted ends and longitudinal or radial slots.

Very large loading fractions can be satisfied provided that a suitable burning rate is available and structural integrity can be maintained. The internal-burning tube and finocyl are applicable when $L/D \sim 2$; the conocyl is applicable when $2 < L/D < 4$; and the slotted tube and segmented tube are applicable when $L/D > 3$. Suitability of slotted configurations depends on available process technology because of the complexities involved in forming the slots. The end burner may be applicable when burning rate is too high for use of an internal-burning grain and the upper limit of burning rate is adequate to satisfy duration.

Boost-sustain grains.—The grain designer should attempt to satisfy boost-sustain requirements with one of the boost-sustain concepts shown in figure 20. Combinations of the grain configurations defined in section 2.2.2.1 are applicable. A web fraction should be considered for each grain, it being recognized that in single-propellant tandem and some concentric configurations the sustain web burned during boost operation increases the total sustain web fraction needed for sustain duration. When the difference in durations of boost and sustain exceeds the range of burning rate achievable with a single propellant, it is necessary to use a dual-propellant grain, with the sustain grain having the lower burning rate. Dual-propellant grain configurations require additional manufacturing steps, but the added cost usually is not prohibitive.

In tandem configurations, special consideration should be given to (1) structural aspects of the transition region between the two configurations, and (2) shift in center of gravity.

General considerations.—The grain designer should understand that the classical grain configurations, although not proven to be completely unique, probably encompass all of the practical possibilities of grain configurations that are capable of providing reasonable thrust-time performance. Therefore, these configurations or variations thereof should be explored thoroughly before undefined grain configurations are

sought. In the final analysis, combinations of characteristic features of various configurations should be considered, particularly when required burning neutrality and volumetric loading fraction are difficult to achieve simultaneously. The grain design may be enhanced by addition of geometric elements, as in the following examples (ref. 26):

- Slotting a high-web-fraction progressive star to obtain neutrality
- Adding a conocyl to a standard high-web-fraction star to obtain neutrality
- Adding small star points to a low-web-fraction slotted tube to increase volumetric loading fraction
- Coning the ends of a tubular grain to obtain neutral burning
- Providing dual-length radial partial slots (not to the case wall) to provide desired burning patterns

Frequently, more than one grain configuration may be applicable to a given motor. In such cases, tradeoff variables related to ballistic performance, processing advantages, and structural aspects should be identified and evaluated further to provide an analytical basis for selection of the configuration.

3.2.2.3 Geometric Analysis

Techniques for estimating the variation of burning-surface area, burning perimeter, and port area with web distance burned shall simulate burning-front regression in actual motor operation.

It is recommended that analysis of burning-front regression be treated independently of ballistic analysis only when pressure drop and erosive burning are deemed insignificant; otherwise, burning-front regression depends on gas dynamic variables and should be treated in conjunction with performance-prediction analysis. Computer programs such as those in references 1, 57, 58, and 122 are required because of the complexity in solving the gas dynamic equations. Computer methods for generating burning perimeters, surfaces, and port areas are recommended when practical. The analysis should ensure that no detached sliver exists.

It is recommended that drafting techniques be used for burning-surface determination when computer programs are not available or computer methods are too costly. Scales used should be consistent with accurate measurement of the lines and areas denoting burning surfaces and port areas. Burning surfaces derived by drafting techniques should be checked by numerically integrating the scaled burning surfaces and comparing the integral with the

volume obtained independently as the product of length and cross section. The volume of propellant and burning surface-web are related by

$$V_p = \int A_b dw_x \quad (38)$$

Many numerical integration formulas are available for evaluating the integral in equation (38). One of the simplest and easiest to use is Simpson's rule. Stated analytically in terms of current variables, it is (ref. 129, p. 119)

$$\int A_b dw_x = \frac{\Delta w_x}{3} (A_{b,1} + 4 A_{b,2} + 2 A_{b,3} + 4 A_{b,4} + \dots + 4 A_{b,n-1} + A_{b,n}) \quad (39)$$

This equation requires surfaces to be determined at an even number of equal web increments Δw_x . Care should be taken to include all points of discontinuity in the function and its first derivative in calculating the surfaces as well as in providing inputs to computer programs for ballistic calculations. Failure to do so will give incorrect results for equation (39), as shown in figure 30, and for the associated ballistic calculations.

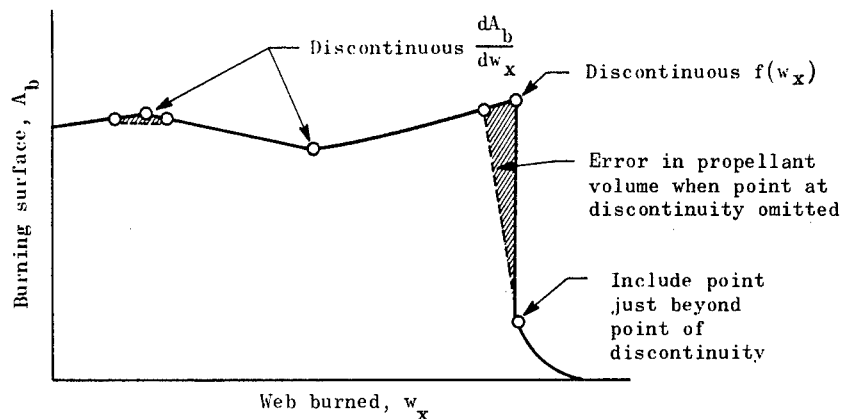


Figure 30.—Points of discontinuity for $A_b = f(w_x)$.

When temperature in the grain cross section is non-uniform, perimeter becomes a function of temperature as well as web burned, and Piobert's law no longer applies, even in two dimensions on a cross-sectional basis. A recommended approach to analysis of a grain containing a burning-rate gradient is based on a generalized two-dimensional analysis for determining perimeters (ref. 130). The burning-rate field is described by point values of burning rate at the intersection of concentric rings and radii emanating from the chamber center. Individual arcs within each sector are taken as isotherms corresponding to the average of the temperature at the extremities of each of the arcs.

3.3 Design Verification Analysis

3.3.1 Steady-State Mass Balance

The rate at which combustion products are generated by the propellant burning surface at the design pressure shall equal the rate at which combustion products are exhausted from and stored in the chamber.

To ensure steady-state mass balance at the desired pressure, the recommended practices of references 8 and 99 should be followed when characterizing the burning-rate sensitivity to pressure and temperature over the ranges of motor operation. Particular attention should be given to pressure/burning rate relation in regions where the pressure exponent n tends to increase or decrease. A requirement for $n < 1$ at motor operating pressure is fundamental to the stable operation of a solid rocket motor (fig. 29).

Equation (35) frequently is used to relate average pressure \bar{P} , average burning surface \bar{A}_b , and average burning rate \bar{r} . It should be recognized, however, that averages based on typical expressions for these three parameters

$$\bar{P} = \frac{1}{t} \int P dt \quad (40)$$

$$\bar{r} = w/t \quad (41)$$

$$\bar{A}_b = V_p/w \quad (42)$$

may not provide a consistent set of values for equation (35) for application to non-neutral pressure–time traces (refs. 93 and 131). Average pressure \bar{P} obtained from equation (35) by use of equations (41) and (42) will not necessarily be the same as \bar{P} from equation (40). In this regard, reference 131 notes that \bar{r} from equation (41) may be in error by as much as one percent for some non-neutral traces of practical interest. Reference 93 cites (for a specific example) that the error in \bar{P} when equation (42) is used for \bar{A}_b is 0.3 percent (based on $n = 0.25$ and a 50-percent progressive pressure–time trace). Even though these errors are small and may be insignificant for relatively neutral traces, the inconsistencies should be understood.

3.3.2 Burning-Rate Augmentation

The grain design shall provide for burning-rate variation induced by factors other than chamber pressure and grain temperature.

It is necessary to estimate the degree of burning-rate augmentation in the initial assessment of burning rate for web-fraction determination (sec. 3.1.2.4). Effects of erosive burning

should be considered in determining the average operating pressure (sec. 3.1.2.1). These preliminary estimates of erosive burning effects should be accurate in order to minimize the number of iterations required in the final analysis. Such estimates are best established from actual performance data of similar motors.

The performance prediction (sec. 3.3.3) should include a reliable analysis of erosive burning. Recommended techniques are presented in reference 99. In particular, it is recommended that calculation of erosive burning rates take into account gas velocity, mass flux, reference burning rate, and grain complexity. The method should account for the dependence of relative augmentation on the level of chamber pressure.

Potential effects of burning-rate augmentation at the propellant/liner interface should be recognized in case-bonded grains, including both end-burning and internal-burning configurations. These effects should be evaluated quantitatively on the basis of empirical data or laboratory burning-rate tests simulating motor conditions.

The grain designer should recognize the potential effect on burning rate and motor performance induced by acceleration forces from a spin environment, when applicable. Although burning-rate augmentation from spin may not be amenable to accurate prediction, an indication of the severity must be considered. A variety of test data that may be applicable to specific designs and may provide the basis for an estimate has been reported (see refs. cited in sec. 2.3.2). Further, testing of the propellant's sensitivity to this environment, either with slab samples or in subscale motors having grain design characteristics of the full-scale motor, is appropriate.

3.3.3 Performance Prediction and Iteration

The predicted ballistic performance shall satisfy, within tolerances given or implied, the ballistic requirements for MEOP, thrust, impulse, and duration.

The methods recommended in reference 99 should be applied in the performance prediction phase of grain design. Required inputs from the grain design are propellant properties (sec. 2.1.1.2), nozzle variables (sec. 2.1.2.2), and grain geometry variables (sec. 2.2.2.3). The grain design should be considered complete only when the required performance is substantiated by appropriate performance prediction and analysis and the grain is deemed structurally adequate.

Because the ballistic variables are applied in implicit functions, performance requirements usually will not be satisfied in the first analysis. The practices and procedures recommended for adjusting the design variables to satisfy the performance analysis are given below.

3.3.3.1 MEOP

The most common discrepancy requiring iteration is the first prediction of MEOP. Even when the desired maximum pressure is achieved in the first analysis, subsequent design revisions necessary to correct thrust or duration will affect maximum pressure. The methods for adjusting MEOP therefore apply also to thrust and duration (secs. 3.3.3.2 and 3.3.3.3).

In general the deficient MEOP should be modified by (1) altering the burning surface corresponding to maximum pressure, (2) revising burning rate or nozzle diameter or both to decrease (or increase) motor operating pressure, or (3) coning the aft end of the flow channel.

Alteration of burning surface.—Some configurations have sufficient flexibility to permit a change to initial or maximum burning surface without significantly affecting other ballistic properties. The function of the slot length in the slotted tube, for example, is to provide an independent control of initial burning surface and a degree of control of maximum pressure (ref. 67). The radius r_2 in the star configuration (fig. 11) provides an initially progressive burning surface and has been suggested as a control for initially high pressure (ref. 132). Another means for decreasing initial surface independently of specific grain geometries is the application of surface restrictors (ref. 113). This practice is recommended, however, only when other methods are not adequate.

Revisions to nozzle and burning rate.—The initial estimate of relative values of average thrust and pressure usually is reliable; i.e., when the estimated average pressure is attained, the estimated average thrust also will be attained. The independent requirement is thrust, not pressure. Therefore, any alteration to the operating pressure level necessitates revisions to the nozzle and burning rate to preserve the capability of the motor to deliver the required thrust.

Coning the propellant grain.—Proper tapering or coning of the flow channel will balance the mass flowrate and flow volume. The resulting reduced velocity at the aft end of the grain will tend to minimize the initial pressure peak (ref. 27).

The relationships between thrust, pressure, burning rate, and nozzle throat area are illustrated in figure 31. A decrease in pressure level requires an increase in nozzle throat area and burning rate to maintain the same thrust level. The surest way to determine exactly the burning rate and throat area for a desired average thrust and pressure value is to prepare a parametric presentation such as that depicted in figure 31. Approximately nine complete performance estimates are required to derive three constant-burning-rate lines, and several more to establish the constant-pressure lines. Therefore, the practicality of this approach when computerized techniques are involved depends on computer expense, available setup time, etc.

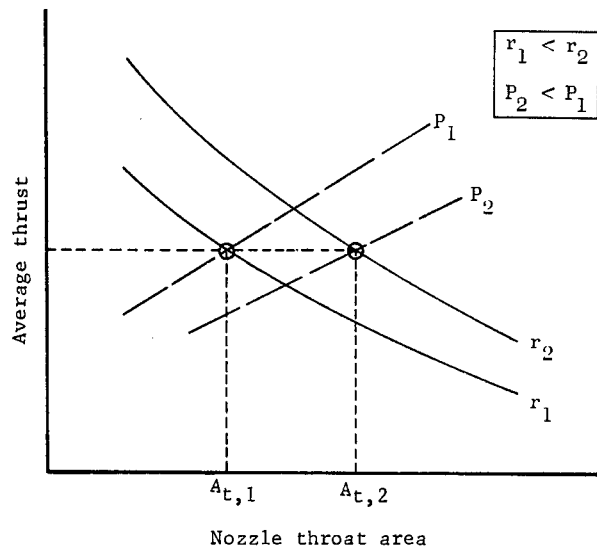


Figure 31.—Dependence of thrust on pressure, nozzle throat area, and burning rate.

Subsequent iterations, however, can be based on the simplified equations. When maximum and average pressure have been derived from the first performance prediction, the required revision to the design pressure to satisfy the MEOP limit can be estimated. With pressure and thrust values known, the revised nozzle throat area is obtained from equation (14) and the revised burning rate from equation (35). If the MEOP requirement is not satisfied by the second iteration, the two point values thus obtained on the first and second estimate should be sufficient for an accurate and final adjustment to burning rate or nozzle throat area or both for the third performance analysis.

3.3.3.2 Average Thrust

Thrust depends primarily on mass flowrate and delivered specific impulse. Therefore, predicted thrust can be varied by adjustment of the variables burning rate and nozzle throat area. However, the analyst must be mindful of the dependence of thrust coefficient, and hence impulse, on pressure.

Thrust less than required.—If MEOP limit will accommodate the necessary increase in pressure, the burning rate should be increased to correct pressure and thrust to the desired levels. The correction to burning rate may be obtained approximately by

$$r_2 = r_1 (P_2/P_1)^{1-n} \quad (43)$$

where the subscripts 1 and 2 correspond to the first and second analysis, respectively, and both burning rate values correspond to a common pressure. Erosive-burning variables render equation (43) an approximation that will slightly overcorrect burning rate, the degree depending on erosive burning severity.

If maximum pressure will exceed the MEOP limit when burning rate is increased, an increase in nozzle throat area as well as burning rate will be necessary to obtain the increased thrust with a smaller increase in pressure (fig. 31).

Thrust greater than required.—The preceding procedure should be reversed to effect a decrease in thrust. For an efficient ballistic design, the estimated MEOP should coincide with the limit on MEOP. Therefore, when one revises design variables to effect a pressure change, an effort should be made to display an estimated maximum pressure commensurate with the stipulated MEOP.

3.3.3.3 Duration and Impulse

Procedures for correcting thrust apply also to duration because of the dependence of average thrust on duration and impulse. When both thrust and duration cannot be made to coincide with desired values, a discrepancy exists in impulse. The only solution, apart from a change in propellant formulation or in nozzle design, is an increase (or decrease) in propellant weight. Adjustment must be made to either grain length or grain cross section to bring about an increase (or decrease) in propellant weight. Normally grain length cannot be varied, and propellant weight variations should be achieved by revision to cross-sectional dimensions. For example, if the estimated thrust satisfies requirements and duration is less than desired, (1) grain cross section must be increased, with revised burning rate dependent on web revision, or (2) if permitted, grain length must be increased with a commensurate decrease in burning rate.

When previous design revisions regarding MEOP considerations result in a lower operating pressure, a deficiency in total impulse may result because of the dependence of impulse on pressure (eqs. (1) and (11)). Except for possible changes in the nozzle design to increase the C_F efficiency factor, the only solution is to increase propellant weight, and the preceding procedures apply.

3.3.4 Design Acceptability and Optimization

The grain design shall be the most nearly optimum ballistic design permitted by the structural constraints, manufacturing capability, schedule, and cost.

The first level of ballistic design optimization should be applied when more than one configuration will satisfy ballistic requirements. The optimum configuration usually can be

identified by the ballistic merits alone (sec. 3.2.2.2). Otherwise, a structural or process requirement invariably will distinguish one grain configuration as optimum.

Within the design freedom of a single configuration, the designer should endeavor to (1) minimize the sliver content and (2) minimize the ratio P_{max}/\bar{P}_b . An absolute optimum design can be identified rarely if ever. A relatively optimum design, however, can be recognized by comparison or trade study. The designer should evaluate a reasonable number of variations, depending on schedule and budget constraints, and thereby provide a grain design that can be defined as optimum by comparative methods.

REFERENCES

1. Barron, J. G., Jr.; Cook, K. S.; and Johnson, W.C.: Grain Design and Internal Ballistics Evaluation Program (IBM 7094 FORTRAN IV). Program No. 64101 (AD 818321), Hercules Powder Co., Bacchus Works (Magna, UT), July 1967.
2. Whetstone, A. E.; Threewit, T. R.; and Billheimer, J. S.: Basic Grain Design and the 564 Interior Ballistics Computer Program. Rep. STM-143 (AD 805284), Aerojet-General Corp., June 10, 1961.
3. Billheimer, J. S.: The Ballistic Interface in Grain Configuration for Structural Analysis. Rep. AFRPL-TR-69-57 (Solid Rocket Structural Integrity Information Center, Univ. of Utah), Air Force Rocket Propulsion Lab., vol. 6, no. 2, Apr. 1969, pp. 1-40.
4. Billheimer, J. S.; and Wagner, F. R.: The Morphological Continuum in Solid Propellant Grain Design. Preprint P94, 19th Congress of International Astronautical Federation (New York, NY), Oct. 13-19, 1968.
5. Vogel, J. M.: A Quasi-Morphological Approach to the Geometry of Charges for Solid Rocket Propellants: The Family Tree of Charge Designs. Jet Propulsion, vol. 26, no. 2, Feb. 1956, pp. 102-105.
6. Anon.: Solid Rocket Motor Igniters. Space Vehicle Design Criteria Monograph, NASA SP-8051, March 1971.
7. Anon.: Solid Propulsion Nomenclature Guide. CPIA Publ. 80 (AD 465058), Chemical Propulsion Information Agency, Johns Hopkins Univ., May 1965.
8. Anon.: Solid Propellant Selection and Characterization. Space Vehicle Design Criteria Monograph, NASA SP-8064, June 1971.
9. Dudley, D. P.; Veitt, P. W.; and Billheimer, J. S.: The Man-Computer Link in Solid Propellant Rocket Preliminary Design and Optimization. Preprint 68-489, ICRPG/AIAA 3rd Solid Propulsion Conference (Atlantic City, NJ), June 4-6, 1968.
10. Anon.: Recommended Procedure for the Measurement of Specific Impulse of Solid Propellants. ICRPG Solid Propellant Rocket Static Test Working Group, CPIA Publ. 174, Aug. 1968.
11. Anon.: Solid Propellant Manual (U). CPIA/M2, Chemical Propulsion Information Agency, Johns Hopkins Univ., Apr. 1969. (Confidential)
12. Warren, F. A.: Rocket Propellants. Reinhold Publishing Corp., 1958.
13. Summerfield, M.; Sutherland, G. S.; Webb, M. J.; Taback, H. J.; and Hall, K. P.: Burning Mechanism of Ammonium Perchlorate Propellants. Solid Propellant Rocket Research, Part B, Martin Summerfield, ed., Academic Press, Inc., 1960, pp. 141-182.

14. Taylor, J.: Solid Propellant and Exothermic Compositions. Interscience Publishers, Inc., 1959.
15. Anon.: Engineering Design Handbook, Explosive Series, Solid Propellants, Part One. AMC Pamphlet AMCP 706-175, Headquarters, U.S. Army Materiel Command (Washington, DC), Sept. 1964.
16. Sampson, R.G.; and Maneely, D. J.: Design and Performance Scale-up of Large Solid Rocket Motors (U). Paper 3d, 62nd National Meeting, Am. Inst. Chem. Eng. (Salt Lake City, UT), May 21-24, 1967. (Confidential)
17. Brooks, W. T.: A Method for More Reproducible Burning Rate Determination. J. Spacecraft Rockets, vol. 7, no. 12, Dec. 1970, pp. 1488-1489.
18. Herrington, L. E.: Correlation of Motor and Strand Composite Propellant Burning Rate. AIAA J., vol. 2, no. 9, Sept. 1964, pp. 1671-1673.
19. Anon.: Solid Propellant Extended Environmental Capability Evaluation Program (U). Final Report, AFRPL-TR-66-155, Rocketdyne Solid Rocket Div., North American Rockwell Corp. (McGregor, TX), Aug. 1968. (Confidential)
20. Smith, R. C., Jr.: High Pressure Performance Studies. Quarterly Technical Summary Report, TR-PL-9716-02-1, Atlantic Research Corp. (Alexandria, VA), Dec. 1968. (Confidential)
21. Sutton, G. P.: Rocket Propulsion Elements. Third ed., John Wiley & Sons, Inc., 1963.
22. Shapiro, A. H.: The Dynamics and Thermodynamics of Compressible Fluid Flow. Vol. I, The Ronald Press Co., 1953.
23. Barrere, M.; Jaumotte, A.; Fraeijs de Veubeke, B.; and Vandekerckhove, J.: Rocket Propulsion. D. Van Nostrand Co., Inc., 1960.
24. Rao, G. V. R.: Evaluation of Conical Nozzle Thrust Coefficient. ARS J., vol. 29, no. 8, Aug. 1959, pp. 606-607.
25. Landsbaum, E. M.: Thrust of a Conical Nozzle. ARS J., vol. 29, no. 3, Mar. 1959, pp. 212-213.
26. Anon.: Rocket Motor Manual (U). CPIA/M1, Chemical Propulsion Information Agency, Johns Hopkins Univ., July 1970. (Confidential)
- *27. Gibby, H.: Ignition Transients Control Through Propellant Grain Coning. Rep. MP-63-232-U, Wasatch Div., Thiokol Chemical Corp. (Brigham City, UT), Oct. 16, 1963.
28. Fenech, E. J.; and Billheimer, J. S.: Use of Internal Grain Configuration to Predict Erosive Burning Constant. Paper 61-8, Western States Section, The Combustion Institute (Pacific Palisades, CA), Apr. 1961.

*Dossier for design criteria monograph "Solid Propellant Grain Design and Internal Ballistics." Unpublished, 1970. Collected source material available for inspection at NASA Lewis Research Center, Cleveland, OH.

- *29. Glick, R. L.; and Thurman, J. L.: An Analysis of the Circumferential Slot Effects on the Internal Ballistics of the TX354 Motor. Rep. U-65-11A, Huntsville Div., Thiokol Chemical Corp. (Huntsville, AL), Feb. 22, 1965.
30. Anon.: Solid Propellant Processing Factors in Rocket Motor Design. Space Vehicle Design Criteria Monograph, NASA SP-8075, Oct. 1971.
31. Anon.: Solid Propellant Grain Structural Integrity Analysis. Space Vehicle Design Criteria Monograph, NASA SP-8073 (to be published).
32. Oxley, J. H.: Development of the CONDOR Solid Propulsion System—A Status Report (U). Bulletin of 26th JANNAF Solid Propulsion Meeting (Washington, DC), July 14-16, 1970, Vol. I, CPIA Publ. 196, May 1970, pp 3-19. (Confidential)
33. Hecht, J. F., Sr.: Poseidon Gas Generator Development (U). Bulletin of 4th ICRPG Solid Propulsion Meeting (Chicago, IL), May 20-22, 1969, Vol. I, CPIA Publ. 188, Apr. 1969, pp. 17-28. (Confidential)
34. Fulbright, J. L.; and Miller, W. H.: Failure Analysis of Solid Propellant Grains Based on Dissected Motor Properties. Bulletin of ICRPG Mechanical Behavior Working Group (Pasadena, CA), Dec. 5-6, 1967, Vol. I, CPIA Publ. 158, Oct. 1967, pp. 377-392.
- *35. Bermender, N. W.: A Method to Reduce the Temperature Sensitivity of Solid Propellant Rocket Motors by Automatically Controlling the Burning Area. Rep. DDM 61-17, Rocketdyne Solid Rocket Div., North American Rockwell Corp. (McGregor, TX), Aug. 18, 1961.
36. Fuller, W. H.; and Platt, R.T.: Dual Propellant Grain Geometries for High Performance Rockets (U). Bulletin of 17th Meeting JANAF-ARPA-NASA Solid Propellant Group (Denver, CO), May 23-25, 1961, Vol. II, SPIA, May 1961, pp. 185-202 (AD 326146). (Confidential)
37. Hinderer, B. F.: Development of the Mk 38 Mod 0 Rocket Motor for the SPARROW III-6b Missile (U). Bulletin of 18th Interagency Solid Propulsion Meeting (Seattle, WA), Vol. IV, CPIA Publ. 18A, July 1963, pp. 577-596 (AD 346945). (Confidential)
38. Anon.: Qualification Test, Mk 25 Mods 0, 1, and 2 Rocket Motor (U). Rep. R-4003-4, Rocketdyne Solid Rocket Div., North American Rockwell Corp. (McGregor, TX), July 8, 1960. (Confidential)
- *39. Burchfield, P. B.: Design Parameters for a Tubular Charge Burning Internally on One and Both Ends. Rep. ADM 59-15, Rocketdyne Solid Rocket Div., North American Rockwell Corp. (McGregor, TX), Oct. 12, 1959.
- *40. Wagner, F. R.: Burning Surface Area and Other Formulas for Internal-Burning, Cylindrically Perforated Grains with Unrestricted Burning from Both Ends. Rep. UTEC ME 67-089, Univ. of Utah, Dec. 27, 1967.

*Dossier for design criteria monograph "Solid Propellant Grain Design and Internal Ballistics." Unpublished, 1970. Collected source material available for inspection at NASA Lewis Research Center, Cleveland, OH.

41. Simmons, D.A.; and Westphal, L. O.: 260-SL-3 Motor Firing Results. Bulletin of 4th ICRPG Combustion Conference (Menlo Park, CA), Oct. 2-13, 1967, Vol. I, CPIA Publ. 162, Dec. 1967, pp. 381-387.
42. Shafer, J. I.: Solid Rocket Propulsion. Space Technology, ch. 16, Howard S. Seifert, ed., John Wiley & Sons, Inc., 1959.
- *43. Shafer, J. I.: Development of the Star Configuration. Unpublished, 1970.
44. Avery, W. H.; and Beek, J., Jr.: Propellant Charge Design of Solid Fuel Rockets. Rep. 5809, Office of Scientific Research and Development, June 1946.
- *45. Vogel, J. M.: The Design of Solid-Propellant Grains for Rocket Motors. Rep. 308-19-52RF, Rocketdyne Solid Rocket Div., North American Rockwell Corp. (McGregor, TX), 1952.
46. Bartley, C.E.; and Mills, M. M.: Solid Propellant Rockets. Jet Propulsion Engines, Sec. H, E. O. Lancaster, ed., Princeton Univ. Press, 1959.
47. Piasecki, L.; and Robillard, G.: Generalized Design Equations for an Internal-Burning Star-Configuration Solid-Propellant Charge and Method of Calculating Pressure-Time and Thrust-Time Relationships. JPL Memo 20-135, Jet Propulsion Lab., Calif. Inst. Tech. (Pasadena, CA), Sept. 18, 1956.
48. Vandekerckhove, J.: Internal-Burning Star and Wagon-Wheel Designs for Solid Propellant Grains. Publication de l'Institut d'Aeronautique, Université Libre de Bruxelles, 1958 (Available also as ref. 23, sec. 6.2).
49. Stone, M. W.: A Practical Mathematical Approach to Grain Design. Jet Propulsion, vol. 28, no. 4, Apr. 1958, pp. 236-244.
50. Vandekerckhove, J. A.: Comment on: A Practical Approach to Grain Design. Jet Propulsion, vol. 28, no. 11, Nov. 1958, pp. 766-768.
51. Anon.: Quarterly Progress Report on Interior Ballistics for Apr. to July 1955. Rep. P-55-15, Redstone Arsenal Research Div., Rohm and Haas Co. (Huntsville, AL), Aug. 1955. (Confidential)
52. Jackson, F.: Star Center Burning Surfaces. CARDE TM 312/60, Canadian Armament Research and Development Establishment, Dec. 1960.
53. Lumpkin, H.K.: Mathematical Approach to Solid Propellant Grain Design. ARGMA TN 1G5N, Army Rocket and Guided Missile Agency, Ordnance Missile Laboratories Div. (Huntsville, AL), Dec. 21, 1959.

*Dossier for design criteria monograph "Solid Propellant Grain Design and Internal Ballistics." Unpublished, 1970. Collected source material available for inspection at NASA Lewis Research Center, Cleveland, OH.

54. Silman, K. E.; and Treutler, H.: Some Aspects of the Problem of Plastic Propellant Charge Design (U). Bulletin of 15th Meeting JANAF Solid Propellant Group (Washington, DC), June 16-18, 1959, Vol. I, SPIA, June 1959, pp. 193-230. (Confidential)
55. Kasky, B.: Grain Design Handbook. Rep. 3Y12, Rocket Development Laboratories, Ordnance Missile Laboratories, Redstone Arsenal (Huntsville, AL), June 8, 1956.
56. Anon.: Quarterly Progress Report On Interior Ballistics. Rep. P-56-1, Redstone Arsenal Research Div., Rohm and Haas Co. (Huntsville, AL), Feb. 10, 1956. (Confidential)
57. Anon.: Solid Propellant Rocket Motor Internal Ballistics Computer Program, (Program Manual). Rep. RK-TR-67-7 (AD 822349), The Boeing Co. (Seattle, WA), Sept. 1967.
58. Threewit, T.R.; Rossini, R. A.; and Uecker, R. L.: The Integrated Design Computer Program and the ACP-1103 Interior Ballistics Computer Program. Rep. STM-180 (AD 466965), Aerojet-General Corp., Dec. 1, 1964 (Suppl. 1, Mar. 1, 1965; suppl. 2, Nov. 20, 1965).
59. Stone, M. W.: Modified Wagon Wheel Grain Design. Rep. S-30 (AD 257620), Redstone Arsenal Research Div., Rohm and Haas Co. (Huntsville, AL), May 15, 1961.
60. Stone, M. W.: Modified Wagon Wheel Grain Design. Rep. S-33 (AD 273012), Redstone Arsenal Research Div., Rohm and Haas Co. (Huntsville, AL), Feb. 14, 1962.
61. Stone, M.W.: Modified Wagon Wheel Grain Design. Rep. S-36 (AD 285192), Redstone Arsenal Research Div., Rohm and Haas Co. (Huntsville, AL), Oct 1962.
62. Peretz, A.: A Practical Mathematical Approach to the Dendrite Design of Solid Propellant Grains. J. Spacecraft Rockets, vol. 6, no. 8, Aug. 1969, pp. 944-946.
63. Whetstone, A. E.; Threewit, T.R.; and Rossini, R. A.: Intermediate Grain Design and the ACP-564B Interior Ballistics Computer Program. Rep. STM-148, Aerojet-General Corp., Feb. 20, 1962.
64. Stone, M. W.: The Slotted Tube Grain Design. Rep. S-27 (AD 248599), Redstone Arsenal Research Div., Rohm and Haas Co. (Huntsville, AL), Dec. 23, 1960.
65. Stone, M. W.: Slotted Tube Grain Design. ARS J., vol. 31, no. 2, Feb. 1961, pp. 223-228.
66. Anon.: Qualification of the Mk 47 Mod 0 Rocket Motor for XAIM-54A (PHOENIX) Guided Missile (U). Rep. R-4485, Rocketdyne Solid Rocket Div., North American Rockwell Corp. (McGregor, TX), Feb. 19, 1968. (Confidential)
67. Stone, W. C.: Practical Method for Compensation of Erosive Pressure Peaks. ARS J., vol. 31, no. 9, Sept. 1961, pp. 1288-1289.
68. Crooks, J. R.: Skybolt Propulsion System (U). Bulletin of 18th Meeting JANAF-ARPA-NASA Solid Propellant Group (Pittsburgh, PA), June 5-7, 1962, Vol. I, SPIA, June 1962, pp. 113-122. (Confidential)

69. Barth, K.: Weapon System 133B, Second-Stage Minuteman Wing VI Motor Data Book (U). GM TR016500478 (AD 352215), Aerojet-General Corp., Aug. 1, 1964. (Confidential)
- *70. Speak, C. A.: Application of the Finocyl Configuration. Unpublished, 1970.
71. Groetzinger, W. H., III: In-Tube-Burning Rockets for Advanced Light Assault Weapons (U). Rep. S-208, Redstone Arsenal Research Div., Rohm and Haas Co. (Huntsville, AL), Apr. 1969. (Confidential)
72. Burkes, W. M.: Eject Motor Characteristics for Tube-Launched Weapon Systems (U). Paper presented at AIAA 5th Propulsion Joint Specialist Conference (U.S. Air Force Academy, CO), June 9-13, 1969. (Confidential)
73. Brooks, W. T.: Development of Propulsion for Forward Area Air Defense (U). Paper presented at AIAA 5th Propulsion Joint Specialist Conference (U.S. Air Force Academy, CO), June 9-13, 1969. (Confidential)
74. Thibodaux, J. G.; Swain, R.L.; and Wright, G.: Analytical and Experimental Studies of Spherical Solid-Propellant Rocket Motors (U). NACA RM L57G12a, 1957. (Confidential)
75. Andrews, W. G.; and Reed, D.R.: Spherical Rocket Motors for Space and Upper Stage Propulsion. IAF Paper P24, 19th Congress of International Astronautical Federation (New York, NY), Oct. 13-19, 1968.
76. Roach, J. E.; and Martino, E. A.: Spherical Rocket Engines (U). Bulletin of 16th Meeting JANAF Solid Propellant Group (Dallas, TX), June 14-16, 1960, Vol. II, SPIA, June 1960, pp. 61-72 (AD 317113). (Confidential)
77. Segal, H. M.: Design Method for Spherical Grains. ARS J., vol. 30, no. 4, Apr. 1960, pp. 370-371.
78. Segal, H. M.: Preliminary Thrust-Time Curve for a Spherically Shaped Solid Propellant Rocket Motor. ARS J., vol. 31, no. 10, Oct. 1961, pp. 1447-1450.
79. Anon.: Research Study to Advance the State of the Art of Solid Propellant Grain Design (U). Quarterly Progress Report, E248-59A, Elkton Div., Thiokol Chemical Corp. (Elkton, MD), Aug. 1959. (Confidential)
80. Berti, J. W.; and Wrubel, J. A.: Calculating Burning Surface Areas of Internal Burning Spherical Charges. ARS J., vol. 32, no. 8, Aug. 1962, pp. 1283-1285.
81. Ritchey, H. W.: Tailor-Made Thrust. Jet Propulsion, vol. 25, no. 10, Oct. 1955, p. 550.
82. Anderson, S. E.: Design and Evaluation of a Propulsion Unit for a Single-Stage Hercules (U). Rep. S-48, Redstone Arsenal Research Div., Rohm and Haas Co. (Huntsville, AL), July 8, 1964. (Confidential)

*Dossier for design criteria monograph "Solid Propellant Grain Design and Internal Ballistics." Unpublished, 1970. Collected source material available for inspection at NASA Lewis Research Center, Cleveland, OH.

83. Anderson, S. E.: Scale-up and Demonstration Firings of a Low-Signature NF Propellant (U). Rep. S-169, Redstone Arsenal Research Div., Rohm and Haas Co. (Huntsville, AL), June 1968. (Confidential)
84. McClendon, S. E.: Mission Performance Advantage and Flexibility Afforded by Solid Rocket Propulsion Utilizing a Dual Area Nozzle (U). Bulletin of AIAA 6th Propulsion Joint Specialist Conference (San Diego, CA), June 15-19, 1970, CPIA Publ. 202, June 1970, pp. 209-236. (Confidential)
85. Rogers, K. H.: Mathematical Design of a Sliverless Rocket Engine. Preprint 1616-61, ARS Solid Propellant Rocket Conference (Salt Lake City, UT), Feb. 1-3, 1961.
- *86. Vogel, J. M.: Solid and Hybrid Rocket Technology. Rep. UTC 268, Vol. I, United Technology Center (Sunnyvale, CA), June 1961.
87. Podel, H. C.: The Practical Application of a Bi-Propellant Grain System in Large Solid Rocket Engines (U). Bulletin of 16th Meeting JANAF Solid Propellant Group (Dallas, TX), June 14-16, 1960, Vol. II, SPIA, June 1960, pp. 1-22 (AD 317113). (Confidential)
- *88. Kershner, R. B.: Interior Ballistics of Rockets. Solid Propellant Technology, AIAA Selected Reprint Series, Vol. 10, F. A. Warren, ed., Feb. 1970 (Available also as Interior Ballistics of Rockets. Rocket Fundamentals, Ch. 3. OSRD no. 3992, B. L. Crawford, Jr., ed., George Washington Univ., Allegany Ballistics Lab., Dec. 26, 1944).
89. Anon.: Qualification Test Report for F-104 G ZELL Rocket Motor. Rep. R-4249A, Rocketdyne Solid Rocket Div., North American Rockwell Corp. (McGregor, TX), July 12, 1964.
90. Anon.: Development of XM-34 Rocket Motor. Rep. 740-4-58, Rocketdyne Solid Rocket Div., North American Rockwell Corp. (McGregor, TX), Oct. 1958. (Confidential)
- *91. Brooks, W. T.: Burning Surfaces of the Slab Configuration. Unpublished, 1970.
92. Lewis, S. R.: Design of Solid Propellant Gas Generators for Transient Operation. Paper presented at ICRPG/AIAA 2nd Solid Propulsion Conference (Anaheim, CA), June 6-8, 1967.
93. Rossini, R. A.; Billheimer, J. S.; and Threewit, T. R.: Configuration Efficiency: A New Measure of Ballistic Quality for a Grain Design. ARS J., vol. 31, no. 12, Dec. 1961, pp. 1761-1764.
94. Epstein, L. I.: The Design of Cylindrical Propellant Grains. Jet Propulsion, vol. 26, no. 9, Sept. 1956, pp. 757-759.
95. Huggett, C.: Combustion of Solid Propellants. High Speed Aerodynamics and Jet Propulsion, Vol. II - Combustion Processes, Sec. M, B. Lewis, R. N. Pease, and H. S. Taylor, eds., Princeton Univ. Press, 1956.

*Dossier for design criteria monograph "Solid Propellant Grain Design and Internal Ballistics." Unpublished, 1970. Collected source material available for inspection at NASA Lewis Research Center, Cleveland, OH.

96. Peterson, E. G.; Nielsen, C. C.; Johnson, W. C.; Cook, K. S.; and Barron, J. G.: Generalized Coordinate Grain Design and Internal Ballistics Evaluation Program. Preprint 68-490, ICRPG/AIAA 3rd Solid Propulsion Conference (Atlantic City, NJ), June 4-6, 1968.
97. Anon.: A Research Study to Advance the State-of-the-Art of Solid Propellant Grain Design. Quarterly Progress Report, E181-60, Vol. I, Elkton Div., Thiokol Chemical Corp. (Elkton, MD), Oct. 28, 1960.
98. Gorny, L. J.: A Generalized Approach to Rapid Evaluation of Solid Propellant Grain Geometries. Preprint 2316-62, ARS Solid Propellant Rocket Conference (Waco, TX), Jan. 24-26, 1962.
99. Anon.: Solid Rocket Motor Performance Analysis and Prediction. Space Vehicle Design Criteria Monograph, NASA SP-8039, May 1971.
100. Miller, W. H.; and Barrington, D. K.: A Review of Contemporary Solid Rocket Motor Performance Prediction Techniques. *J. Spacecraft Rockets*, vol. 7, no. 3, Mar. 1970, pp. 225-237.
- *101. Blatz, P. J.: On the Ballistic Behavior of Constant-Pressure-Exponent Solid Propellants. Preprint SC-PP-67-141, Science Center, North American Rockwell Corp. (Los Angeles, CA), Jan. 1968.
102. Robillard, G.; and Lenoir, J. M.: The Development of a New Erosive Burning Law. Publ. 91, Jet Propulsion Lab., Calif. Inst. Tech. (Pasadena, CA), Apr. 1, 1957.
103. Saderholm, C. A.: A Characterization of Erosive Burning for Composite H-Series Propellant. Paper presented at AIAA Solid Propellant Rocket Conference (Palo Alto, CA), Jan. 29-31, 1964.
104. Green, L., Jr.: Erosive Burning of Some Composite Solid Propellants. *Jet Propulsion*, vol. 24, no. 1, Jan.-Feb. 1954, pp. 9-15, 26.
105. Lawrence, W. J.; Matthews, D. R.; and Deverall, L. I.: The Experimental and Theoretical Comparison of the Erosive Burning Characteristics of Composite Propellants. Preprint 68-531, ICRPG/AIAA 3rd Solid Propulsion Conference (Atlantic City, NJ), June 4-6, 1968.
106. Geckler, R. D.; and Sprenger, D. F.: The Correlation of Interior Ballistic Data for Solid Propellants. *Jet Propulsion*, vol. 24, no. 1, Jan.-Feb. 1954, pp. 22-26.
107. Vandekerckhove, J. A.: Erosive Burning of a Colloidal Solid Propellant. *Jet Propulsion*, vol. 28, no. 9, Sept. 1958, pp. 599-603.
108. Lawrence, W. J.; and Deverall, L. I.: The Erosive Burning Behavior of Selected Composite Propellants. Bulletin of 4th ICRPG Combustion Conference (Menlo Park, CA), Oct. 2-13, 1967, Vol. I, CPIA Publ. 162, Dec. 1967, pp. 459-465.
109. Zucrow, M. J.; Osborn, J. R.; Murphy, J. M.; and Kershner, S. D.: Investigation of Velocity Upon Burning Rate of Solid Propellants (U). Rep. F-63-3, JPC 352 (AD 346175), Jet Propulsion Center, Purdue Univ., Dec. 1963. (Confidential)

*Dossier for design criteria monograph "Solid Propellant Grain Design and Internal Ballistics." Unpublished, 1970. Collected source material available for inspection at NASA Lewis Research Center, Cleveland, OH.

110. Kreidler, J. W.: Erosive Burning: New Experimental Techniques and Methods of Analysis. Preprint 64-155, AIAA Solid Propellant Rocket Conference (Palo Alto, CA), Jan. 29-31, 1964.
111. Marklund, T.; and Lake, A.: Experimental Investigation of Propellant Erosion. ARS J., vol. 30, no. 2, Feb. 1960, pp. 173-178.
112. Viles, J. M.: Measurement of Erosive Burning Rates. Rep. S-213, Redstone Arsenal Research Div., Rohm and Haas Co. (Huntsville, AL), Jan. 1969.
113. Gibby, H.: Ignition Transient Control through Inhibiting of Propellant Grain. J. Spacecraft Rockets, vol. I, no. 6, Nov.-Dec. 1964, pp. 692-693.
114. Northam, G. B.; and Lucy, M. H.: On the Effects of Acceleration Upon Solid Rocket Performance. Preprint 68-530, 3rd ICRPG/AIAA Solid Propulsion Conference (Atlantic City, NJ), June 4-6, 1968.
115. Crowe, C. T.; and Willoughby, P. G.: Effect of Spin on the Internal Ballistics of a Solid-Propellant Motor. Preprint 66-523, AIAA Fourth Aerospace Sciences Meeting (West Coast), June 27-29, 1966.
116. Glick, R. L.: An Analytical Study of the Effects of Radial Acceleration Upon the Combustion Mechanism of Solid Propellant. Rep. 42-66, Thiokol Chemical Corp. (Huntsville, AL), Dec. 1966.
117. Sturm, E.J.; and Reichenback, R. E.: An Experimental Study of the Effect of Solid Ingredient Particle Size on Burning Rates of Composite Propellants in Acceleration Fields. Bulletin of 4th ICRPG Combustion Conference (Menlo Park, CA), Oct. 2-13, 1967, Vol. I, CPIA Publ. 162, Dec. 1967, pp. 467-479.
118. Manda, L. J.: Compilation of Rocket Spin Data. Vol. I, NASA CR-66625, 1968; Vol. II, NASA CR-66641, 1968; Vol. III, NASA CR-66679, 1968.
119. Anon.: A Research Study to Advance the State-of-the-Art of Solid-Propellant Grain Design. Summary Report E92-63 (AD 420826), Elkton Div., Thiokol Chemical Corp. (Elkton, MD), Oct. 1963.
120. Coy, J. B.: Influence of Strain on Burning Rate (U). Quarterly Summary Report, CIT/JPL-QSR-38-4, Jet Propulsion Lab., Calif. Inst. Tech. (Pasadena, CA), July 1961. (Confidential).
121. Saylak, D.: The Effect of Strain on the Burning Rate of Solid Propellants. Bulletin of Second ICRPG Working Group on Mechanical Behavior (Hill Air Force Base, UT), Nov. 19-21, 1963, CPIA Publ. 27, Oct. 1963 (AD 345530). (Confidential)
- *122. Cunningham, J. M.: Gas Dynamics and Its Influence on Erosive Burning in Prediction of Ballistic Performance of Solid Rocket Motors. Rep. DDM 70-1, Rocketdyne Solid Rocket Div., North American Rockwell Corp. (McGregor, TX), Mar. 16, 1970.

*Dossier for design criteria monograph "Solid Propellant Grain Design and Internal Ballistics." Unpublished, 1970. Collected source material available for inspection at NASA Lewis Research Center, Cleveland, OH.

123. Liepmann, H. W.; and Roshko, A.: Elements of Gas Dynamics. John Wiley & Sons, Inc., 1963.
- *124. Speak, C. A., et al.: State-of-the-Art Performance Reproducibility. Unpublished, 1970.
- *125. Speak, C. A.: Specific Impulse; Standardization of Nomenclature, Correction Procedures and Performance Efficiency Calculations. Report TWR-3506, Wasatch Div., Thiokol Chemical Corp. (Brigham City, UT), Aug. 20, 1969.
126. Brown, L. M.; and Cockrell, B.C.: Micro-Motor Evaluation of Specific Impulse (U). Bulletin of 18th Meeting JANAF-ARPA-NASA Solid Propellant Group (Pittsburgh, PA), June 5-7, 1962, Vol. III, SPIA, June 1962. (Confidential)
127. Peterson, J. A.: The Selection of the Optimum Solid Propellant. Paper presented at 53rd National Meeting, Am. Inst. Chem. Eng. (New York, NY), May 1964.
128. Gordon, L. J.: Ballistic Effects of Pyrolyzed Liner in Solid Propellant Motor Firings. ARS J., vol. 30, no. 5, May 1960, pp. 502-503.
129. Nielsen, K. L.: Methods in Numerical Analysis. The Macmillan Co., 1960.
- *130. Chan, G. O.: Generalized Two-Dimensional Burning Perimeters with Temperature Gradient. Unpublished, 1970.
131. Brock, F. H.: Average Burn Rate, Average Pressure Relationships in Solid Rockets. J. Spacecraft Rockets, vol. 3, no. 12, Dec. 1966, pp. 1802-1803.
132. Billheimer, J. S.: Case-Bonded Grain Designs for High Loading Long Duration Solid Propellant Motors (U). Bulletin of 15th Meeting, JANAF Solid Propellant Group (Washington, DC), June 16-18, 1959, Vol. I, SPIA, June 1959, pp. 231-246. (Confidential)
-
- *Dossier for design criteria monograph "Solid Propellant Grain Design and Internal Ballistics." Unpublished, 1970. Collected source material available for inspection at NASA Lewis Research Center, Cleveland, OH.

GLOSSARY

Symbols and terms used in the text in general are consistent with the nomenclature guide in reference 7 and with usage in the industry. Each symbol and many of the terms used in the monograph are listed in this section with an explanation sufficient for identification. When symbols appearing in material extracted directly from a reference did not conform exactly to definitions given below, the reference symbols were not used. Parenthetical units are in the International System of Units (SI Units).¹

<u>Symbol</u>	<u>Definition</u>	<u>Appears In</u>
$A_b, A_{b,i}$	area of propellant burning surface, in. ² (m ²) (i = 1, 2, etc)	eqs. (19), (22), et al.
\bar{A}_b	average burning surface, in. ² (m ²)	eq. (42)
A_e	flow area at nozzle exit plane, in. ² (m ²)	eq. (14)
A_p	flow area at grain port, in. ² (m ²)	eqs. (17), (18), (37)
$A_t, A_{t,i}$	flow area at nozzle throat, in. ² (m ²) (i = 1, 2)	eqs. (14), (17b), et al.; fig. 31
a, a _i	coefficient of pressure or constant in burning rate equations (i = 1, 2)	eqs. (3), (4), et al.; fig. 3
b	coefficient of pressure in burning rate equations	eqs. (4), (5)
C_D	discharge coefficient, kg/(N-sec)	eqs. (1), (34), (35)
C_F	nozzle thrust coefficient, dimensionless	eq. (1)
$C_{F, act}$	actual thrust coefficient reflecting all nozzle losses	eqs. (11), (14)
C_F°	ideal thrust coefficient	eq. (10)
$C_{F, vac}^\circ$	ideal thrust coefficient in vacuum	eqs. (11), (14)
c*	characteristic exhaust velocity, ft/sec (m/sec)	eqs. (1), (34), et al.
D	outside diameter of grain, in. (m)	eqs. (16), (17), et al.
D_r	outside diameter of rod element in rod-and-shell configuration, in. (m)	fig. 10
d	inside diameter of grain, in. (m)	definitions following eq. (16); eqs. (22), (23)

¹Mechtly, E.A.: The International System of Units. Physical Constants and Conversion Factors, Revised. NASA SP-7012, 1969.

<u>Symbol</u>	<u>Definition</u>	<u>Appears In</u>
d_s	inside diameter of shell element in rod and shell configuration, in. (m)	fig. 10
F	thrust, lbf (N)	eqs. (14), (19)
\bar{F}_a	action-time average thrust, lbf (N)	fig. 2
\bar{F}_b	burning-time average thrust or average boost thrust, lbf (N)	figs. 2, 21
F_{max}	maximum thrust, lbf (N)	fig. 2
\bar{F}_s	average sustain thrust, lbf (N)	fig. 21
g_c	gravitational conversion constant, 32.17 lbf-ft/lbf-sec ²	eqs. (1), (34), (35)
I	impulse, lbf-sec (N-sec)	fig. 1
I_{sp}	propellant specific impulse, lbf-sec/lbm (N-sec/kg)	eq. (1)
I_{spd}	measured (delivered) propellant specific impulse, lbf-sec/lbm (N-sec/kg) (ratio of I_{tot} to propellant weight, corresponding to \bar{P} , ϵ , P_{amb} , and a [half angle] of the motor [ref. 10])	eqs. (2), (15), (19)
I_{sps}	standard deliverable propellant specific impulse, lbf-sec/lbm (N-sec/kg) (value of I_{spd} corrected to $P_c = 1000$ psia, $P_{amb} = 14.7$ psia, optimum ϵ , $a = 0^\circ$ [ref. 10])	sec. 2.1.1.2.1
I_{tot}	total impulse, lbf-sec (N-sec) (total integral of thrust-time)	eq. (15)
I_{spd}^o	theoretical delivered propellant specific impulse, lbf-sec/lbm (N-sec/kg) (theoretical I_{sp} corresponding to particular values of \bar{P} , ϵ , P_{amb} , and a [ref. 10])	eq. (2)
I_{sps}^o	standard theoretical propellant specific impulse, lbf-sec/lbm (N-sec/kg) (theoretical I_{sp} at standard conditions of $P_c = 1000$ psia, $P_e = P_{amb} = 14.7$ psia, optimum ϵ , $a = 0^\circ$ [ref. 10])	sec. 2.1.1.2.1
$1/J$	port-to-throat area ratio, A_p/A_t	definition following eq. (17b)

<u>Symbol</u>	<u>Definition</u>	<u>Appears In</u>
K_n	burning surface-to-throat area ratio, A_b/A_t	eqs. (6), (8)
L	grain length, in. (m)	eqs. (20), (22), et al.
L_a	linear dimension in wagon wheel, dendrite, and dogbone, in. (m)	figs. 12, 13, 15
L_i	linear dimension in anchor, in. (m) ($i = 1, 2$)	fig. 14
ℓ	slot length in slotted tube, in. (m)	fig. 16
\bar{M}	average molecular weight, lbm/lbm-mole (kg/kg-mole)	sec. 2.1.1.2.1
MEOP	maximum expected operating pressure, lbf/in. ² (N/m ²) (upper limit on maximum pressure)	fig. 2
\dot{m}	propellant mass flowrate, lbm/sec (kg/sec)	eq. (19)
\dot{m}_e	propellant mass flowrate consistent with nozzle discharge capability, lbm/sec (kg/sec)	eq. (34)
\dot{m}_g	propellant mass flowrate generated in the chamber, lbm/sec (kg/sec)	eq. (33)
N	configuration symmetry number, number of star points	eqs. (27), (28)
n	pressure exponent in de Saint Robert's burning-rate law	eqs. (3), (35), (36), (43)
P, P_i	pressure, lbf/in. ² (N/m ²) ($i = 1, 2, 3, 4$)	eqs. (6), (7), (9), (43)
\bar{P}	average pressure, lbf/in. ² (N/m ²)	eq. (40)
\bar{P}_a	action-time average chamber pressure, lbf/in. ² (N/m ²)	fig. 2
P_{amb}	ambient barometric pressure, lbf/in. ² (N/m ²)	eqs. (10), (11), (14)
\bar{P}_b	burning-time average chamber pressure or average boost pressure, lbf/in. ² (N/m ²)	fig. 2
P_c	chamber pressure, lbf/in. ² (N/m ²)	eqs. (3), (4), et al.
P_e	exit plane pressure, lbf/in. ² (N/m ²)	eqs. (10), (11), (14)
P_{max}	maximum chamber pressure, lbf/in. ² (N/m ²)	fig. 2

<u>Symbol</u>	<u>Definition</u>	<u>Appears In</u>
Q	burning perimeter of grain, in. (m)	eq. (18)
R	outer radius of grain, in. (m)	eq. (31)
r, r_i	propellant burning rate, in./sec (m/sec) ($i = 1, 2, 3, 4$)	eqs. (3) through (5), et al; figs. 3, 6
\bar{r}	average burning rate, in./sec (m/sec)	eq. (41)
r	1/2 slot width in slotted tube, in. (m)	fig. 16
r_i	radii in grain configurations, in. (m) ($i = 1, 2, 3, 4$)	eq. (31) and figs. 11, 12, 13, 15
S	burning perimeter varying with w_x , in. (m)	eq. (27)
T	temperature, °F or °R (K)	fig. 1
T_c	propellant combustion temperature, °R (K)	sec. 2.1.1.2.1
T_i	grain conditioned temperature, °F (K)	eqs. (6) through (9), (36)
t	time, sec	(general use)
t_a	action time, sec	fig. 2
t_b	burning time or boost time, sec	fig. 2; eq. (16)
t_s	sustain time, sec	fig. 21
V_a	chamber volume available for propellant, in. ³ (m ³)	eqs. (15), (20)
V_c	instantaneous free volume of combustion chamber, in. ³ (m ³)	sec. 2.1.1.2.1
V_ℓ	volumetric loading fraction, V_p/V_a	eqs. (15), et al.
V_p	propellant volume, in. ³ (m ³)	eqs. (15), (32), (38)
W_p	propellant weight, lbm (kg)	definitions following eq. (15)
w	web thickness of propellant, in. (m)	eq. (31)
w_f	web fraction, w/R	eqs. (16), et al.

<u>Symbol</u>	<u>Definition</u>	<u>Appears In</u>
w_x	variable web burned, in. (m)	eqs. (22) through (24), et al.
X	configuration factor	eq. (18)
x	burning dimension, in. (m)	fig. 6
Y*	critical burn distance, in. (m)	figs. 11, 14
y	burning dimension, in. (m)	fig. 6
y_c	grain inner radius in anchor, in. (m)	fig. 14
α	nozzle divergence half angle or half angle of inscribed cone, deg	eqs. (12), (13)
α	configuration angle in star, wagon wheel, dendrite, and dogbone, deg	eq. (30) and figs. 11, 12, 13, 15
β	configuration angle in wagon wheel and dendrite, deg	figs. 12, 13
γ	$\frac{\text{specific heat at constant pressure}}{\text{specific heat at constant volume}}$	eq. (10)
Δ	a positive or negative change in the value of a variable	(general use)
ϵ	nozzle area expansion ratio, A_e/A_t	eqs. (10), (11)
ϵ	strain, in./in. (m/m)	fig. 1
η	configuration angle in star, deg	eqs. (27) through (29) and fig. 11
η_T	nozzle thrust coefficient efficiency factor	eqs. (11), (14)
η_θ	c* efficiency factor	sec. 2.1.1.2.1
η_μ	deliverable motor efficiency	eq. (2)
θ	angle of end-burning geometry defined by non-uniform burning rate, deg	fig. 6
θ_{ex}	nozzle exit plane lip angle, deg	eq. (13)
λ	nozzle divergence correction factor	eqs. (11) through (14)

<u>Symbol</u>	<u>Definition</u>	<u>Appears In</u>
ξ	configuration angle in star, wagon wheel, dendrite, and dogbone, deg	eqs. (29) through (31) and figs. 11, 12, 13, 15
π_K	temperature sensitivity of pressure at a particular value of K_n , %/°F (%/K)	eqs. (6), (36), and fig. 3
$\pi_{P/r}$	temperature sensitivity of pressure at a particular value of P/r , %/°F (%/K)	eq. (9) and fig. 3
ρ_p	propellant mass density, lbm/in. ³ (kg/m ³)	eqs. (15), (19), et al
σ	standard deviation	sec. 3.1.1.1
σ	stress, lbf/in. ² (N/m ²)	fig. 1
σ_K	temperature sensitivity of burning rate at a particular value of K_n , %/°F (%/K)	eq. (8) and fig. 3
σ_P	temperature sensitivity of burning rate at a particular value of P , %/°F (%/K)	eqs. (7), (36), and fig. 3
ϕ	configuration angle in anchor, deg	fig. 14

<u>Term</u>	<u>Definition</u>
burning rate	literally, the rate at which the propellant burns; in grain design, the rate at which the web decreases in thickness during motor operation
burning surface	all the surface of the grain that is not restricted from burning at any given time during propellant combustion
configuration	the perforation geometry of a propellant grain
configuration efficiency	the ratio of the total impulse to the impulse that could be delivered with an optimum nozzle at an average pressure equal to the maximum pressure
cylindrical grain	a grain in which the internal cross section is constant
end effects	the effect on total burning surfaces of internal-burning grains contributed by burning in the longitudinal direction
envelope	external boundary defining the limits on diameter and length of the grain

<u>Term</u>	<u>Definition</u>
erosive burning rate	burning rate that includes augmentation induced by gas flow over the burning surface
grain	integral piece of propellant in a solid rocket motor
grain conditioned temperature	the temperature of the propellant grain just before ignition
impulse	the product of average thrust and the time during which it acts; mathematically, the integral of the thrust-time function over a definite time interval
internal-burning grain	a grain in which the surface of the perforation is a burning surface
mandrel	casting tool that forms the grain perforation
mass addition	a technique of analysis that evaluates the gas dynamics within the motor in terms of addition of small amounts of mass at specific locations
mass flux	mass flowrate through a given area expressed as the ratio of mass flowrate and port area
neutral burning	a condition in which thrust, pressure, or burning surface remains approximately constant with respect to time or to web burned
perforation	central cavity of a propellant grain
perimeter	outer boundary of the flow area at a given station in the motor
pressure overshoot	a maximum (or relative maximum) point that occurs on the pressure-time curve at ignition
progressive burning	a condition in which thrust, pressure, or burning surface increases with respect to time or to web burned
progressivity ratio	ratio of final to initial burning surface
radial-burning grain	a grain that burns in the radial direction either outward (e.g., an internal-burning grain) or inward (e.g., an internal-external burning tube or rod and tube)
regressive burning	a condition in which thrust, pressure, or burning surface decreases with time or web burned

<u>Term</u>	<u>Definition</u>
restricted surface	surface that is prevented from burning
sliver	propellant remaining at the time of web burnout
three-dimensional configuration	a grain whose burning surface is described by three-dimensional analytical geometry (one that considers end effects)
threshold velocity	the gas velocity at which burning-rate augmentation (erosive burning) begins
two-dimensional configuration	a grain whose burning surface is described by two-dimensional analytical geometry (cross section is independent of length)
two-phase flow	simultaneous flow of solid particles (e.g., condensed metal oxide) and combustion gases
web	the minimum thickness of the grain from the initial ignition surface to the insulated case wall or to the intersection of another burning surface at the time when the burning surface undergoes a major change; for an end-burning grain, the length of the grain

<u>Abbreviation</u>	<u>Identification</u>
AIAA	American Institute of Aeronautics and Astronautics
AFRPL	Air Force Rocket Propulsion Laboratory
ARGMA	Army Rocket and Guided Missile Agency
ARS	American Rocket Society
CARDE	Canadian Armament Research and Development Establishment
CPIA	Chemical Propulsion Information Agency
ICRPG	Interagency Chemical Rocket Propulsion Group
JANNAF	Joint Army-Navy-NASA-Air Force
JANAF-ARPA-NASA	Joint Army-Navy-Air Force-Advanced Research Project Agency-National Aeronautics and Space Administration
SPIA	Solid Propulsion Information Agency

NASA SPACE VEHICLE DESIGN CRITERIA MONOGRAPHS ISSUED TO DATE

ENVIRONMENT

SP-8005	Solar Electromagnetic Radiation, Revised May 1971
SP-8010	Models of Mars Atmosphere (1967), May 1968
SP-8011	Models of Venus Atmosphere (1968), December 1968
SP-8013	Meteoroid Environment Model—1969 (Near Earth to Lunar Surface), March 1969
SP-8017	Magnetic Fields—Earth and Extraterrestrial, March 1969
SP-8020	Mars Surface Models (1968), May 1969
SP-8021	Models of Earth's Atmosphere (120 to 1000 km), May 1969
SP-8023	Lunar Surface Models, May 1969
SP-8037	Assessment and Control of Spacecraft Magnetic Fields, September 1970
SP-8038	Meteoroid Environment Model—1970 (Interplanetary and Planetary), October 1970
SP-8049	The Earth's Ionosphere, March 1971
SP8067	Earth Albedo and Emitted Radiation, July 1971
SP-8069	The Planet Jupiter (1970), December 1971
SP-8085	The Planet Mercury (1971), March 1972

STRUCTURES

SP-8001	Buffeting During Atmospheric Ascent, revised November 1970
SP-8002	Flight-Loads Measurements During Launch and Exit, December 1964
SP-8003	Flutter, Buzz, and Divergence, July 1964
SP-8004	Panel Flutter, July 1964

SP-8006	Local Steady Aerodynamic Loads During Launch and Exit, May 1965
SP-8007	Buckling of Thin-Walled Circular Cylinders, revised August 1968
SP-8008	Prelaunch Ground Wind Loads, November 1965
SP-8009	Propellant Slosh Loads, August 1968
SP-8012	Natural Vibration Modal Analysis, September 1968
SP-8014	Entry Thermal Protection, August 1968
SP-8019	Buckling of Thin-Walled Truncated Cones, September 1968
SP-8022	Staging Loads, February 1969
SP-8029	Aerodynamic and Rocket-Exhaust Heating During Launch and Ascent, May 1969
SP-8030	Transient Loads From Thrust Excitation, February 1969
SP-8031	Slosh Suppression, May 1969
SP-8032	Buckling of Thin-Walled Doubly Curved Shells, August 1969
SP-8035	Wind Loads During Ascent, June 1970
SP-8040	Fracture Control of Metallic Pressure Vessels, May 1970
SP-8042	Meteoroid Damage Assessment, May 1970
SP-8043	Design-Development Testing, May 1970
SP-8044	Qualification Testing, May 1970
SP-8045	Acceptance Testing, April 1970
SP-8046	Landing Impact Attenuation for Non-Surface-Planing Landers, April 1970
SP-8050	Structural Vibration Prediction, June 1970
SP-8053	Nuclear and Space Radiation Effects on Materials, June 1970
SP-8054	Space Radiation Protection, June 1970

- SP-8055 Prevention of Coupled Structure-Propulsion Instability (Pogo), October 1970
- SP-8056 Flight Separation Mechanisms, October 1970
- SP-8057 Structural Design Criteria Applicable to a Space Shuttle, January 1971
- SP-8060 Compartment Venting, November 1970
- SP-8061 Interaction With Umbilicals and Launch Stand, August 1970
- SP-8062 Entry Gasdynamic Heating, January 1971
- SP-8063 Lubrication, Friction, and Wear, June 1971
- SP-8066 Deployable Aerodynamic Deceleration Systems, June 1971
- SP-8068 Buckling Strength of Structural Plates, June 1971
- SP-8072 Acoustic Loads Generated by the Propulsion System, June 1971
- SP-8077 Transportation and Handling Loads, September 1971
- SP-8079 Structural Interaction with Control Systems, November 1971
- SP-8082 Stress-Corrosion Cracking in Metals, August 1971
- SP-8083 Discontinuity Stresses in Metallic Pressure Vessels, November 1971
- SP-8095 Preliminary Criteria for the Fracture Control of Space Shuttle Structures, June 1971

GUIDANCE AND CONTROL

- SP-8015 Guidance and Navigation for Entry Vehicles, November 1968
- SP-8016 Effects of Structural Flexibility on Spacecraft Control Systems, April 1969
- SP-8018 Spacecraft Magnetic Torques, March 1969
- SP-8024 Spacecraft Gravitational Torques, May 1969
- SP-8026 Spacecraft Star Trackers, July 1970
- SP-8027 Spacecraft Radiation Torques, October 1969

SP-8028	Entry Vehicle Control, November 1969
SP-8033	Spacecraft Earth Horizon Sensors, December 1969
SP-8034	Spacecraft Mass Expulsion Torques, December 1969
SP-8036	Effects of Structural Flexibility on Launch Vehicle Control Systems, February 1970
SP-8047	Spacecraft Sun Sensors, June 1970
SP-8058	Spacecraft Aerodynamic Torques, January 1971
SP-8059	Spacecraft Attitude Control During Thrusting Maneuvers, February 1971
SP-8065	Tubular Spacecraft Booms (Extendible, Reel Stored), February 1971
SP-8070	Spaceborne Digital Computer Systems, March 1971
SP-8071	Passive Gravity-Gradient Libration Dampers, February 1971
SP-8074	Spacecraft Solar Cell Arrays, May 1971
SP-8078	Spaceborne Electronic Imaging Systems, June 1971
SP-8086	Space Vehicle Displays Design Criteria, March 1972

CHEMICAL PROPULSION

SP-8052	Liquid Rocket Engine Turbopump Inducers, May 1971
SP-8048	Liquid Rocket Engine Turbopump Bearings, March 1971
SP-8064	Solid Propellant Selection and Characterization, June 1971
SP-8075	Solid Propellant Processing Factors in Rocket Motor Design, October 1971
SP-8039	Solid Rocket Motor Performance Analysis and Prediction, May 1971
SP-8051	Solid Rocket Motor Igniters, March 1971
SP-8025	Solid Rocket Motor Metal Cases, April 1970
SP-8041	Captive-Fired Testing of Solid Rocket Motors, March 1971